

AD-A159 723

AN ASSESSMENT OF WAVE AND WIND DATA FOR USE IN DESIGN
OF TENSION LEG PLAT (U) DAVID W TAYLOR NAVAL SHIP
RESEARCH AND DEVELOPMENT CENTER BET W H BUCKLEY

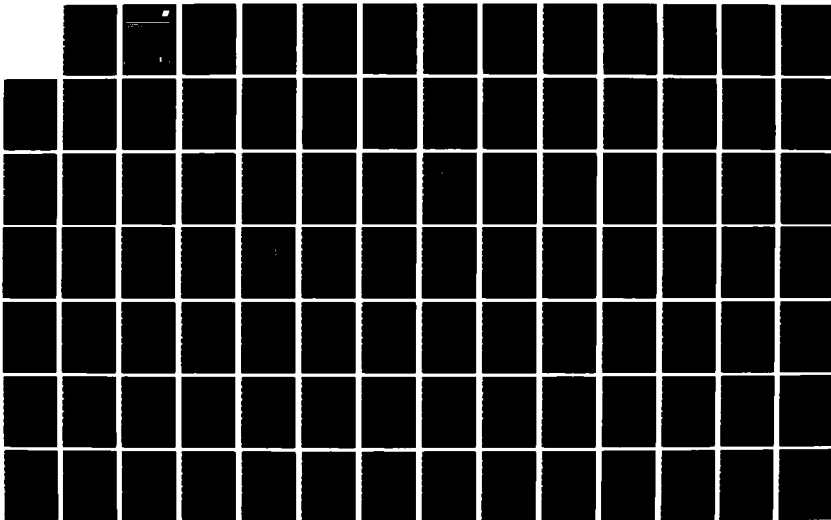
1/2

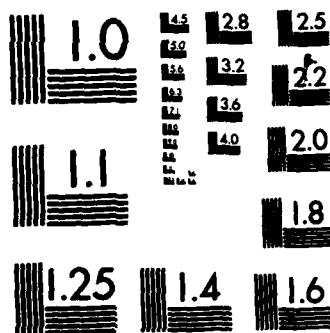
UNCLASSIFIED

JUL 84 USCG-M-84-5 DTICG23-83-F-04433

F/G 8/3

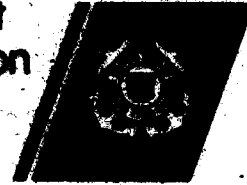
NL





MICROCOPY RESOLUTION TEST CHART
NATIONAL BUREAU OF STANDARDS-1963-A

U.S. Department
of Transportation
United States
Coast Guard



2

AD-A159 723

AN ASSESSMENT OF WAVE AND WIND DATA FOR USE IN DESIGN OF TENSION LEG PLATFORMS—U.S. OFFSHORE AREAS

William H. Buckley

David W. Taylor Naval Ship
Research and Development Center

This document is available to the public
through the National Technical Information
Service, Springfield, Virginia 22161.

Office of Merchant Marine Safety
Washington, D.C. 20593

DTIC FILE COPY

July 1984
Final Report

USCG-M-84-5(16718)

DTIC
ELECTE
S OCT 4 1985 D
A

85 10 03 084

1. Report No. USCG-M-84-5 (16718)	2. Government Accession No. AD-A159 723	3. Recipient's Catalog No.
4. Title and Subtitle Assessment of Wave and Wind data for use in Design of Tension Leg Platform - U.S. Offshore areas	5. Report Date July 1984	6. Performing Organization Code
7. Author(s) William H. Buckley	8. Performing Organization Report No.	10. Work Unit No. (TRAIS)
9. Performing Organization Name and Address David Taylor Naval Ship Research and Development Center. Code 1730.6 Bethesda, MD 20084	11. Contract or Grant No. DTCG 23-83-F-04433	13. Type of Report and Period Covered FINAL REPORT June 1983 - Jan. 1984
12. Sponsoring Agency Name and Address U.S. Coast Guard (G-MTH-5/13) 2100 Second Street, SW Washington, D.C. 20593	14. Sponsoring Agency Code	
15. Supplementary Notes		
<p>(cont p 1)</p> <p>16. Abstract</p> <p>Climatic summary wave and wind data obtained from NOAA ocean data buoys of potential interest in Tension Leg Platform (TLP) design are summarized. Selected wave and wind data from those storms which produced maximum measured values of significant wave height are then examined in detail. Based upon these data, which is supplemented by wave data from hurricane Camille, an envelope of extreme values of significant wave height and modal period is defined. This envelope also identifies seaways of extreme steepness. Characteristic normalized spectra are defined for certain portions of the envelope and in the case of seas of limiting steepness, critical time domain waves are identified.</p> <p>Dynamic response characteristics of a model of the Hutton TLP are reviewed in order to help identify wave and wind data of special interest in determining cumulative service and extreme structural loadings for TLP's. Initiatives for extending the frequency and time domain wave and wind data of this report to individual NOAA data buoy locations are then identified. <i>Kayman 429</i></p>		
17. Key Words Extreme wave and wind Environmental Condition Tension Leg Platform <i>Hutton TLP</i> <i>North Atlantic</i>	18. Distribution Statement Document is available to the public through the National Technical Information Service, Springfield, VA 22161	
19. Security Classif. (of this report) Unclassified	20. Security Classif. (of this page) Unclassified	21. No. of Pages 110

TABLE OF CONTENTS

	Page
LIST OF FIGURES.	v
LIST OF TABLES	viii
ABSTRACT	1
1.0 INTRODUCTION.	1
2.0 RECENT DEVELOPMENTS IN WAVE AND WIND DATA ACQUISITION AND ANALYSIS. . . .	2
2.1 NOAA Climatic and Maximum Significant Wave Height Data	2
2.1.1 General	2
2.1.2 Presumptions Inherent in the Analysis of Climatic Wave and Wind Data.	7
2.1.3 Climatic Wave and Wind Data Compiled from NOAA Data Buoy Measurements.	7
2.1.4 Additional Information Available from the NOAA Data Base	9
2.1.5 Wave Height Spectra for Maximum Significant Wave Heights.	12
2.2 Time Series Characteristics of the Larger Waves in Extreme Seaways.	20
2.2.1 General	20
2.2.2 The Half-Cycle Analysis Method and Its Application to Hurricane Camille Wave Data.	23
2.2.3 Circumstantial Evidence Regarding the Existence and Characteristics of Large Non-Gaussian Waves	30
3.0 RESPONSE CHARACTERISTICS OF TENSION LEG PLATFORMS AND REQUIRED WAVE AND WIND DATA.	34
3.1 General.	34
3.2 Hutton TLP Response Characteristics.	34
3.2.1 Basic Tethered Responses.	34
3.2.2 Results of Model Tests in Waves	34
3.3 Potentially Critical Wave and Wind Conditions.	40
3.3.1 Service Load Environments	40
3.3.2 Extreme Load Environments	40
4.0 RECOMMENDATIONS FOR THE ESTABLISHMENT OF WAVE AND WIND CRITERIA	43
4.1 Assumptions Regarding the Specification of Extreme Wave Conditions.	45
4.2 Wave Height Spectra.	46
4.3 Extreme Time Series Waves.	46
4.4 Wind Velocity Spectra.	46

	Page
4.5 Assessment of Critical Wave Conditions for Tension Leg Platforms.	47
4.6 Coordination of Wave and Wind Data for Critical Storm Conditions	47
ACKNOWLEDGMENTS.	48
REFERENCES	49
APPENDIX A - WAVE AND WIND DATA FOR SELECTED STORMS.	51
A1. Buoy Location 41001: Winter Storm of 3 March 1980.	52
A2. Buoy Location 42003: Hurricane Frederic, 12 September 1979	52
A3. Buoy Location 44004: Winter Storm of 8 February 1980	53
A4. Buoy Location 46001: Winter Storm of 28 November 1979.	53
A5. Buoy Location 46003: Winter Storm of 16 December 1979.	55
A6. Buoy Location 46005: Winter Storm of 26 November 1981.	55
A7. Buoy Location 46006 and 46022: Winter Storm of 9 February 1983.	55
APPENDIX B - AN OBSERVATION OF EPISODIC WAVE PACKETS	91
APPENDIX C - UNIQUENESS OF SYNOPTIC WIND FIELDS ASSOCIATED WITH THE OCCURRENCE OF EXTREME SIGNIFICANT WAVE HEIGHTS AND MODAL PERIODS	95
APPENDIX D - COMPARISON OF HURRICANE AND SEVERE WINTER STORM WAVES	99

Pages 94 and 98 are not missing but are
misnumbered.

Per Mr. Wm. H. Buckley, DTNSRDC/Code 1730.6

Accession For	
NTIS CRA&I	<input checked="" type="checkbox"/>
DTIC TAB	<input type="checkbox"/>
Unannounced	<input type="checkbox"/>
Justification	
By _____	
Distribution/	
Availability Codes	
Dist	Avail and/or Special
<div style="display: flex; justify-content: space-between;"> AI </div>	



LIST OF FIGURES

	Page
1 - Wave Height Data Archived at the National Climatic Data Center - North Atlantic and Gulf of Mexico	3
2 - Wave Height Data Archived at the National Climatic Data Center - North Pacific	4
3 - Location of NOAA Data Buoys for Which Climatic Summary Data are Available - North Atlantic and Gulf of Mexico.	5
4 - Location of NOAA Data Buoys for Which Climatic Summary Data are Available - North Pacific.	6
5 - Suggested Data Format for Climatic Summary of Wave Height Spectra.	11
6 - Suggested Format for Climatic Wind Data.	13
7 - Wave Height Spectra for Selected Severe Environmental Conditions	14
8 - Maximum Measured Significant Wave Heights vs Frequency Corresponding to Modal Period.	15
9 - Normalized Wave Height Spectra for Steep Wave Conditions ($H_{m0}/T_p^2 = 0.25$)	17
10 - Generalized Wave Height Spectrum for Wave Conditions of Extreme Steepness.	18
11 - Development of Winter Storm at Buoy Location 46005, 26 November 1981	19
12 - Development of Winter Storm at Buoy Location 44004, 7-8 February 1980.	21
13 - Normalized Wave Height Spectra for Maximum Significant Wave Height Conditions	22
14 - Half-Cycle Counting of Random Data	24
15 - Characterization of Half-Cycle Excursions Within the HACYM	24
16 - Estimate of Expected Half-Cycle Events for Gaussian Realizations Conforming to Three Wave Spectra from Hurricane Camille.	26
17 - Distribution of Occurrence of Half-Cycle Time Increments for Measured and Simulated Wave Data	27
18 - Summary of Half-Cycle Wave Height Events from Thirteen Half-Hour Gaussian Realizations Which Exceeded the Gaussian Expectation Boundary	28

	Page
19 - Summary of Half-Cycle Wave Height Events from Hurricane Camille (1000-1617 Hours) Which Exceeded the Gaussian Expectation Boundary	28
20 - Half-Cycle Count Distributions of Measured Data for Three Half-Hours of Hurricane Camille Wave Data.	29
21 - Large Non-Gaussian Waves Measured During Hurricane Camille	31
22 - Wind Velocity Spectrum Measured During Hurricane Camille (1500-1530 Hours).	36
23 - Time Series Wind Velocity and Wave Height Data Measured During Hurricane Camille at 1522 Hours.	37
24 - Significant Wave Height vs Frequency Corresponding to Modal Period for Particular Geographic Locations	38
A1 - Wave and Wind Data from Buoy Location 41001: Winter Storm of 3 March 1980.	58
A2 - Surface Weather Map for Buoy Location 41001 at 1200Z on 3 March 1980.	59
A3 - Wave Height Spectra from Buoy Location 41001: Winter Storm of 3 March 1980.	60
A4 - Track of Winter Storm Relative to Buoy Location 41001: 3 March 1980	61
A5 - Track of Hurricane Frederic Relative to Buoy Location 42003: 12 September 1979.	62
A6 - Wave and Wind Data from Buoy Location 42003: Hurricane Frederic 12 September 1979	63
A7 - Wave Height Spectra from Buoy Location 42003: Hurricane Frederic 12 September 1979	64
A8 - Wave and Wind Data from Buoy Location 44004: Winter Storm of 7 February 1980	65
A9 - Track of Winter Storm Relative to Buoy Location 44004: 7 February 1980.	66
A10 - Surface Weather Map for Buoy Location 44004 at 1800Z on 7 February 1980	67
A11 - Wave Height Spectra from Buoy Location 44004: Winter Storm of 7 February 1980	68

	Page
A12 - Track of Winter Storm Relative to Buoy Location 46001: 28 November 1979	69
A13 - Wave and Wind Data from Buoy Location 46001: Winter Storm of 28 November 1979.	70
A14 - Surface Weather Map for Buoy Location 46001 at 0600Z on 28 November 1979.	71
A15 - Wave Height Spectra from Buoy Location 46001: Winter Storm of 28 November 1979.	72
A16 - Wave Height Spectra from Buoy Location 46001: Winter Storm of 28 November 1979 - 09Z to 12Z Hours	73
A17 - Surface Weather Map for Buoy Location 46003 at 1800Z on 15 December 1979.	74
A18 - Track of Winter Storm Relative to Buoy Location 46003: 15 December 1979	75
A19 - Wave Data from Buoy Location 46003: Winter Storm of 15 December 1979	76
A20 - Wave Height Spectra from Buoy Location 46003: Winter Storm of 15 December 1979.	77
A21 - Track of Winter Storm Relative to Buoy Location 46005: 26 November 1981	78
A22 - Surface Weather Map for Buoy Location 46005 at 1200Z on 26 November 1981.	79
A23 - Wave and Wind Data from Buoy Location 46005: Winter Storm of 26 November 1981.	80
A24 - Wave Height Spectra from Buoy Location 46005: Winter Storm of 26 November 1981.	81
A25 - Wave and Wind Data from Buoy Location 46006: Winter Storm of 9 February 1983	82
A26 - Wave Height Spectra from Buoy Location 46006: Winter Storm of 9 February 1983 - 0700Z to 1000Z.	83
A27 - Wave Height Spectra from Buoy Location 46006: Winter Storm of 9 February 1983 - 1100Z to 1300Z.	84
A28 - Track of Winter Storm Relative to Buoy Location 46006: 9 February 1983.	85

	Page
A29 - Surface Weather Map for Buoy Location 46006 at 1200Z on 9 February 1983	86
A30 - Wave and Wind Data from Buoy Location 46022: Winter Storm of 9 February 1983	87
A31 - Wave Height Spectra from Buoy Location 46022: Wave Energy from Winter Storm of 9 February 1983	88
C1 - Sea Level Pressure Chart (mb.) at 1200 GMT March 6, 1962	97
C2 - Sea Level Pressure Chart (mb.) at 1200 GMT March 7, 1962	97
D1 - Maximum Measured Significant Wave Heights vs Frequency Corresponding to Modal Period - Including North Sea Storm.	101
D2 - Similarity of Waves in a North Sea Winter Storm and Hurricane Camille.	102

LIST OF TABLES

1 - Percentage Occurrence of Significant Wave Heights by Geographic Location.	8
2 - Comparison of Maximum Wind Speed in Severe Storms and Maximum Measured Wind Speed.	10
3 - An Initial Characterization of Large Non-Gaussian and Episodic Waves	32
4 - Response Periods for Tension Leg Platforms	35
5 - Wave Parameters for 10 Areas in United States Waters of 91.4 m (300 ft) Depth or Greater	42
6 - Hurricane Camille Wind Data: Ratio of Peak Gust to Average Wind Velocity.	44
A1 - Summary of Observation Periods and Average Observation Rates for Selected Buoys	89
A2 - Typical Reporting Ranges, Sampling Intervals and Averaging Periods for NOAA Buoy Measured Wave and Wind Parameters.	90
B1 - Selected Data from the Weather Log of the BALD EAGLE March 7-10, 1969	93

ABSTRACT

Climatic summary wave and wind data obtained from NOAA ocean data buoys of potential interest in Tension Leg Platform (TLP) design are summarized. Selected wave and wind data from those storms which produced maximum measured values of significant wave height are then examined in detail. Based upon these data, which is supplemented by wave data from hurricane Camille, an envelope of extreme values of significant wave height and modal period is defined. This envelope also identifies seaways of extreme steepness. Characteristic normalized spectra are defined for certain portions of the envelope and in the case of seas of limiting steepness, critical time domain waves are identified.

Dynamic response characteristics of a model of the Hutton TLP are reviewed in order to help identify wave and wind data of special interest in determining cumulative service and extreme structural loadings for TLP's. Initiatives for extending the frequency and time domain wave and wind data of this report to individual NOAA data buoy locations are then identified.

1.0 INTRODUCTION

↳ Interest in deep water oil production platform design has increased considerably in recent years. One of the promising concepts for outer continental shelf installations is a semi-submersible, column stabilized floating platform held in place by pre-loaded tendons anchored to the ocean floor. Because of the unique character of the tethering arrangement this concept is commonly referred to as a Tension Leg Platform (TLP). One of the important problems associated with TLP design criteria concerns the wave and wind data to be employed in structural design, particularly for extreme environmental conditions.

Two recent developments have begun to provide important information with respect to wave characteristics to be employed in TLP design. The first is the publication of climatic wave and wind data by the National Oceanic and Atmospheric Administration (NOAA) based upon long term measurements at a number of U.S. offshore ocean data buoy locations, reference 1*. The second is the development of a method of analyzing time series wave data which is capable of identifying non-Gaussian events in the data. An analysis of hurricane Camille wave data using this method has identified distinctive, non-Gaussian waves of extreme steepness which occurred near the height of the storm. A related study of extreme wave encounters by ships has provided an initial characterization of four types of large, non-Gaussian waves.

These developments together with selected portions of the ocean buoy data are examined in section 2.0 in order to arrive at an initial characterization of extreme seaways in both the frequency and time domains. Response characteristics of TLP's are examined in section 3.0 in order to identify those wave energy frequencies and

*References are listed on page 49.

time domain wave characteristics which are likely to be of particular interest in design of TLP's. The significance of the wave data of section 2.0 and certain extreme wind data from hurricane Camille are then examined. Based upon the findings of sections 2.0 and 3.0 data acquisition and analysis initiatives are recommended in section 4.0 which need to be implemented in order to improve the scope of the climatic and extreme wave and wind data presented in this report.

2.0 RECENT DEVELOPMENTS IN WAVE AND WIND DATA ACQUISITION AND ANALYSIS

The publication by NOAA of a climatic summary of wave and wind data gathered from U.S. coastal locations, reference 1, represents an important milestone in the assessment of offshore wave conditions. These data are reviewed here with respect to the frequency of occurrence of significant wave heights at individual buoy locations. In addition, certain of the associated storm wave and wind data are reviewed in detail in Appendix A together with data from a more recent Pacific storm having an unusually high modal period.

The half-cycle method of analyzing time series data is described briefly as well as the results of applying the method to hurricane Camille wave data. Findings of a study of extreme wave encountered by ships in winter storms is presented together with an initial characterization of large non-Gaussian and episodic waves.

2.1 NOAA Climatic and Maximum Significant Wave Height Data

2.1.1 General

NOAA data buoys now furnish, among other information, hourly wave height (point) spectra which are derived from 20 minute duration measurements of buoy accelerations due to wave action together with hourly wind velocity and direction measurements of 8.5 minute duration. (Reporting range, sampling interval, and other data analysis information are given in Table A2). Significant wave height (H_{m0}) is estimated from the area under the variance spectrum for each data measurement interval. For recently acquired wave data, modal period (T_p), which corresponds to the peak ordinate of the variance spectrum, is also tabulated along with significant wave height. Buoy locations from which wave data have been gathered at one time or another are summarized in Figures 1 and 2. Among these, 18 buoy locations have produced approximately 3 years or more of wave data, see Figures 3 and 4. It is data from these locations that are the basis of the climatic summary data of reference 1.

As discussed in reference 2, pp. 63-78, certain characteristics and limitations of the wave data should be noted:

- a) Wave Data and Wave Spectrum Analyzer Measurement Systems.
Wave spectral data obtained using the older Wave Spectrum Analyzer systems should be checked for accuracy before use. Reference 2 in fact recommends that only data from the presently installed Wave Data Analyzer (WDA) measurement systems be considered where accuracy of the spectral data is particularly important. All maximum significant wave height data reviewed in this report were obtained using the WDA system.

Buoy ID.	Location	Period of Record	Number of Observations
06992	59.5N 142.0W	76-77	1308
06993	59.5N 142.3W	76-77	1528
06994	58.3N 157.0W	76-77	1031
46001	58.0N 148.0W	72-82	37442
46002	42.5N 130.0W	75-82	39452
46003	52.0N 156.0W	76-82	18943
46004	51.0N 136.0W	76-82	21178
46005	48.0N 131.0W	76-82	29053
46006	40.7N 137.0W	77-82	22716
46007	59.2N 152.7W	77-79	539
46008	57.1N 151.7W	77-79	3712
46010	46.2N 124.2W	79-82	19395
46011	34.9N 120.9W	80-82	18200
46012	37.4N 122.7W	80-82	15039
46013	38.2N 123.3W	81-82	12579
46014	38.2N 124.0W	81-82	13006
46022	40.8N 124.5W	82-82	7046
46023	34.3N 120.7W	82-82	6425
46024	33.0N 119.2W	82-82	6181
46025	33.8N 119.3W	82-82	4537
46026	37.8N 122.7W	82-82	3411
51001	23.4N 162.3W	81-82	12767

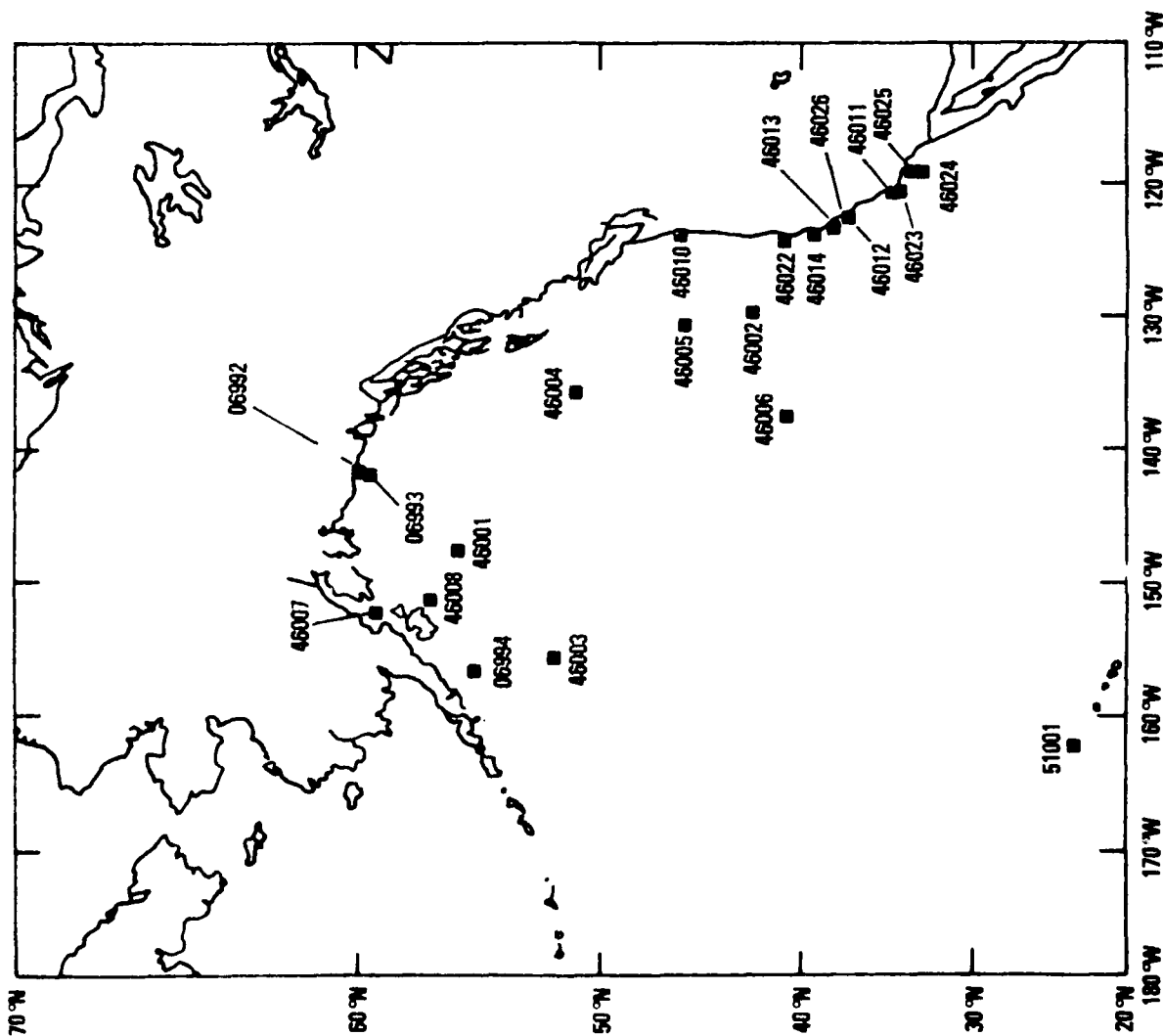


Figure 2 - Wave Height Data Archived at the National Climatic Data Center - North Pacific

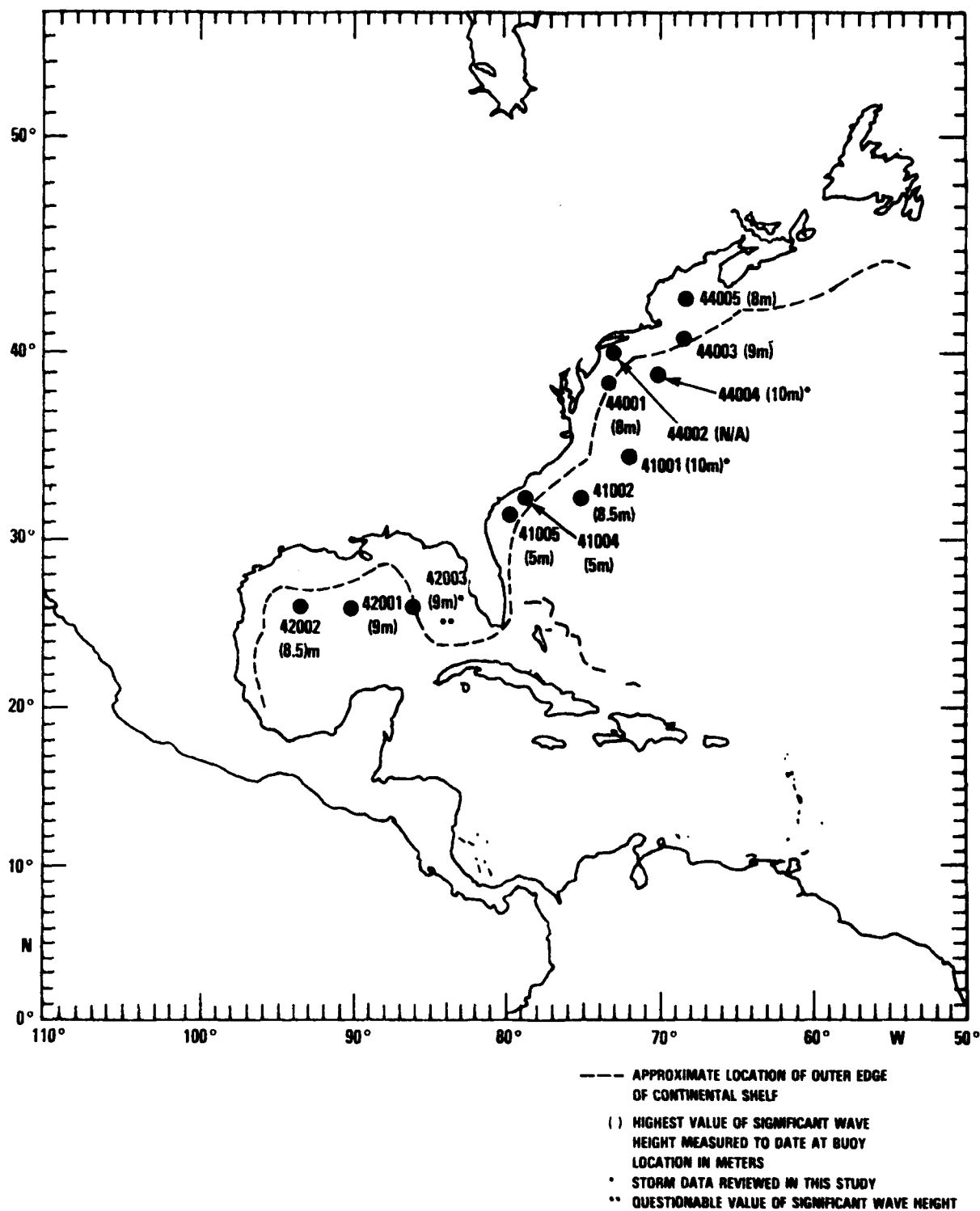


Figure 3 - Location of NOAA Data Buoys for Which Climatic Summary Data are Available - North Atlantic and Gulf of Mexico

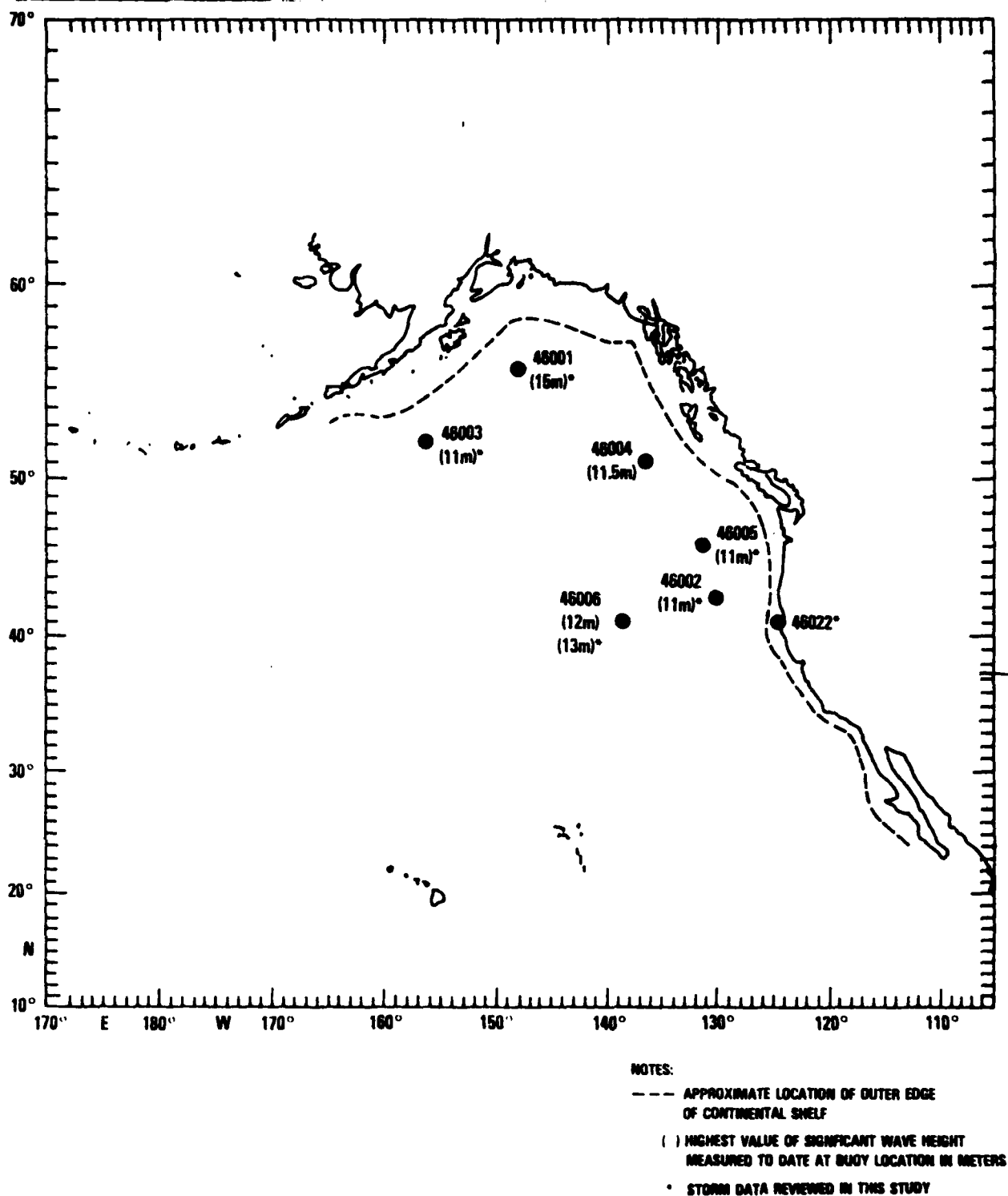


Figure 4 - Location of NOAA Data Buoys for Which Climatic Summary Data are Available - North Pacific

b) Low Frequency Swell Data

The method employed to correct for "noise" effects in low frequency accelerometer measurements has resulted in very low frequency swell waves (periods greater than 20 seconds) often not being detected. This difficulty applies primarily to situations where the swell wave energy is small compared to wind driven wave energy at higher frequencies. It should be noted that this limitation does not apply to wave spectral data from the severe storms which are examined in this report. (It has recently been determined by NOAA's National Data Buoy Center that archived buoy accelerometer data can be reprocessed to overcome this problem so that detection of long period swells in Pacific Ocean data, for example, can still be accomplished).

2.1.2 Presumptions Inherent in the Analysis of Climatic Wave and Wind Data

The following are important presumptions regarding the utilization and analysis of climatic wave and wind data.

- a) Climatic wave and wind data will be used to implement fatigue and crack growth analyses of TLP structural components and for this purpose frequency domain wave data (i.e. wave height variance spectra) are of primary interest. Extreme wave events on the other hand because of potential non-linear loading effects should be defined in time domain format.
- b) Storms associated with extreme wave conditions are not necessarily included in a 3 year sample of wave data and thus should be considered separately.
- c) Wave loadings predominate over wind loadings so that it is reasonable to focus attention initially on climatic wave data.
- d) Wave loadings typically increase non-linearly with wave height so that particular attention should be given to occurrence data associated with high sea states.

2.1.3 Climatic Wave and Wind Data Compiled from NOAA Data Buoy Measurements

Table 1 summarizes annual percentage occurrences of significant wave height (H_{m0}) intervals for 18 data buoy locations. These data are taken directly from reference 1. In order to call attention to occurrences of the higher significant wave heights, these data have been grouped in the right hand side of the table into percentage occurrences of significant wave heights up to 5.5 meters (\approx 18 feet) and for significant wave heights above 5.5 meters. (The choice of 5.5 meters is largely subjective. It reflects a rough estimate of a significant wave height below which a linear response of a TLP is very likely to occur as well as a lower limit for the appearance of one type of large non-Gaussian wave, see section 2.2).

Based upon this grouping it can be seen that significant wave heights greater than 5.5 meters occurred 0.1% of the time or less in the Gulf of Mexico and the Georgia Embayment areas over the 3 year or more data survey period. An occurrence level of 0.1% is considered to correspond a storm occurrence rate on the order of 1 or 2 storms per year since $0.001 \text{ times } (365 \times 24) \text{ hours} = 8.76 \text{ hours per year}$. The effect of off-shore buoy location in two east coast areas is also evident. Buoy

TABLE 1 - PERCENTAGE OCCURRENCE OF SIGNIFICANT WAVE HEIGHTS BY GEOGRAPHIC LOCATION

NOAA Buoy Location	Percentage Occurrence of Significant Wave Height Intervals (Hm ₀ in meters)												Max. Hm ₀ (meters)	Geographic Location
	0-0.5	0.5-1.5	1.5-2.5	2.5-3.5	3.5-4.5	4.5-5.5	5.5-6.5	6.5-7.5	7.5-8.5	8.5-9.5	9.5-10	>10	0-5.5 and up	
44005	1.6	50.0	29.0	11.9	4.8	1.8	0.6	0.2	0	0	0	0	99.1	Gulf of Maine
44003	0	27.6	36.8	20.0	8.8	3.6	1.9	0.8	0.3	*	0	0	96.8	Georges Bank
44002														Hudson Canyon
44004														East of Cape May
44001	0.5	54.9	30.2	11.1	2.8	0.4	0.1	0.1	*	0	0	0	99.9	Baltimore Canyon
41001	0.1	33.6	36.8	15.6	8.1	3.6	1.3	0.5	0.3	*	0	0	97.8	East of Cape Hatteras
41002	0.7	44.1	35.6	13.2	4.8	1.1	0.4	0.1	*	0	0	0	99.5	East of Savannah, Georgia
41004	0.2	55.9	32.8	9.5	1.5	0.2	0	0	0	0	0	0	100.1	Georgia Embayment
41005	0.1	58.9	30.6	7.4	2.7	0.3	0	0	0	0	0	0	100	Georgia Embayment
42003	2.8	63.1	26.3	6.0	1.5	0.3	0.1	*	*	*	0	0	100	Gulf of Mexico
42001	3.8	67.5	23.3	4.1	0.8	0.2	0.1	*	*	0	0	0	99.7	Gulf of Mexico
42002	2.5	62.9	27.0	6.2	1.0	0.3	0.1	*	0	0	0	0	99.9	Gulf of Mexico
46006	0	20.8	37.7	21.9	11.0	5.1	2.2	0.8	0.4	0.1	*	*	96.5	West of Cape Mendocino, Calif.
46002	0	11.1	37.5	27.0	14.3	6.2	2.5	1.0	0.4	0.1	*	*	96.1	West of Cape Blanco, Calif.
46005	*	12.5	34.6	28.0	15.2	6.1	2.4	0.7	0.3	0.1	*	*	96.4	West of Columbia River
46004	0	11.3	29.9	26.7	17.9	8.4	3.4	1.5	0.8	0.1	0	*	94.2	West of Vancouver, B.C.
46001	*	14.6	33.5	25.6	14.9	6.8	2.9	1.1	0.4	0.1	*	0.1	95.4	Gulf of Alaska
46003	0	10.6	28.3	28.2	17.2	9.1	3.5	1.8	0.7	0.2	0.2	0.1	93.4	South of Kodiak, Alaska

*Non-zero percentage rounded to zero.

**Questionable data due to limiting of accelerometer measuring buoy motions.

location 44001 on the continental shelf near the Baltimore Canyon area experienced significant wave heights above 5.5 meters only 0.2% of the time whereas Buoy Location 44004 approximately 115 nautical miles to the east in deep water found an occurrence rate of 4.3%. Further south, buoy locations 41004 and 41005 on the continental shelf in the Georgia Embayment area experienced occurrence rates of 0% whereas at buoy location 41002 approximately 175 nautical miles to the east in deep water an occurrence rate of 0.5% was measured. Data from buoy location 44003 near the outer edge of Georges Bank suggests, however, that continental shelf locations are not necessarily safe from the higher occurrence rates. In this instance the 5.5 meter level was exceeded 3% of the time or for about $0.03 \times 24 \times 365 = 263$ hours per year.

The highest occurrence rates for significant wave heights greater than 5.5 meters occurred in deep water off the west coast of Canada (5.8% at buoy location 46004) and south of the Aleutian Islands (6.5% at buoy location 46003).

The fact that maximum wave heights do not necessarily correlate well with climatic data trends is also illustrated. Buoy location 46003 finds significant wave heights greater than 5.5 meters 6.5% of the time while buoy location 46001 in the Gulf of Alaska finds a lower rate of 4.5%. However, the maximum significant wave height measured at the former is 11 meters whereas that measured at the latter was 15 meters. (By reaching beyond the immediate data base a more extreme example can be offered. During hurricane Camille a significant wave height of 13.5 meters was measured in an area where significant wave heights greater than 5.5 meters occurred only 0.1% of the time).

Extreme values of wind velocity in the climatic data base are presented in Table 2. In order to provide some indication as to whether or not extreme values of wind velocity coincide with extreme values of significant wave height, the maximum winds associated with each have been tabulated together with the dates and hours of the individual occurrences. In some cases the data of reference 1 did not permit the determination of the maximum wind velocity which was measured during the storm that resulted in maximum significant wave height. (For certain buoy locations, however, the data of Appendix A provided the desired information). The data of Table 2 reveal that with two exceptions (buoy locations 41001 and 42003) the maximum wind velocity measured at a buoy did not correspond to the date on which the maximum value of significant wave height was measured. (See also the discussion of section 3.3.2).

2.1.4 Additional Information Available from the NOAA Data Base

The data of reference 1 constitute an especially important climatic data base. However, as noted in 2.1.2(a) above the wave data most desired are climatic wave spectra*. While a separate computer program will be required to extract this information from the data base, data of the type shown in Figure 5 can be provided for use in estimating TLP cumulative service loads.

*i.e. data which permit one to identify the typical distribution of wave energy associated with each significant wave height class interval for a given buoy location.

TABLE 2 - COMPARISON OF MAXIMUM WIND SPEED IN SEVERE STORMS AND MAXIMUM MEASURED WIND SPEED

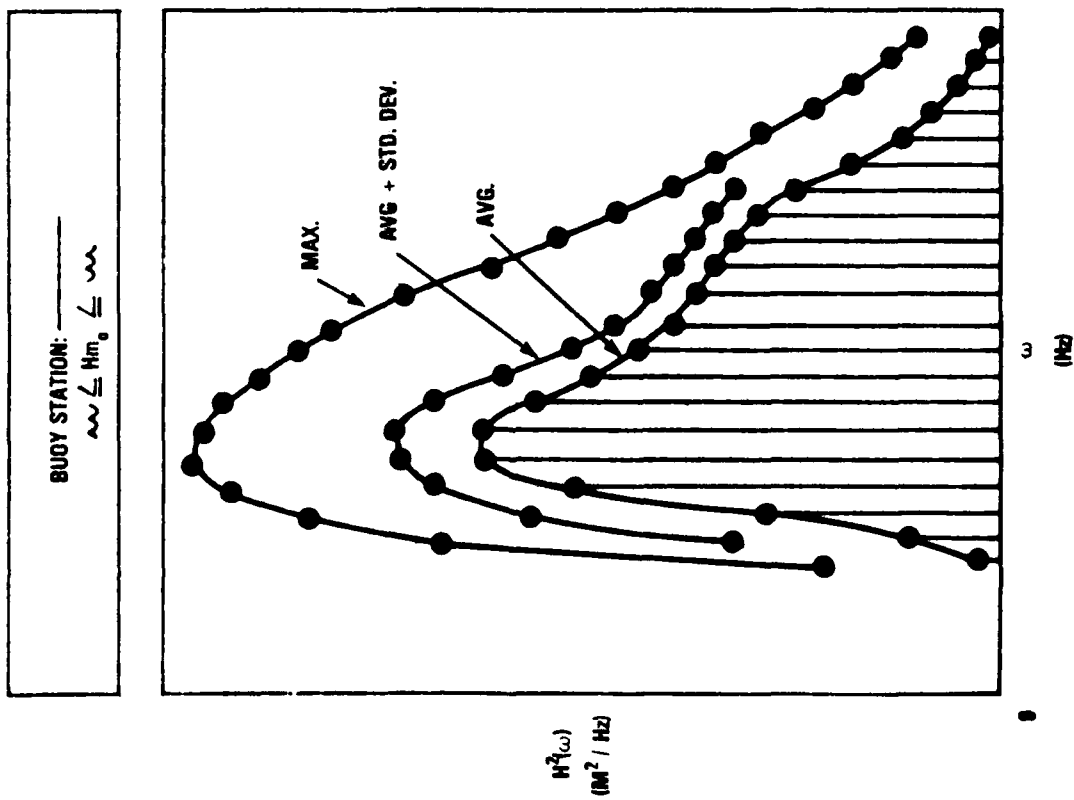
Buoy Location	Maximum 8.5 Minute Averaged Wind Speeds					Maximum Hm _o (meters)	Geographic Location
	V _w * Storm (knots)	Date	Hour (GMT)	V _w ** Max. (knots)	Date	Hour (GMT)	
44005	46	12/16/81	1700	48	01/18/79	2100	Gulf of Maine
44003	↕	N/A	↕	40	01/05/80	1900	Georges Bank
44002	↕	N/A	↕	43	02/06/78	2100	Hudson Canyon
44004	52.5	02/07/80	1600	55	02/19/79	2100	East of Cape May
44001	52	08/09/76	2300	53	02/02/76	1100	Baltimore Canyon
41001	61	03/03/80	0900	61	03/03/80	0900	East of Cape Hatteras
41002	47	02/02/76	0300	60	08/09/76	0600	East of Savannah, Georgia
41004	34	10/23/80	2300	38	12/28/80	1400	Georgia Embayment
41005	↕	N/A	↕	40	09/04/79	1800	Georgia Embayment
42003	66	09/12/79	0000	66	09/12/79	0000	Gulf of Mexico
42001	43	08/08/80	1400	52	09/22/75	1700	Gulf of Mexico
42002	41	11/13/80	1400	72	09/01/77	0500	Gulf of Mexico
46006	↕	N/A	↕	56	12/20/81	1200	West of Cape Mendocino, Calif.
46002	↕	N/A	↕	55	02/13/79	0000	West of Cape Blanco, Calif.
46005	48	11/12/81	0700	51	04/12/79	1700	West of Columbia River
46004	46	09/18/81	0100	52	11/30/79	0600	West of Vancouver, B.C.
46001	50	11/27/79	2100	53	03/11/77	0900	Gulf of Alaska
46003	42	12/15/79	1900	54	09/17/76	1500	South of Kodiak, Alaska

*Maximum wind velocity measured during storm which produced the highest value of significant wave height.

**Maximum wind velocity measured at buoy location.

***Questionable data due to limiting of accelerometer measuring buoy motions.

N/A - Not available from climatic data summary.



FREQ. (Hz)	0.01	0.5
PERIOD (sec)	100	2
AVG. ORD. (m ² /Hz)		
STD. DEV. (m ² /Hz)		
MAX. ORD. (m ² /Hz)		
DATE/TIME		

Figure 5 - Suggested Data Format for Climatic Summary
of Wave Height Spectra

The procedure suggested for determining climatic wave spectra for a particular buoy location is as follows:

(1) Develop a computer program which will identify by significant wave height class intervals the date and time of all archived spectra having significant wave heights within each interval.

(2) For all spectra associated with a particular class interval, determine at each constituent frequency of the spectra, the average of the ordinates, their standard deviation, and the maximum value together with the date and time of its occurrence. Plot and tabulate these data as shown in Figure 5.

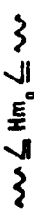
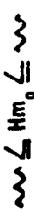
The reason for suggesting that standard deviation and individual maximum values be determined, is that a particular response transfer function for a TLP may have a peak within the frequency range of the average spectrum so that a designer may wish to account for platform response at this peak for wave energy ordinates higher than the average value. Knowledge of the standard deviation and the maximum measured ordinate will permit the designer to account for a reasonable amount of environmental exposure at the response peak. Recording of the time and date of the occurrence of the maximum ordinate permits retrieval from the data base of the particular spectrum which produced maximum wave energy at a response frequency of interest.

Up to this point no consideration has been given to winds acting in combination with waves. Reference 1 contains a considerable amount of climatic wind data and the reader is left to select those statistics which he finds most appropriate. However, it is also suggested that the computer program recommended for determining climatic wave spectra be structured to provide wind occurrence data of the type shown in Figure 6. It is recognized that the wind direction information is of limited value in the absence of concurrent directional wave spectra information. However, since this will not always be the case the cataloguing of directional wind data is recommended. In any event the totals of the right hand side of the table are needed to estimate concurrent wind loading effects.

2.1.5 Wave Height Spectra for Maximum Significant Wave Heights

The NOAA wave spectrum data base with the addition of one wave spectrum measured during hurricane Camille, see reference 3, provides an overview of spectra corresponding to a range of maximum measured significant wave heights. Figure 7 presents those spectra corresponding to highest measured values of significant wave height which are contained in this combined data base. Values of maximum energy density plotted at the corresponding modal periods for the remaining storms of Appendix A are also shown to indicate the relatively extreme nature of the three spectra which are plotted in Figure 7.

Figure 8 defines an empirical boundary of maximum measured values of significant wave height vs. the frequency corresponding to modal period. The boundary was constructed in the following manner. Based upon an examination of the time series character of the largest waves measured during hurricane Camille using half-cycle analyses methods (see section 2.2 below), it was concluded that the largest waves in the seaway near the height of the storm were of extreme steepness. Data point (10) of Figure 8 is thus considered to be an extreme value of the parameter significant wave height (H_{m0}) divided by modal period (T_p) squared. The rationale

BUOY STATION: _____
 Hm₀ 

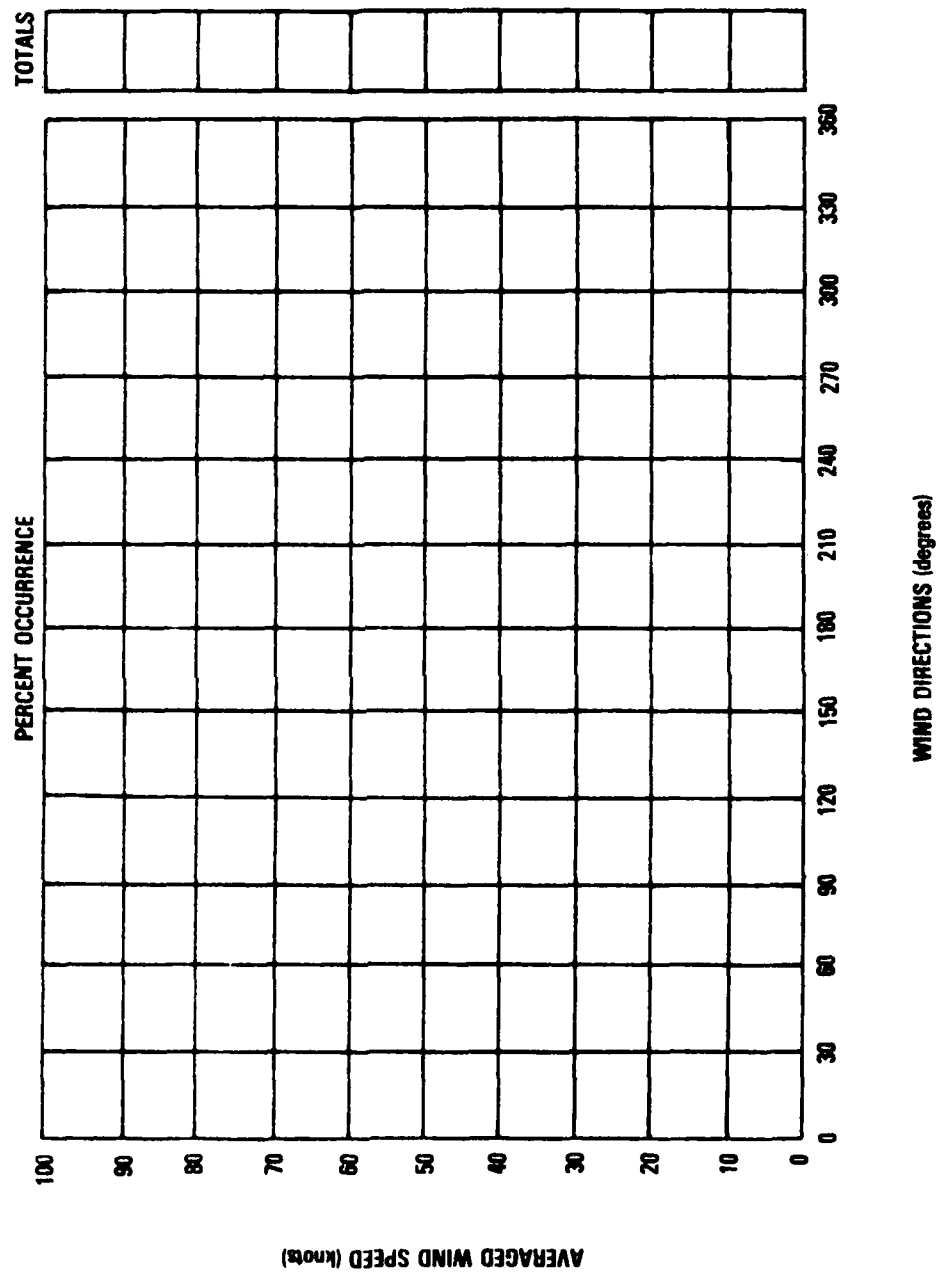


Figure 6 - Suggested Format for Climatic Wind Data

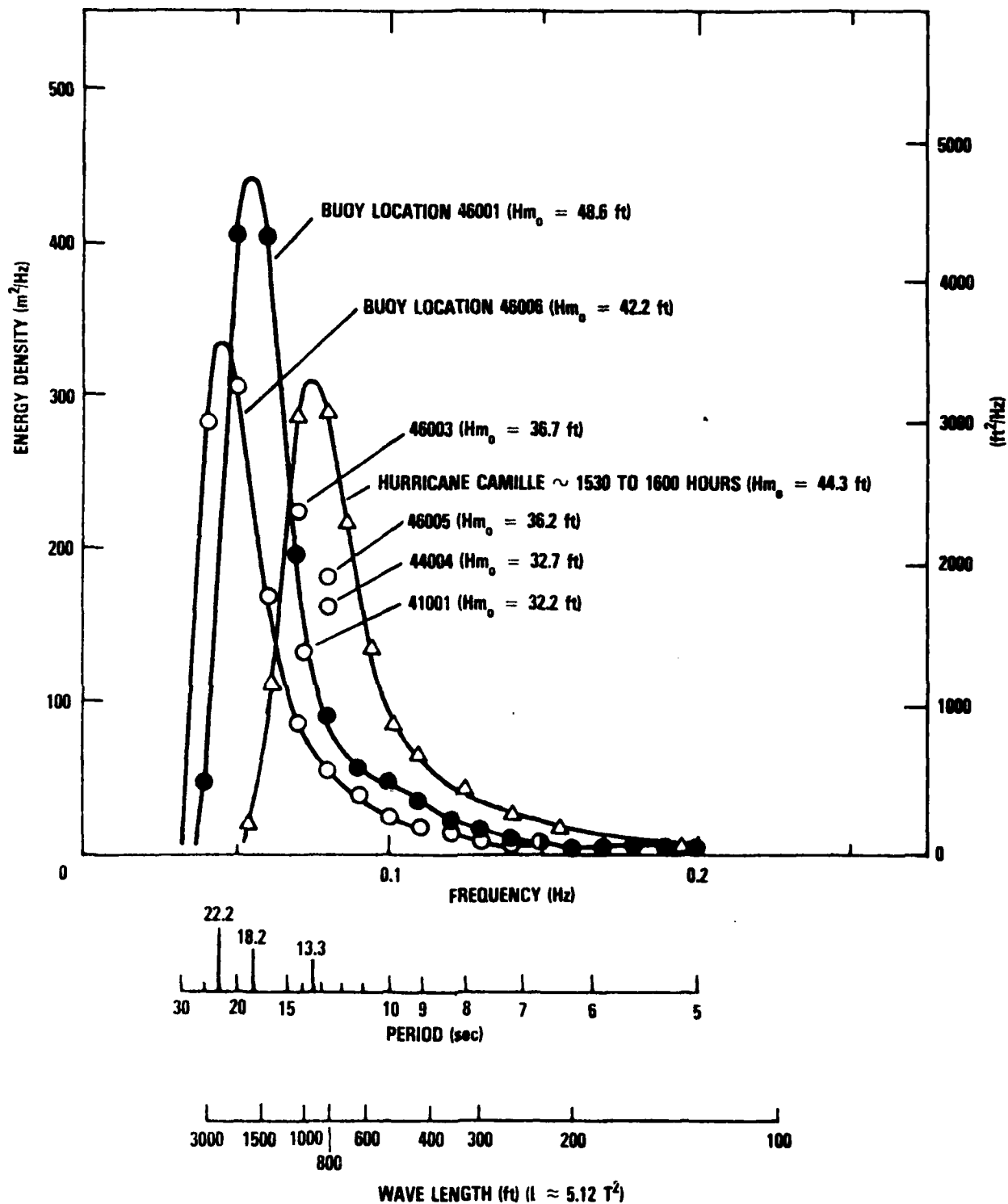


Figure 7 - Wave Height Spectra for Selected Severe Environmental Conditions

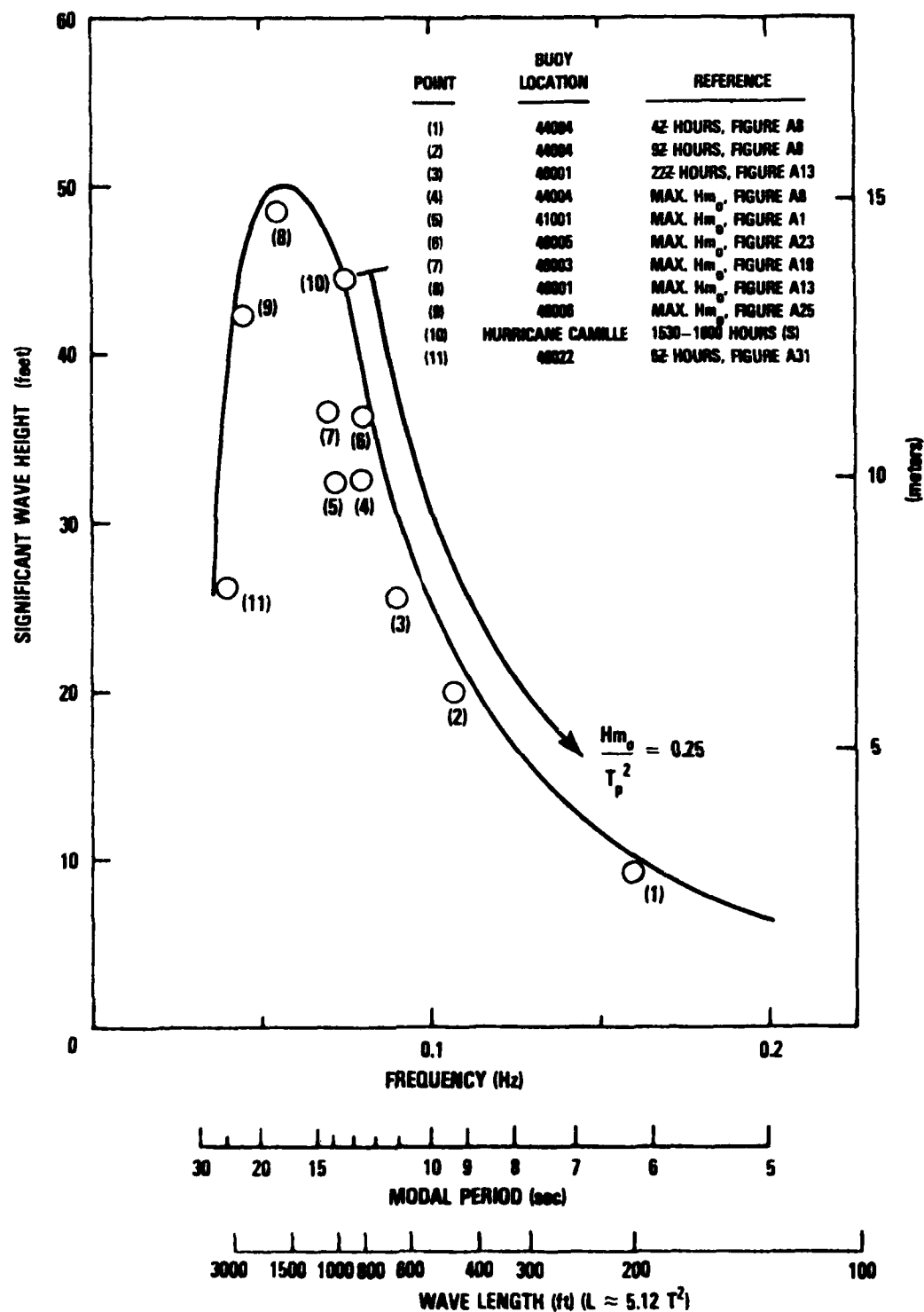


Figure 8 - Minimum Measured Significant Wave Heights vs Frequency Corresponding to Modal Period

for selection of this parameter is that $H_{m0}/5.12T_p^2$ can be considered a rough index of general wave steepness for unimodal wave spectra assuming that the length of regular waves is roughly equal to $5.12T_p^2$. For simplicity the dimensional constant 5.12 has been dropped. The initial presumption then is that a curve of significant wave height vs frequency corresponding to $H_{m0}/T_p^2 = 0.25$, which passes thru point (10), will identify values of significant wave height vs frequency corresponding to unusually steep seas for lesser values of significant wave height. Data points (1) thru (7) of Figure 8, which correspond to high values of this parameter from the storm data of Appendix A, suggest that the parameter H_{m0}/T_p^2 indeed identifies seaways of physically limited steepness. The upper boundary of the curve between 0.075 Hz ($T_p = 13.3$ seconds) and 0.04 Hz ($T_p = 25$ seconds) is based on the measured significant wave heights of points (8) and (9) rounded to wave heights of 50 and 45 feet respectively.

Figure 9 has been prepared in order to investigate the energy distribution characteristics of spectra associated with the boundary $H_{m0}/T_p^2 = 0.25$. In particular, spectra corresponding to data points (1), (2), (6) and (10) which fall on or near the boundary have been considered. Before comparing these spectra, the energy ordinates of each of the four spectra were normalized by dividing them by the square of the significant wave height of the associated spectrum. This was done in order to overcome the inherent disparity in height among the four dimensional spectra. It can be seen that the general shape and size of the spectra corresponding to points (2), (6) and (10) are quite similar. This not true of the one corresponding to point (1), however, and it is evident that wave energy present at lower frequencies results in a broader spectrum shape and a lower value of maximum energy density. In the process of identifying particular times during the chronological plots of significant wave height and modal period of Appendix A when significant wave height was low and the parameter H_{m0}/T_p^2 was high, it became evident that in the lower sea states associated with early storm development appreciable low frequency (swell wave) energy is generally present which results in few instances of low sea states with high values of H_{m0}/T_p^2 . (This difficulty should be overcome when climatic spectra information for the Gulf of Mexico are available). The spectrum of point (1) also illustrates that the parameter H_{m0}/T_p^2 is insufficient for identifying spectra which contain very steep waves such as those from hurricane Camille. If an additional criterion is imposed requiring that maximum energy density of the measured spectrum divided by H_{m0}^2 equal or exceed 1.5, then spectra of remarkably similar shape result. Overlaying of the spectra of points (2), (6), and (10) of Figure 9 reveals that the normalized spectrum shape presented in Figure 10 provides a good approximation for the significant wave height range from $H_{m0} = 44.3$ feet to 20 feet. This empirical results suggests that spectra associated with extremely steep waves can be defined knowing only the limiting combinations of significant wave height and modal period defined by the H_{m0}/T_p^2 boundary of Figure 8 and the normalized spectrum shape of Figure 10. These empirical findings answer a basic question for the designer, namely, if a TLP response parameter peak is known to exist at a particular frequency say 0.1 Hz ($T_p = 10$ seconds), then the highest significant wave height likely to be encountered is 25 feet (Figure 8) and the associated wave energy spectrum is given by Figure 10 when the ordinates are multiplied by 25 squared and T_p is set equal to 10 seconds.

Wave conditions associated with the $H_{m0}/T_p^2 = 0.25$ boundary are highly transient since they typically correspond to a steep, rapidly developing seaway. Figure 11 plots the hourly development of the winter storm which produced the highest significant

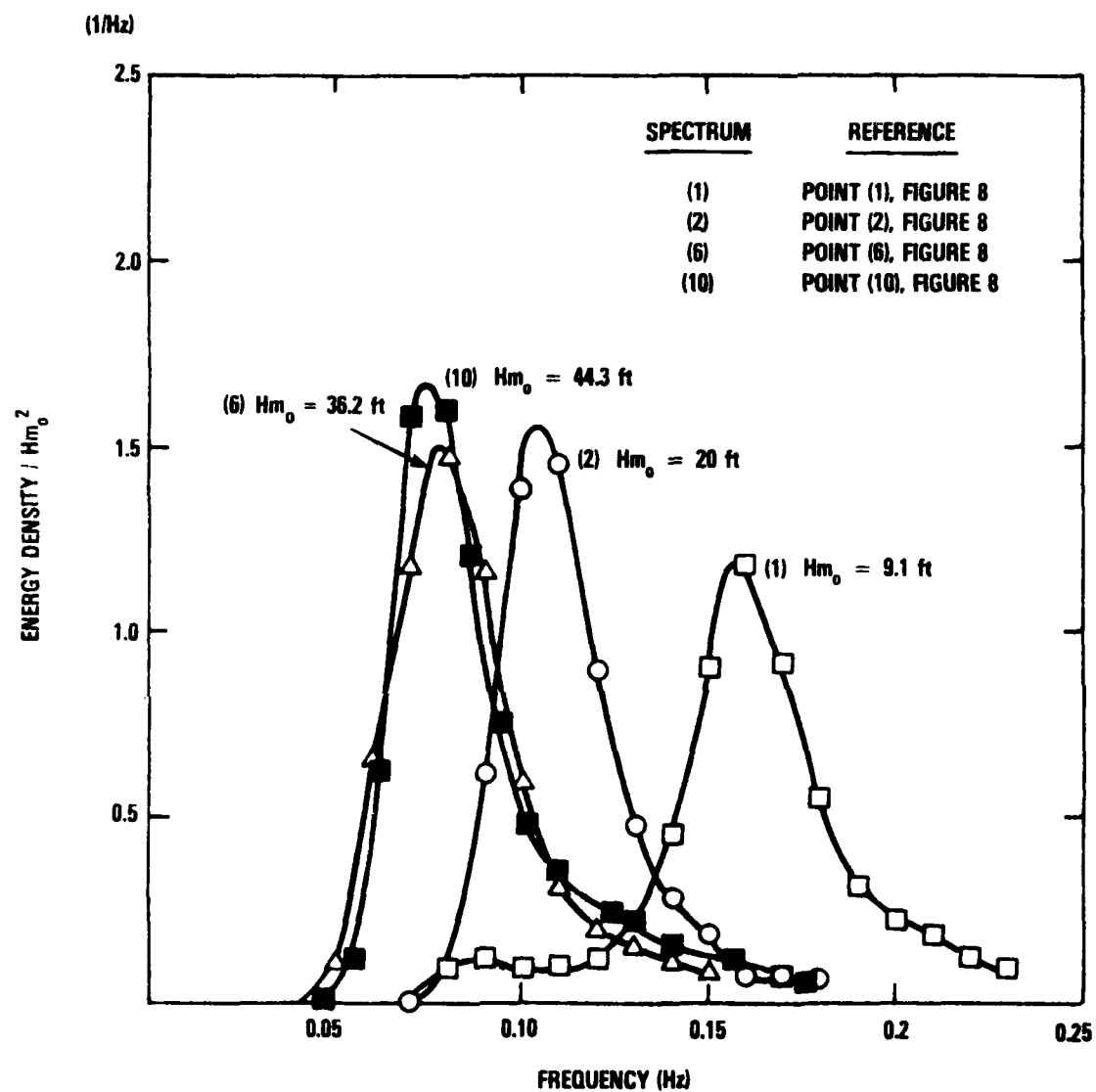


Figure 9 - Normalized Wave Height Spectra for Steep Wave Conditions
 $(H_{m_0}/T_p^2 = 0.25)$

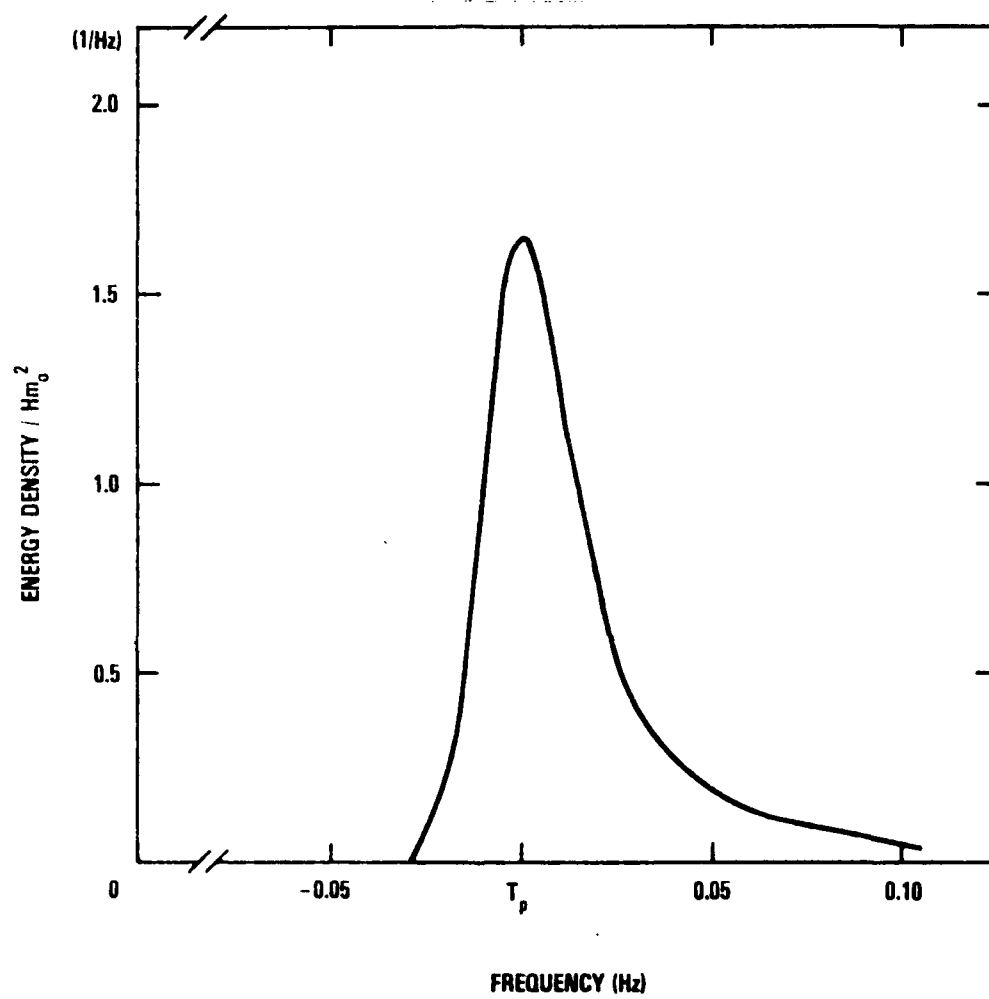


Figure 10 - Generalized Wave Height Spectrum for Wave Conditions of Extreme Steepness

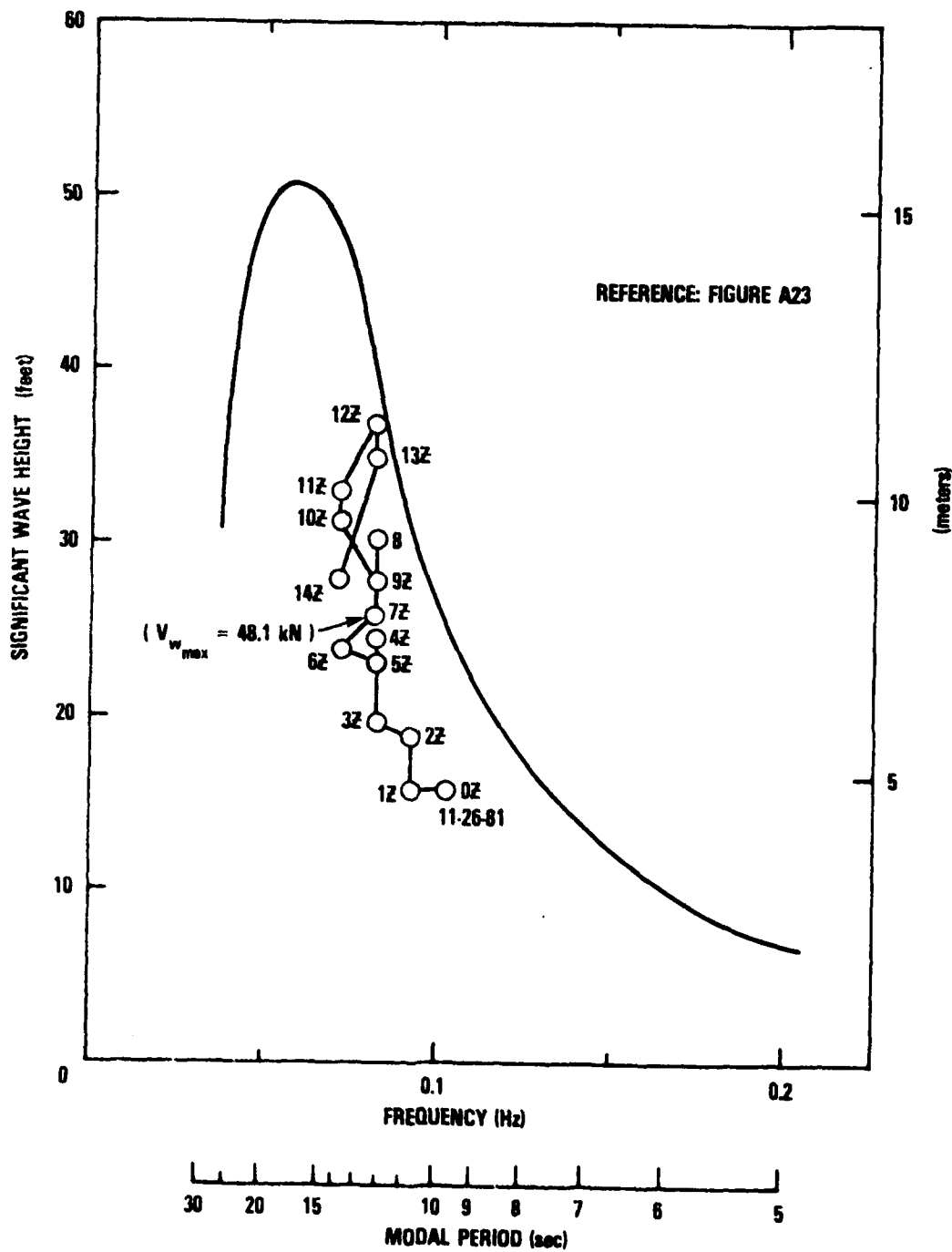


Figure 11 - Development of Winter Storm at Buoy Location 46005, 26 November 1981

wave height measured at buoy location 46005 (see Appendix A). At 0Z on the 26th a fairly substantial seaway existed ($H_{m0} = 15.6$ feet, $T_p = 10$ seconds). Subsequently the rising winds associated with the storm produced a maximum significant wave height of 36.2 feet at 12Z which approached the $H_{m0}/T_p^2 = 0.25$ boundary for a period of about 1 to 2 hours.

The storm of 7-8 February 1980 at buoy location 44004 (Appendix A) is of somewhat of greater interest since the significant wave height and modal period early in the storm development were much lower than at buoy location 46005 as shown in Figure 12. During the development of this storm the $H_{m0}/T_p^2 = 0.25$ boundary was followed rather closely from 0Z until about 9Z hours. It is also apparent that significant wave remained within an interval of $\pm 10\%$ of any measured value of H_{m0} for hardly more than one hour at a time.

Normalized spectra corresponding to points (8), (9) and (10) in Figure 8 are shown in Figure 13. Values of H_{m0}/T_p^2 are 0.25 for point (10), 0.147 for point (8) and 0.086 for point (9) which implies a relatively dramatic decrease in steepness for the larger waves in the seaway as modal periods increase from 13.3 to 18.2 and to 22.2 seconds. (If this did not occur and the $H_{m0}/T_p^2 = 0.25$ trend were to continue one would expect to find a significant wave height of 123 feet occurring at a modal period of 22.2 seconds!) The spectra of Figure 13 for points (8) and (9) are somewhat more sharply peaked than that for point (10) and reach values of peak energy density divided by H_{m0}^2 of slightly over 2.

2.2 Time Series Characteristics of the Larger Waves in Extreme Seaways

2.2.1 General

For purposes of identifying extreme events in time series wave height data the level crossing rate equations first developed by Rice are commonly employed, reference 4. If one assumes that the wave height variance spectrum is effectively narrow-band the simpler formulations of Longuet-Higgins can also be used, reference 5. In either case serious limitations apply. First, the wave height time series must be assumed to be Gaussian and second the statistic obtained from either formulation is one which relates only to wave height occurrences and therefore does not actually identify the time domain character of the events. Inasmuch as the loading effects of large waves on TLP's can easily involve highly non-linear effects, the lack of a time domain description is a serious deficiency for purposes of predicting peak loadings. Moreover, these methods identify only the expectation of the extreme event, i.e. the average of the maximum values to be expected in the associated stochastic process. As a result there is a 0.5% probability that events greater than the predicted value will occur.

With the advent of modern digital computers, a more rational approach is available through a Gaussian random process simulation. By tailoring the simulation to a specific wave height variance spectrum, a time domain realization of the frequency domain wave height process can be provided so that samples of critical wave events can be selected from the time series as needed for non-linear response analyses. Such an approach, however, raises the basic question of whether the wave height time series from which the variance spectrum was originally obtained was Gaussian or not. This question necessarily arises because in computing the Fourier transform of the time series, i.e. the variance spectrum, phase angle information is

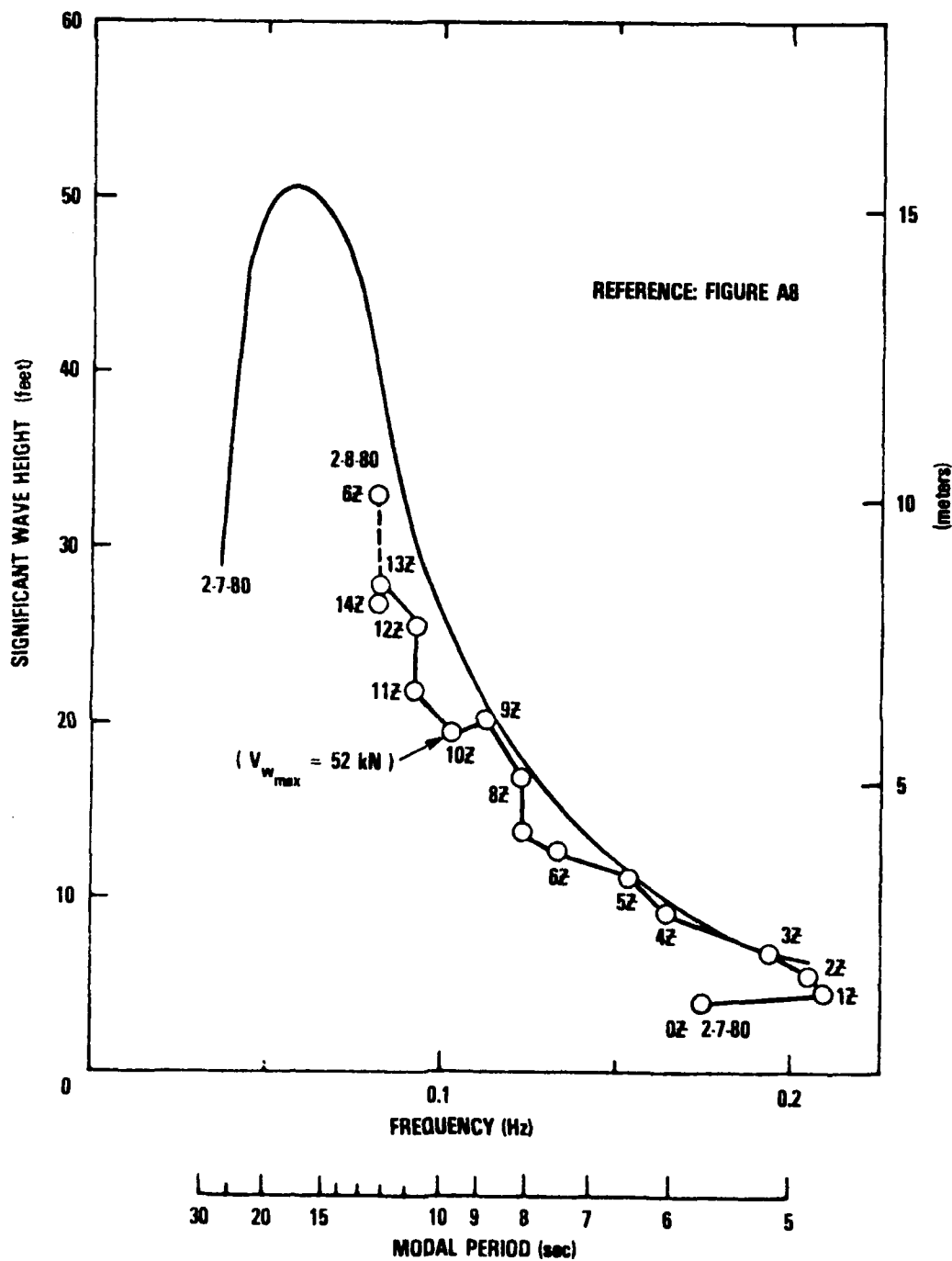


Figure 12 - Development of Winter Storm at Buoy Location 44004,
7-8 February 1980

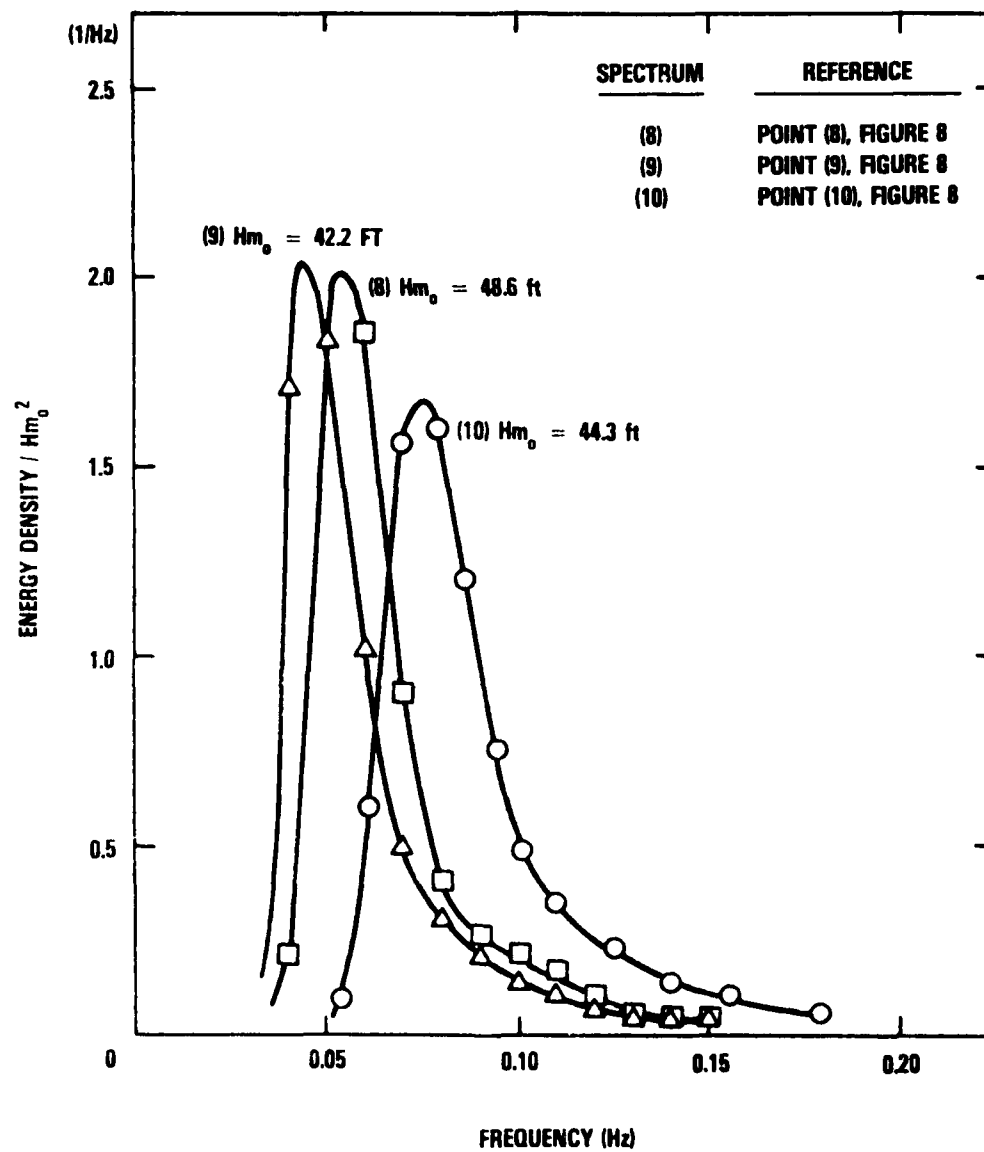


Figure 13 -- Normalized Wave Height Spectra for Maximum Significant Wave Height Conditions

generally not retained so that it is customary in transforming back to the time domain to assume that the probability density distribution of the phase angles of the frequency constituents is uniform between 0 and 2π which effectively results in a Gaussian realization, see reference 4. The recent development of the half-cycle counting method, which is described in reference 6, now provides a method for assessing the non-Gaussian character of the original time series. The following is a brief description of the method and the results of its application to time series wave data corresponding to point (10) of Figure 8.

2.2.2 The Half-Cycle Analysis Method and its Application to Hurricane Camille Time Series Wave Data

Figures 14 and 15 illustrate the basic procedure for half-cycle counting time series data and for entering individual counts into the associated data matrix, or HACYM. The signal is first level banded into uniform intervals on either side of the reference data level. Each data interval has been given a designator (+J through -J) for identification purposes. Whenever a data peak (maximum or minimum) occurs, it is identified with a particular data interval designator. In Figure 14, the half-cycle ① has a first peak of -B and a second peak of +E. As a result, it is entered into the HACYM data bin corresponding to first peak -B and second peak +E. (Note: In Figure 14 the half-cycle identifiers ① through ⑥ have been entered to illustrate the procedure. Normally the data bin would contain a number which corresponds to the number of times the data sample in question had half-cycle excursions corresponding to that particular data bin.) This procedure is repeated for other half-cycle excursions such as ② through ⑥ until all of the data have been processed.

The signal employed here illustrates certain basic features of the dispersion pattern of half-cycle counts within the HACYM. First, matching half-cycles will fall into data bins symmetrically disposed on either side of the null diagonal, i.e. about the diagonal formed by the darkened squares. Thus, if the HACYM were folded along the null diagonal, the data bins containing matching half-cycles would fall one on the other. Second, a half-cycle count located on the reference level diagonal, such as ⑤, has a mean value of zero. Third, the up-going half cycles ①, ③, and ⑤ all appear on the right hand side of the null diagonal, while the down-going half-cycles ②, ④, and ⑥ all appear to the left of the null diagonal.

Figure 15 illustrates the significance of the location of a half-cycle count within the HACYM. In this figure, the data excursion previously designated ① has been characterized in terms of its mean value and amplitude which in this case are 1-1/2 and 3 data intervals respectively. It will be seen in the HACYM of Figure 15 that the location of a half-cycle count with respect to the null diagonal is a direct measure of the amplitude of the half-cycle excursion while the location with respect to the reference level diagonal is a direct measure of its mean value. Half-cycle counts having positive means fall to the right of the reference level diagonal and vice versa.

Previous analyses of time series foil system strain data from the hydrofoil ship PCH-1 and time series wave height data from hurricane Camille found that very coherent distributions of half-cycle counts in the respective HACYM's result from this type of analysis, reference 3. This finding has recently prompted a re-analysis of the Camille wave data with the intent of determining the extent to which the half-cycle wave height events were Gaussian, reference 6. The procedure employed to d:

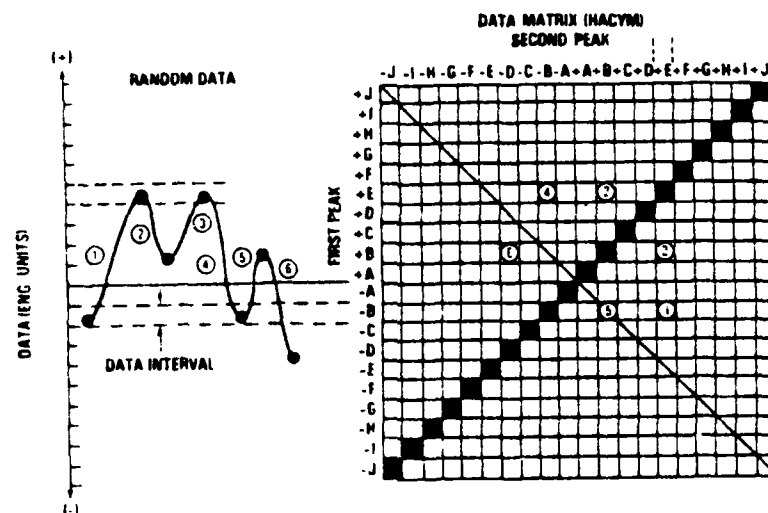


Figure 14 - Half-Cycle Counting of Random Data

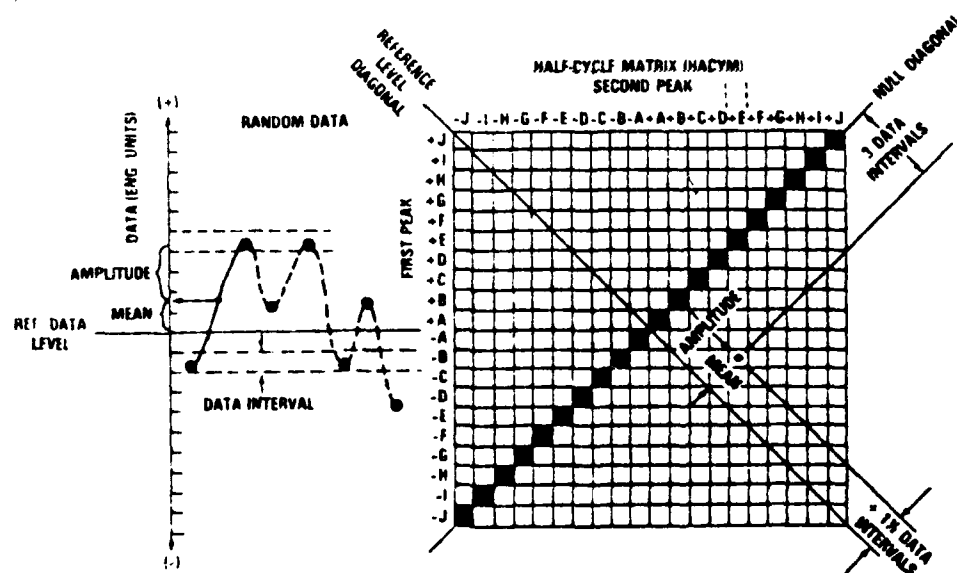


Figure 15 - Characterization of Half-Cycle Excursions Within the HACYM

this involved the generation of Gaussian time series realizations of the wave height process which conformed to the variance spectra for selected half hour data intervals. Both the Gaussian realization and the measured data were then compared in HACYM format to provide a detailed comparison of the respective time series wave events. The results of this investigation are basically as follows.

Three half-hour data intervals of particular interest were selected for analysis. The Gaussian realizations which were generated for the respective variance spectra were run for the equivalent of 10 hours of real time data each. The results were then analyzed in normalized half-cycle matrix format (± 6 standard deviations full scale). An estimate of the expectation of half-cycle events for each half-hour data interval was then obtained by dividing the respective data bin totals by a factor of 20 and rounding fractional numbers to the nearest interger. The results are given in Figure 16.

A chi-square goodness-of-fit test was then conducted comparing the measured and Gaussian half-cycle count distributions with all data bins having fewer than 5 events in the expectation distribution necessarily being excluded (see reference 7, pp. 119-122). The data were accepted as potentially Gaussian at a 5% significance level for each of the three spectra.

In addition, the distributions of actual and expected time intervals between successive peak-trough and trough-peak events were subject to chi-square goodness-of-fit tests, see Figure 17. Again the measured distributions were accepted as potentially Gaussian at a 5% significance level.

It was noted at the time the expectation of normalized half-cycle counts was determined, that a single empirical boundary contained virtually all of the events associated with the three spectra, see Figure 16. Utilizing this finding a comparison was made of events falling outside of the boundary for 13 half-hour intervals of measured data (1000 to approximately 1630 hours) and 13 of the 60 half-hour realizations (selected from every 5th realization). All events which fell outside of the empirical boundary for the Gaussian realizations are summarized in Figure 18 and those for the measured data in Figure 19. It is apparent that the measured data contain more events exceeding the expectation boundary and that the measured data are skewed with respect to the reference level diagonal (upper left to lower right) whereas the Gaussian data are much more symmetrically distributed.

The skewed distribution stems from the fact that the larger waves in the measured data were typically elevated, i.e. the mean of the data excursion from trough to crest or vice versa were well above mean water level, whereas this was generally not true of the Gaussian time series events.

Normalized half-cycle count distributions for the measured data corresponding to the three half-cycle count distributions originally selected for detailed study are shown in Figures 20(a), (b) and (c). During the 1000 to 1030 half-hour interval, the largest waves were noticeably elevated but their amplitudes were hardly more than those associated with the expectation. Between 1130 and 1200 hours an episodic wave was recorded (the four outlying half-cycle counts are inter-connected in the time series data). Otherwise only one other half-cycle event fell outside of the expectation boundary. Beginning at about 1430 hours the largest waves in the time series became distinctly elevated. The 1500-1530 half-hour data interval (Figure

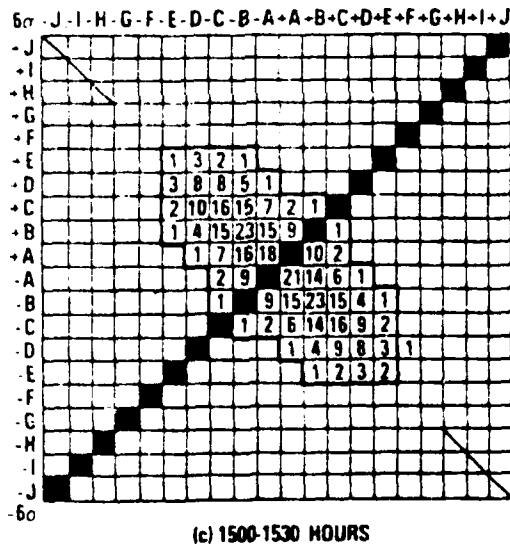
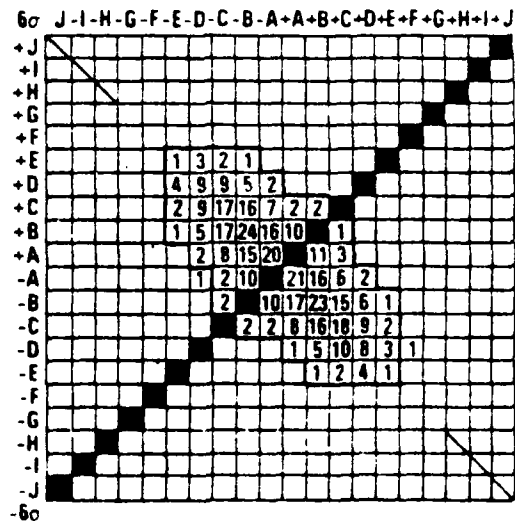
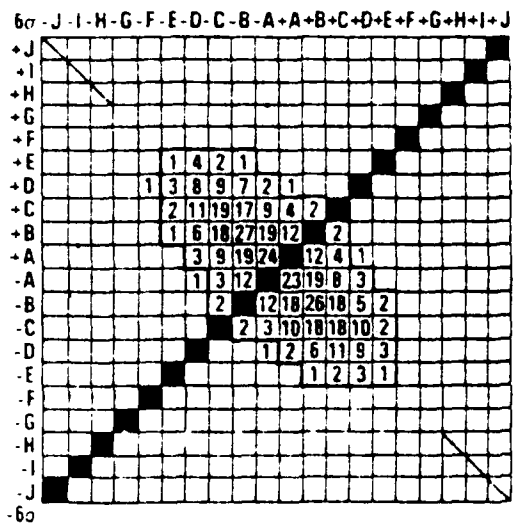


Figure 16 - Estimate of Expected Half-Cycle Events for Gaussian Realizations Conforming to Three Wave Spectra from Hurricane Camille

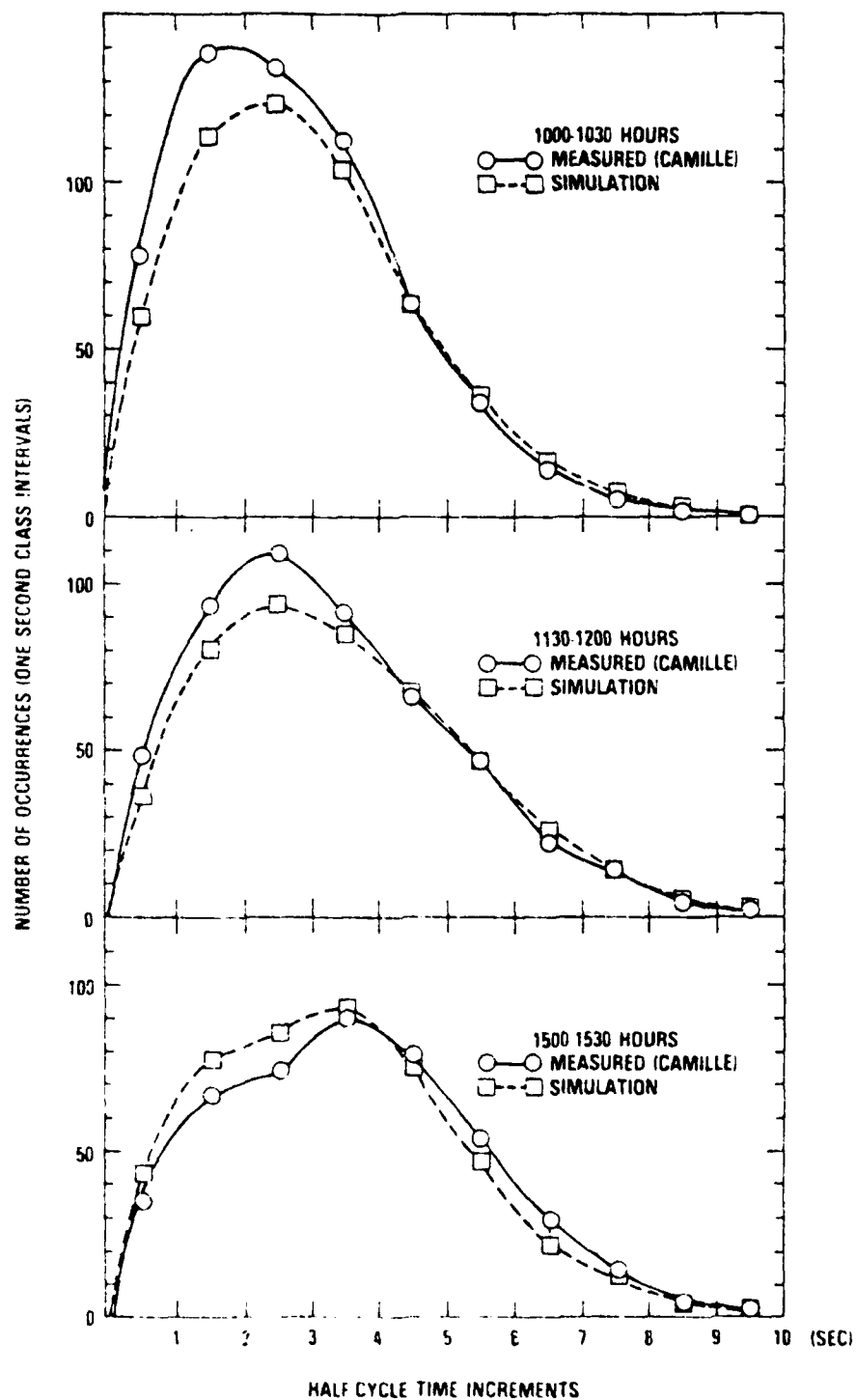


Figure 17 - Distribution of Occurrence of Half-Cycle Time Increments for Measured and Simulated Wave Data

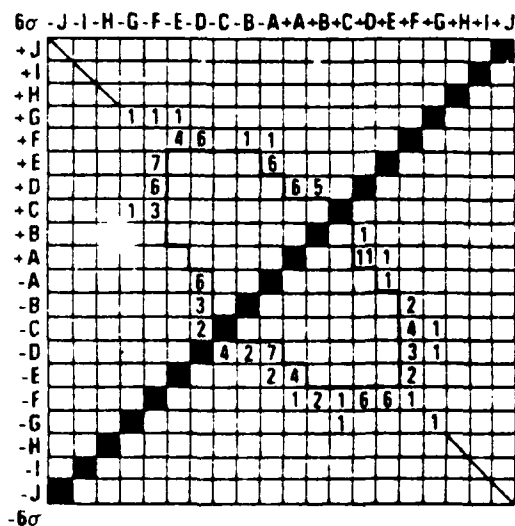


Figure 18 - Summary of Half-Cycle Wave Height Events from Thirteen Half-Hour Gaussian Realizations Which Exceeded the Gaussian Expectation Boundary

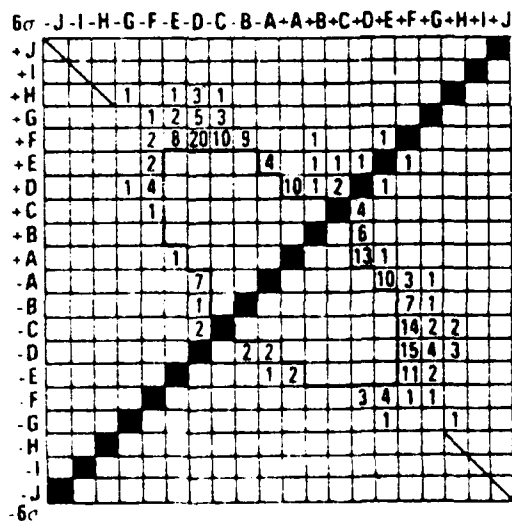
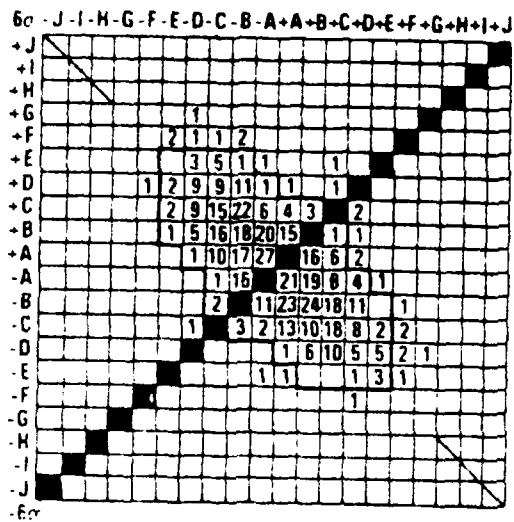
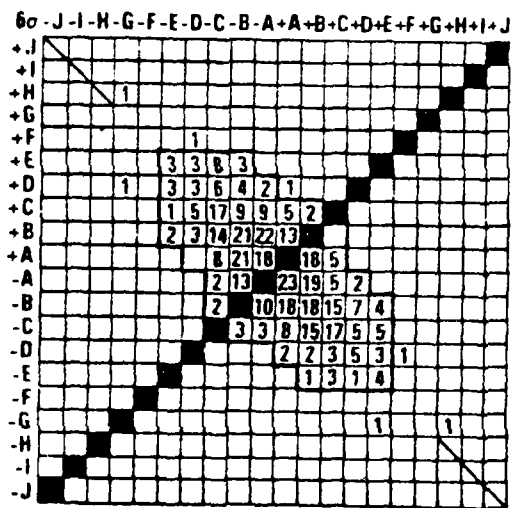


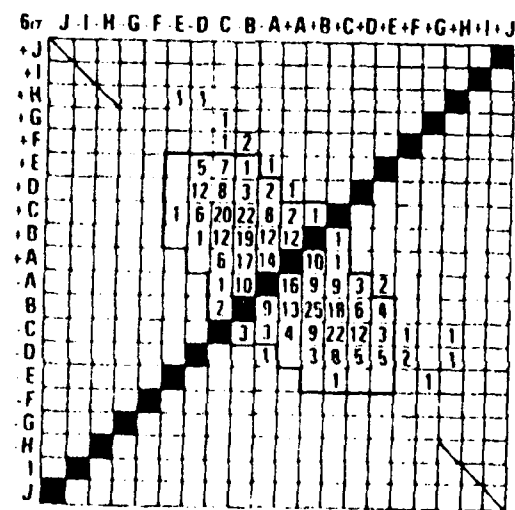
Figure 19 - Summary of Half-Cycle Wave Heights Events from Hurricane Camille (1000-1617 Hours) Which Exceeded the Gaussian Expectation Boundary



(a) 1000-1030 HOURS



(b) 1130-1200 HOURS



(c) 1500-1530 HOURS

Figure 20 - Half-Cycle Count Distributions of Measured Data for Three Half-Hours of Hurricane Camille Wave Data

20(c)) contains some of the largest and most elevated waves in the recorded portion of the storm.

Figure 21 presents time series data for the episodic wave occurring at 1155 hours and for three of the largest waves occurring after 1430 hours when such waves were characteristically steep and elevated. Despite the essentially uni-modal character of the associated wave variance spectra (see Figure 12 of reference 3), these large waves have "between crest" periods substantially less than modal period. Moreover if one assumes that wave lengths vary approximately as the square of the wave period, then the wave occurring at 1522 hours had a length between crests less than half that of waves corresponding to modal period; $(9/13.3)^2 = 0.46$. The waves of Figures 21(b), (c) and (d) lie far off the reference level diagonal in their respective half-cycle matrices, unlike the largest waves in the Gaussian realizations, and they have therefore been characterized as "non-Gaussian". The episodic wave of Figure 21(a) cannot be characterized as non-Gaussian by the same criterion. It is possible, however, that such a wave is the result of a coherent wave growth process rather a random mixing of wave energy constituents so it could be non-Gaussian in a physical as opposed to a mathematical sense.

2.2.3 Circumstantial Evidence Regarding the Existence and Characteristics of Large Non-Gaussian Waves

Buckley, Reference 8, recently completed a study in which ship casualty information was examined and ship master interviews conducted to determine whether evidence could be found that waves similar to those of Figure 21 existed in other than hurricane storm conditions. The results of the study were surprising in that they suggested (a) that the waves of Figure 21 might be unique in a physical sense as well as a mathematical sense and (b) that other classes of unique waves had been observed to occur in severe winter storms. Based upon the circumstantial evidence in hand, an initial characterization of large non-Gaussian and episodic waves was undertaken in reference 8 which is reproduced here in Table 3. The following is an initial assessment of whether or not such waves should be considered in TLP design.

(1) Steep, Elevated Waves

Waves of this type should be considered to exist in rapidly developing seaways which, in extreme cases, approach the $H_{m0}/T_p^2 = 0.25$ boundary of Figure 8, e.g. see Figures 11 and 12. The rationale for this recommendation lies in the presumption that the boundary reflects an attainable extreme for steep, wind driven seaways and the empirical finding that the data of Appendix A approach it but do not exceed it. In particular, since wave spectra meeting the additional criterion (Energy Density/ H_{m0}^2)_{max} > 1.5 have been measured in both a hurricane (Camille) and severe winter storms (Figure 9) it is believed that TLP's should be designed to withstand encounters with the wave conformations of Figure 21(b), (c), and (d).

The major unknown here is believed to be the upper limit of significant wave height on the $H_{m0}/T_p^2 = 0.25$ boundary which is apt to be associated with a particular off-shore location. For purposes of scaling these time series waves to lesser wave heights it is recommended that wave height be decreased in proportion to the ratio of the significant wave height of interest to that of point (10) in Figure 8 (44.3 feet) and that the time scale be shortened in proportion to the square root of this ratio so as to keep the height to length ratio of the waves approximately constant.

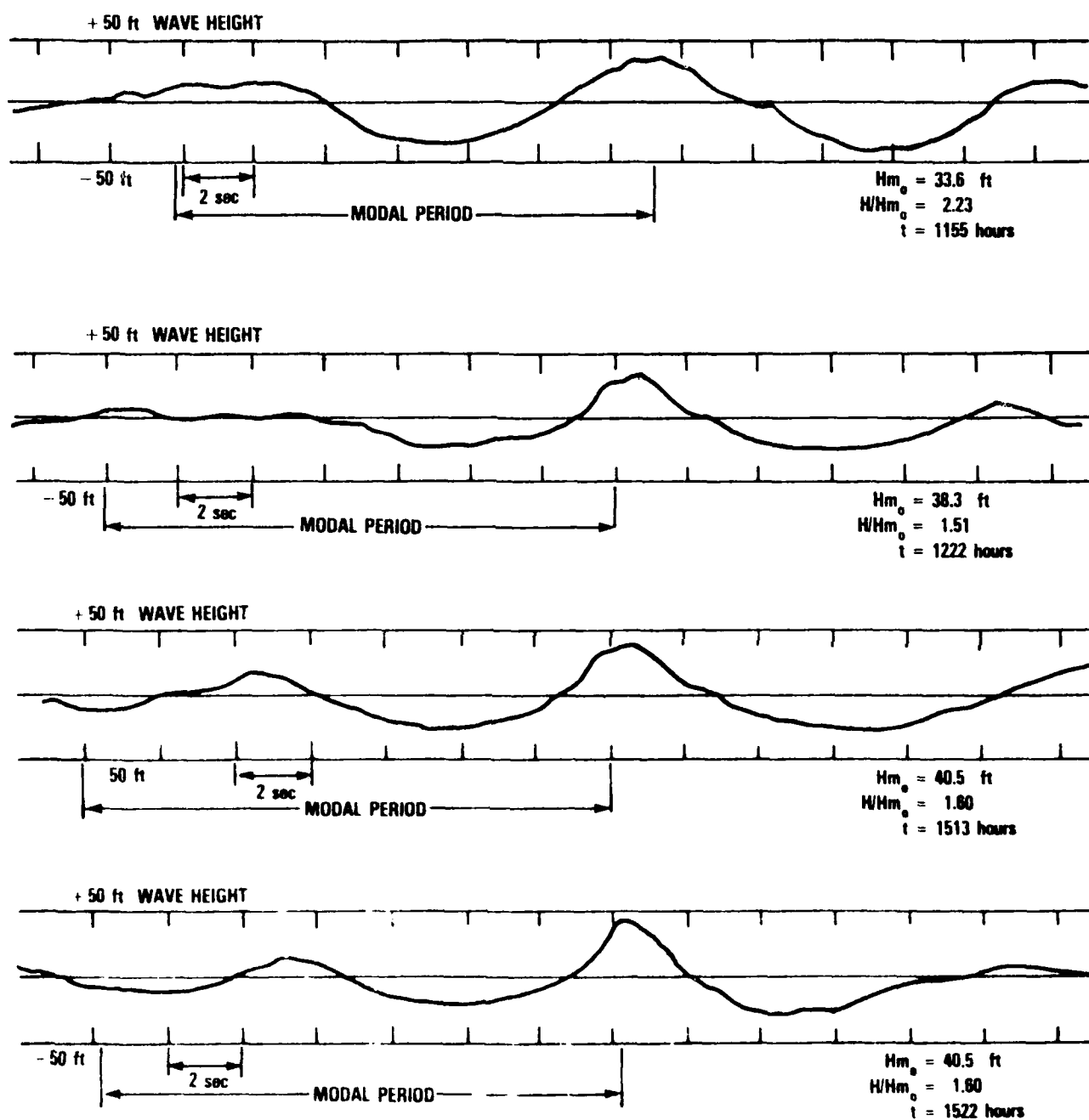


Figure 21 - Large Non-Gaussian Waves Measured During Hurricane Camille

TABLE 3 - AN INITIAL CHARACTERIZATION OF LARGE NON-GAUSSIAN AND EPISODIC WAVES

Type	Characterization	Basis for Characterization*
I. Steep, Elevated Waves	<ul style="list-style-type: none"> o Steep and elevated above mean water level o Period as low as 70% of modal period o Elevation/amplitude ratio ~ 0.5 o Produced by strong, rapidly increasing winds o Long-crested 	<ul style="list-style-type: none"> o Time-series wave data from Hurricane Camille (see Figure 21) o Casualty cases associated with strong rapidly increasing winds <ul style="list-style-type: none"> - SEA-LAND MARKET - LPD-12 - CHESTER A. POLING - F/V FAIR WIND o Observations by officers from ocean weather ships
II. Episodic Waves**		
a. Large Grouped Waves	<ul style="list-style-type: none"> o Group of three large waves in seaway. Second wave frequently largest in group. o Occur in storm winds which are no longer increasing, or which have begun to decrease. 	<ul style="list-style-type: none"> o Waves encountered by CV-62 SEA-LAND McLEAN, LST-1193 o (See A.4 of Appendix A)
b. Episodic Wave Packets	<ul style="list-style-type: none"> o "Three Sisters": group of three long period waves intruding into existing seaway at angles of about 30 degrees from principal wave direction. Generally occur in vicinity of storm with central winds of 60 knots or more. o "Rogue" Wave: large breaking wave intruding into existing seaway at angles up to 50 degrees from principal wave direction. Likely to occur in vicinity of upper altitude "TROF" as it overtakes an existing or developing low. High altitude comma shaped cloud usually associated with "TROF". 	<ul style="list-style-type: none"> o Observations by officers from ocean weather ships as well as ship masters of considerable at-sea experience. o (See Appendix B) o Rogue Wave encounters by U.S. NAVY FRIGATE, CHU FUJINO, MUNCHEN and associated synoptic weather patterns.

*See reference 8.

**These characterizations do not necessarily apply to waves in the Agulhas current (S.E. Coast of Africa).

(2) Episodic Waves

There are no time series data available which are known to correspond specifically to any of the episodic wave types listed in Table 3. The best that can be offered is a somewhat speculative suggestion for modelling the large Grouped Waves of the table using the time series wave data of Figure 21(a). For the time being, it is suggested that for maximum significant wave height conditions (i.e. in the vicinity of point (8) of Figure 8) the time series of Figure 21(a) be proportioned to correspond to a maximum peak to trough wave height of 2.0 times significant wave height and an average time between wave crests equal to approximately 90% of modal period. In the case of point (8), for example, this would result in a wave height of $48.6 \times 2 = 97.2$ feet and an average time interval between wave crests of $0.9 \times 18.2 = 16.4$ seconds. The rationale for this recommendation is that the waves in question are believed at this time to be only mildly episodic so that a ratio of maximum wave height to significant wave height of about 2 to 1 is not unreasonable. A detailed review of the time series wave data of hurricane Camille has indicated that the "between wave crest" periods of the largest waves in the time series is invariably less than modal period. Since the wave energy spectrum of Figure 7 which corresponds to point (8) is quite narrow band, a ratio of wave period to modal period of 0.9 has been suggested with the Camille data in mind.

The time series character of the "three sisters" is unknown at this time and no substantive guidance can be offered. The period and phase speed of these waves have been reported to be noticeably greater than the other large waves in the local seaway and it is known that ship masters are likely to be concerned about them primarily because they can appear at appreciable angles in the local seaway and thus produce severe ship roll angles. An additional characterization of these waves which was found after reference 8 was written is presented here in Appendix B for information.

The "rogue" waves of Table 3 also have not been identified as to their time series wave height characteristics. Because they have been observed at times to be (a) episodic with respect to height and (b) steep and breaking, they are a wave type of potential concern in TLP design. Because they are rarely observed events, descriptive information is scarce and time series wave height measurements are not known to be available.

With regard to the possibility of obtaining time series data in the future, the situation is not entirely hopeless. The findings of reference 8, section 6.1.2, suggest that time series wave height measurements during winter months at NOAA buoy locations 46003, 46001, 46002, and 46005 could produce the desired time series data (see Figure 24 of the reference). Moreover should the speculative assessments of section 6.1.2.1 of the reference regarding imperfect envelope solitons as the origin of "rogue" waves prove correct, then test tank wave making experiments would permit the creation of rogue waves under controlled conditions and hence provide time series wave height measurements during the evolution and unstable collapse of the waves. In the meanwhile, it is regretted that no substantive guidance can be offered regarding design for such waves.

3.0 RESPONSE CHARACTERISTICS OF TENSION LEG PLATFORMS

3.1 General

The purpose of this section is to review available TLP motion and load response information together with the extreme wave information of section 2.0, in order to help identify wave and wind environmental conditions of special interest. This review is not undertaken for particular sites although broad coastal areas of the continental U.S. are considered. The majority of information regarding TLP response is taken from reference 9 since it contains the most comprehensive assessment of TLP response characteristics found to date.

3.2 Hutton TLP Response Characteristics

3.2.1 Basic Tethered Responses

Periods of the basic tethered response modes for the Hutton TLP are given in Table 4 together with values for two other platform designs which are intended to operate in deeper water. It is evident from the boundary of maximum measured significant wave heights vs modal period of Figure 8, that little or no wave energy is likely to be encountered at these motion periods. This is not true, however, of hurricane wind energy near frequencies associated with surge, sway, and yaw modes, see Figure 22. The time series wind velocity data of Figure 23 likewise suggest the presence of low frequency velocity fluctuations of relatively large magnitude. The wind velocity data in each of these figures are taken from the half-hour interval immediately preceding that of point (10) of Figure 8. Reference 9 calls attention to the possibility of subharmonic excitation of the Hutton platform's low frequency response modes by wave energy in the 20-30 second period range. It is evident from the wave data of Figures A15, A16 and A31, that wave energy corresponding to these periods can be encountered off the U.S. west coast. Reference 9 also states, however, that no instabilities were observed in the comprehensive (model) tests carried out on the final Hutton TLP design. Since the reference also states that wind loads during tank tests were simulated by applying a steady horizontal force to the center of the model it is presumed here that the effects of low frequency wind velocity fluctuations were not simulated when the tests were conducted. Reference 12, which discusses the analysis of full-scale motion measurements of a deep water, articulated loading platform with basic response periods of 40, 1, and 2 seconds, concludes that "Non-linear interaction between low-frequency motions caused by wind and wave forces is indicated". In view of this finding, it is suggested that frequency domain wind and wave data for at least extreme environmental conditions are needed in order to determine whether the combined effects of wind and waves can result in significant loadings on the tethering system of a TLP.

3.2.2 Results of Model Tests in Waves

Reference 9 identifies certain general characteristics of the waves which resulted in maximum platform responses during model tests. These findings are summarized here with respect to those wave characteristics which were found to be important.

TABLE 4 - RESPONSE PERIODS FOR TENSION LEG PLATFORMS

Mode	Response Period (sec)		
	Hutton TLP*	Model**	Model***
Heave	2	2	2
Pitch & Roll	2	2.1	2.2
Surge & Sway	50-60	106	92.5
Yaw	42-48	86	70.5
Full Scale Water Depth	1478 m (485 ft)	450 m (1476 ft)	500 m (1641 ft)

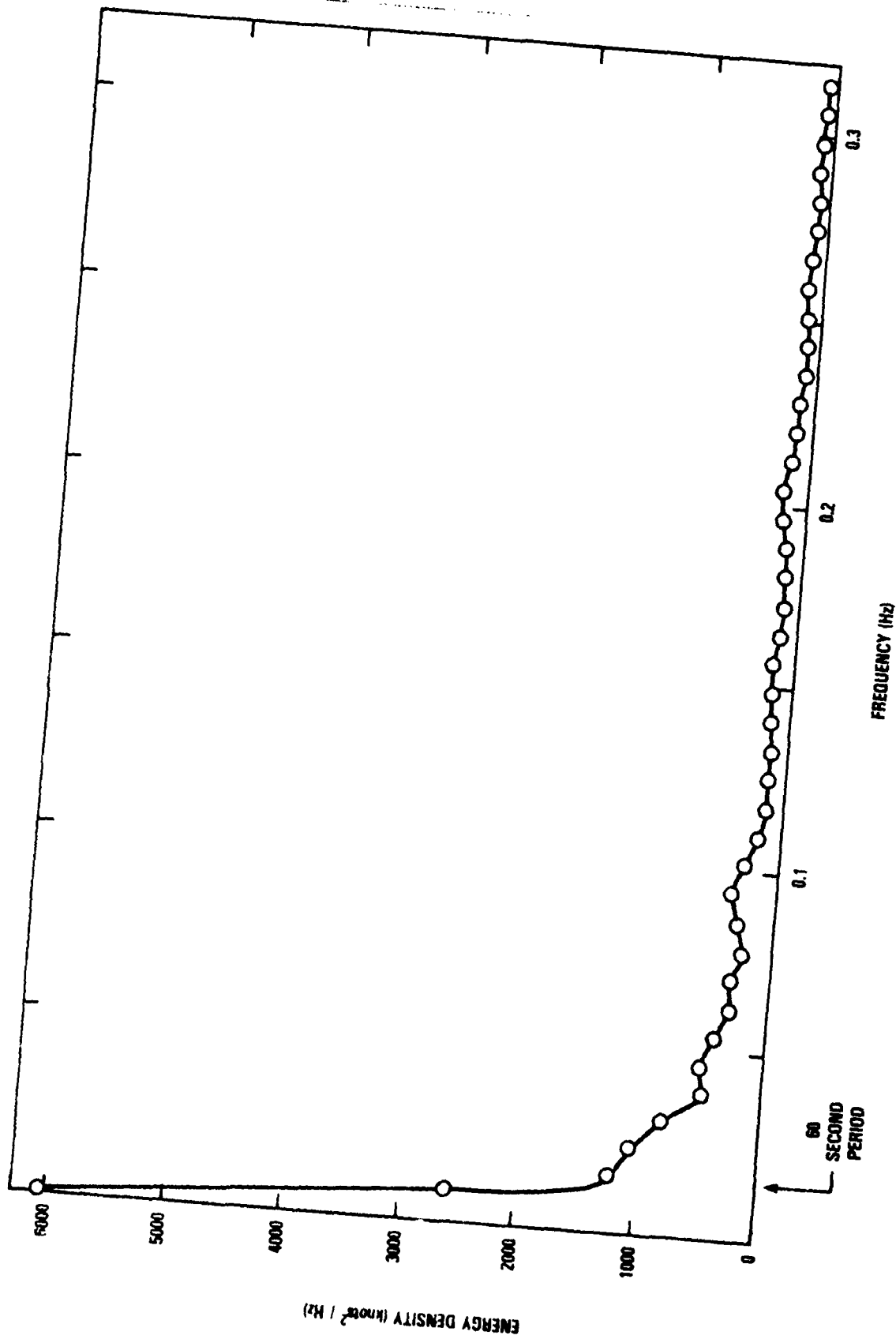


Figure 22 - Wind Velocity Spectrum Measured During Hurricane Camille (1500-1530 Hours)

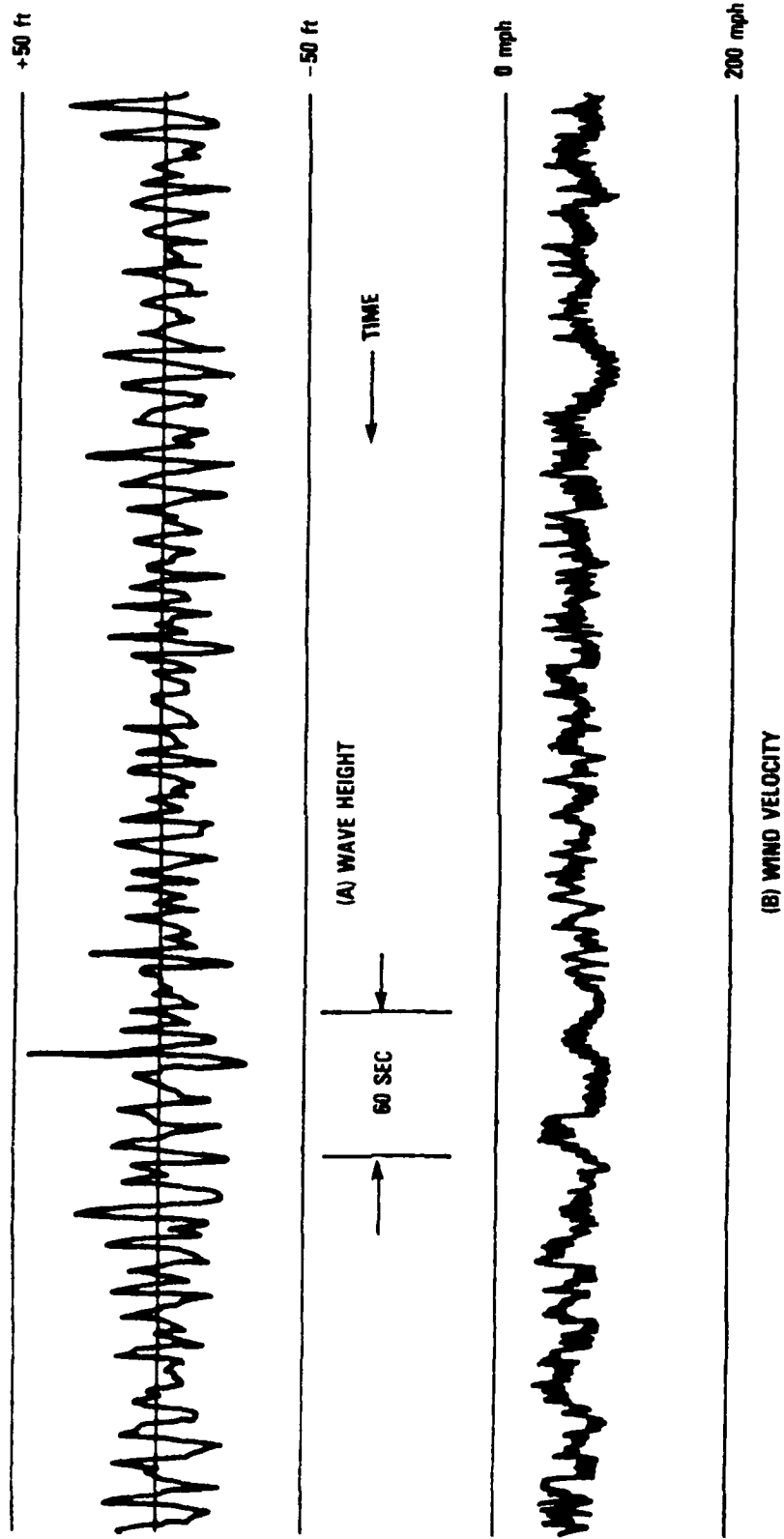


Figure 23 - Time Series Wind Velocity and Wave Height Data Measured
During Hurricane Camille at 1522 Hours

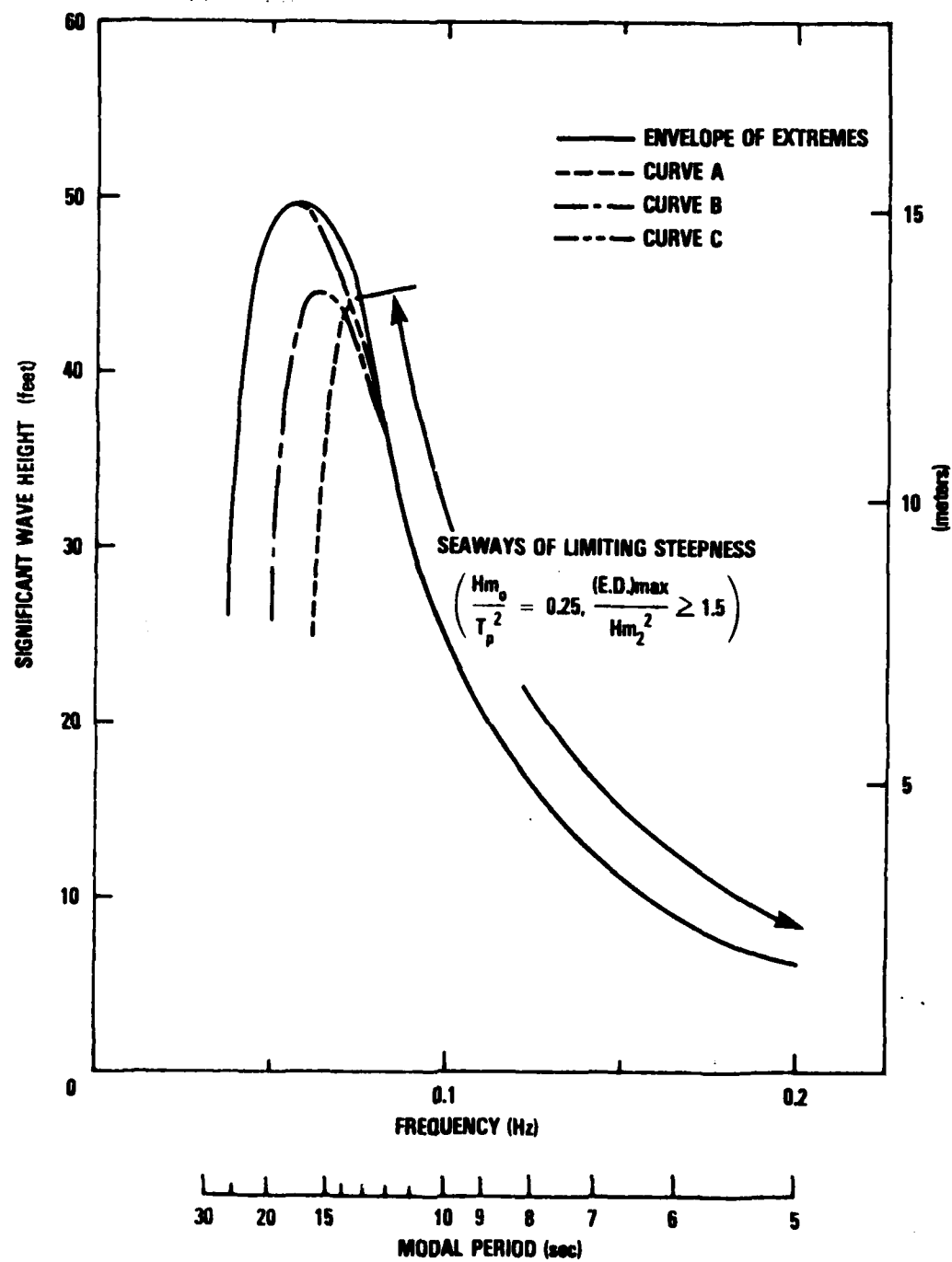


Figure 24 - Significant Wave Height vs Frequency Corresponding to Modal Period for Particular Geographic Locations

(a) Tendon loads

The reference finds that "the short period extreme design wave proves to have the greatest effect on minimum tension leg loads and required pretension". It also noted that pitch moment loads were maximum for wave periods of about 10-11 seconds and that heave forces were maximum at a wave period at or above 25 seconds. Differential buoyancy loads on the legs might well peak at a wave length twice the platform leg spacing of about 250 feet. The associated wave period would be roughly $T = \sqrt{500/5.12} = 10$ seconds which is in general agreement with the measured maximum pitch restraint loads. By the same line of reasoning, heave forces should be maximum for very long wave lengths which is also in general agreement with the experimental result.

With respect to linear, frequency domain analyses of platform pitch moment response, the limiting (deep water) significant wave heights of Figure 8 (e.g. $H_{m0} \text{ max} = 30$ feet at $T_p = 11$ seconds) together with the normalized wave energy spectrum of Figure 10 identify a potentially critical wave energy case. Similarly the maximum significant wave heights of Figure 8 for deep water wave periods greater than 19 seconds are of interests with respect to maximum heave response loads. In either case it is important to note that an investigation of maximum wave induced tendon loads also be undertaken for the steep, time domain waves discussed in section 2.2. Moreover, it should be recognized that the steep, elevated wave of Figure 21(d), which has a peak to peak period of about 9 seconds, was measured in a seaway which had a modal period of 13.3 seconds, see point (10) of Figure 8. The significant wave height of the seaway associated with this particular wave is 44.3 feet as opposed to the 30 feet significant wave height associated with the wave energy spectrum having maximum energy at a modal period of 11 seconds. The steepest wave associated with a wave spectrum having an energy peak at 11 seconds would not be as large as the most critical time domain wave conformation which might be encountered. Reference 9 also calls attention to tendon responses that "were measured in some tests, especially in high, steep waves, which are resonant vertical vibrations of the TLP platform". While the origin of the excitation was not determined it is apparent that the steep, elevated waves of Figures 21(b), (c) and (d) are also likely to be of importance with respect to this particular form of tendon dynamic response.

(b) Surge and Yaw motions

Wave conformations which resulted in maximum surge and yaw motions were not identified presumably because basic platform response periods were well beyond those of waves having realistic maximum wave periods, as well as because no sub-harmonic resonances were observed during the model tests. As noted in 3.2.1 above, inclusion of the combined effects of low frequency wind and wave excitation forces might have produced more definitive results.

(c) Wave Impingement on Deck Bottom Structure

The reference calls attention to the fact that "some tests revealed the occurrence of wave profile modifications due to the presence and motions of the TLP. These modifications included wave run-up around the columns, particularly the down-weather columns, and some local up-welling under the middle of the deck. These effects were most important for high waves with shorter periods." It appears that here again the steep, elevated waves of Figure 21(b), (c) and (d) are of importance.

3.3 Potentially Critical Wave and Wind Conditions

3.3.1 Service Load Environments

Environmental loadings of primary importance with respect to fatigue and crack growth investigations vary considerably with geographic location. The climatic wave data of Table 1, for example, show that significant wave heights greater than 5 meters (16.4 feet) are more than 10 times as likely to occur at deep water locations from Cape Hatteras north and from Cape Mendocino north than in the Gulf of Mexico and Georgia Embayment areas. It is fortunate that the wave spectra information most needed for service load assessments have been archived by NOAA and can be retrieved so as to define average and extreme wave energy distributions for each of the significant wave height class intervals of Table 1. Concurrent 8.5 minutes averaged wind velocity data can also be provided for each wave height class interval.

It is also evident from Table 1 that the occurrence levels of significant wave heights greater than 5 meters for continental shelf locations in the Baltimore Canyon and Georgia embayment areas are relatively low. A marked increase occurs, however, near the outer edge of Georges Bank where the continental shelf extends further to the east. Along the West Coast no similar generalizations can be offered due to the lack of continental shelf wave data in the climatic summary of reference 1 and hence in Table 1. Data have been gathered at certain locations on the continental shelf for periods less than 3 years, however, as indicated in Figure 2 and are presumably available for analysis.

The tendency of the Hutton TLP, for example, to experience increased pitch moment loads in waves of about 10-11 seconds period is of some importance as a case in point. Once climatic wave spectra data are available estimates of tendon service loads which recognize this tendency can be provided for a particular buoy location. Such loads then provide conservative estimates (generally) for adjacent continental shelf locations, or alternatively as a reference point for estimating service loads at a location of interest.

3.3.2 Extreme Load Environments

It is presumed in the comments which follow that the analysis of TLP response to service load environments will be accomplished in the frequency domain and that, given the required analytical capability, initial estimates of extreme loads will be made using frequency domain representations of extreme seas for a specific geographic location. It is further presumed, in view of the limitations of frequency domain modelling in identifying critical time domain waves (see section 2.2) and in predicting non-linear platform responses to such waves, that time-domain analyses based upon deterministic extreme wave conformations will also be required.

(a) Frequency domain representations of extreme seas.

Figure 8 provides an envelope of extreme measured significant wave heights vs corresponding modal frequencies. Figure 10 provides a normalized wave energy spectrum which is intended to apply to transient seaways of extreme steepness. For more fully developed seaways of extreme significant wave height, the normalized wave energy spectra of Figure 13 are recommended for guidance in selecting specific shapes.

Use of the envelope of extremes in Figure 8 may be inappropriate (i.e., excessively conservative) for a particular geographic location. From a qualitative point of view, Figure 24 suggests the type of envelope of extremes which might apply to the Gulf of Mexico (Curve A), deep water locations off the East Coast from Cape Hatteras northward (Curve B), and deep water locations off the West Coast north of Cape Mendocino (Curve C). It is recommended that the envelope of extremes for a given geographic location be established after climatic wave spectra have been obtained for the closest NOAA data buoy locations since this information will be helpful in establishing the left hand side of the envelope curve. For purposes of defining the peak of the curve, it is recommended that consideration be given to the maximum wave height precedents of Table 5 which is taken from reference 13. The data can be utilized if one assumes that significant wave height in this region of the curve is approximately one half of the extreme wave height cited, (see section 2.2.3 (2)). (This is not an assertion that the maximum height criteria of Table 5 are necessarily correct but that prior efforts to define extreme wave heights at specific locations should certainly be considered).

(b) Time domain waves associated with extreme seas

The studies summarized in section 2.2 are believed to confirm that extreme seas can contain large non-Gaussian waves, i.e. waves which would not be predicted by transforming a wave height variance spectrum back into the time domain assuming that the associated random process is Gaussian. While a method now exists for analyzing time series wave height data for purposes of identifying large non-Gaussian waves, data from only one storm (hurricane Camille) have been analyzed to date.* Considering the tendency for large, steep waves to result in certain critical TLP responses, as discussed in section 3.2.2, the availability of the Camille data is fortuitous. An approximate means of transforming the steep, elevated waves measured in Camille to correspond to lower significant wave heights along the $H_{m0}/T_p^2 = 0.25$ boundary of Figure 24, are given in section 2.2.2. A somewhat more approximate means is also suggested for estimating the time domain character of the large, grouped waves found in the more nearly fully-developed seas likely to be associated with the peaks of the envelope curves B and C of Figure 24.

Regretably no time domain approximations for the episodic wave packets of Table 3 can be provided at this time as discussed in section 2.2.2.

(c) Winds associated with extreme seas

Wind data corresponding to time average values (such as the 8.5 minute average associated with the NOAA data buoys) have two important limitations when very gusty winds are involved. First, the wind induced drag load acting on a TLP will be roughly proportional to the square of the time series wind velocity. Since the mean square velocity of a gusty wind can be substantially greater than the square of the mean velocity (50% in the case of Camille from 1500 to 1530 hours), the 8.5 minute wind velocity can lead to a low estimate of the drag load acting

*Reference 14 indicates that Spidsøe and Hilmarsen are also aware that non-Gaussian waves can exist in storm driven seaways. They do not provide time domain characterizations of such waves in their paper, however, so their results can not be incorporated into this study.

TABLE 5 - WAVE PARAMETERS FOR 10 AREAS IN UNITED STATES WATERS OF
91.4 m (300 ft) DEPTH OR GREATER*

Area	Reference Level Wave Height		Wave Steepness	Reference Level Deck Clearance**	
	m	ft		m	ft
Offshore Gulf of Mexico	21.3	70	1/12	14.6	48
Offshore Alaska					
1. Lower Cook Inlet	18.3	60	1/13	17.1	56
2. Icy Bay-Gulf of Alaska	30.5	100	1/15	24.4	80
3. Kodiak Shelf-Gulf of Alaska	27.4	90	1/15	21.9	72
4. Bering Sea/Bristol Bay	25.9	85	1/13	19.2	63
Offshore California					
1. Santa Barbara Channel	13.7	45	1/16	11.6	38
2. Outer Banks	18.3	60	1/15	13.4	44
Offshore Atlantic Coast					
1. Georges Bank	25.9	85	1/12	18.0	59
2. Baltimore Canyon	27.4	90	1/12	18.9	62
3. Georgia Embayment	22.9	75	1/12	16.2	53
*From TABLE A-1 of Reference 13.					
**Above mean low-water (MLW) in Atlantic and Gulf of Mexico; above mean low low-water (MLLW) in Pacific and Gulf of Alaska.					

on the platform. Secondly, the average wind velocity is of little value when platform dynamics are of interest. In this case the energy spectrum of the velocity time series is required.

Time series wind velocity measurements obtained during hurricane Camille are especially valuable since they apply directly to point (10) of Figure 8 and since the mean square wind velocity and energy spectrum can be determined* (see Figure 22 for example). Half-cycle counting of the wind velocity by half-hour intervals has permitted determination of the ratio of peak gust velocity to the half-hour average wind velocity by half-hour intervals during the height of the storm. These data are summarized in Table 6. It can be seen that instantaneous velocities up to 1.9 times the half-hour averaged wind velocity were recorded which reflects the gusty nature of the wind also evident in the time series data of Figure 23.

With respect to hurricane seaways, maximum wind velocity and maximum significant wave height are likely to be coincident, as least for the critical sector of the storm. This is not necessarily the case for winter storms as can be seen in the data of Figures 11 and 12. Chronological plots of this type for other severe winter storms can provide guidance in this regard but only with respect to the 8.5 minute averaged wind velocity. Time series wind velocity data from other sources are required to obtain the desired energy spectrum of wind velocity and mean square wind velocity for uniform time intervals (preferably 8.5 minutes because of the NOAA data base). In the meanwhile the energy spectrum and the ratio or mean square wind velocity to the square of the mean velocity from adjusted Camille data should furnish conservative guidance in estimating corresponding winter storm wind characteristics because of the pronounced gustiness of the wind during this storm.

4.0 RECOMMENDATIONS FOR THE ESTABLISHMENT OF WAVE AND WIND CRITERIA

Recent advances in wave and wind data acquisition and analysis which are summarized in section 2.0 permit the establishment of wave and wind environmental criteria which are more responsive to the needs of TLP designers than criteria established in the past for fixed offshore platforms (such as Table 5). In particular, the establishment of realistic climatic and extreme wave height spectra now appears possible. The present report carries this initiative only to the level of extreme spectra considering data from eighteen NOAA data buoy locations. As mentioned previously this initiative can and should be pursued to the level of extreme and climatic wave spectra at particular data buoy locations using data presently archived by NOAA.

A somewhat limited excursion has also been taken into the realm of deterministic, time domain extreme deep water wave descriptions. It has been encouraged by the results of the application of the half-cycle method of analyzing time series data to hurricane Camille wave data as well as by the results of a recent investigation of

*The anemometer location on the platform was such as to result in somewhat lower velocity measurements than would have been obtained in the free stream at the same height above the water. A velocity correction factor must be applied to these data.

TABLE 6 - HURRICANE CAMILLE WIND DATA: RATIO OF PEAK GUST
TO AVERAGE WIND VELOCITY

Time Interval (hours)	Averaged Wind Speed (knots)	Peak Gust (knots)	Peak Gust Ratio
1000-1030	31.8	52.5	1.65
1030-1100	27.2	52.5	1.93
1100-1130	29.1	52.5	1.80
1130-1200	34.0	57.5	1.69
1200-1230	34.4	62.4	1.81
1230-1300	32.4	57.5	1.77
1300-1330	41.6	72.5	1.74
1330-1400	33.2	57.5	1.73
1400-1430	41.0	77.5	1.89
1430-1500	52.0	87.5	1.68
1500-1530	50.5	87.5	1.73
1530-1600	59.0	92.5	1.57
1600-1617	58.4	92.5	1.58
			Avg. = 1.74

damaging waves which has revealed that certain distinctive types of extreme waves have been observed in winter storms. Wind data, it has been found, are seldom reported in a format which is useful to designers of compliant deep water platforms. The recommended actions of sections 4.2 to 4.6 are intended to lead to the establishment of wave and wind criteria which are realistic in an environmental sense and important considering the unique response characteristics of tension leg platforms.

4.1 Assumptions Regarding the Specification of Extreme Wave Conditions

The approach taken in section 2.1.5 to defining wave energy spectra for extreme seaways as well as the approach taken in section 2.2.3 (1) to identifying the time series character of the largest waves in a seaway of limiting steepness have the following inherent assumptions associated with them. These are reviewed here before proceeding to the subject of wave and wind criteria for use in TLP design because of their basic importance.

(a) Envelope of extreme values of significant wave height vs modal period (or frequency).

This envelope is regarded as a fundamental statement of the extreme wave environments associated with either a general ocean area or a specific location within an ocean area. Justification for its use derives in part from the availability of wave height variance spectra for extreme sea conditions from archived NOAA data. The utility of the envelope depends to a considerable degree upon the uniqueness of the distribution of wave energy vs frequency for any particular segment of the boundary as well as upon the uniqueness of the time series character of the largest waves associated with the same segment. The presumption that such uniqueness exists arises from the implicit assumption that the synoptic wind field and seaway conditions associated with any segment of the envelope of extreme values are themselves unique. The uniqueness of synoptic wind fields associated with the occurrence of maximum significant wave height and modal period is discussed in Appendix C.

(b) Characteristic distributions of wave energy vs frequency

It is presumed that characteristic distributions of wave energy can be determined empirically from measurements in a variety of extreme wave conditions. For U.S. off-shore locations the majority of such data is expected to be provided by NOAA data buoys. The normalized spectra of Figures 9, 10 and 13 represent an initial effort to identify characteristic distributions associated with the envelope of extreme values of significant wave height and modal period shown in Figure 8. (With the exception of the spectra associated with seaways of limiting steepness, no attempt has been made to generalize spectral shapes. There are a number of closed form spectral formulations in the literature from which a "best fit" for the spectra of Figure 13 can be sought to suit individual preferences. For purposes of identifying individual spectra approaching the empirical boundary of Figure 8, the chronological plots of individual storm development such as shown in Figures 11 and 12 are considered to be especially useful).

(c) Characteristic shapes of time series waves

The generally unsubstantiated nature of the assumption that extreme events in the wave height time series can be uniquely characterized is a consequence of

the limited amount of pertinent data now available. (One example of the uniqueness of the time-series character of the largest waves in a seaway of limiting steepness is given in Appendix D.) Only in the case of the steep, elevated waves of Table 3 is a time series characterization offered from environmental measurements so that the need for additional measurements from seaways removed from point (10) of Figure 8 is self evident. It should be noted that characterization of any individual time series wave event must include a statement of the ratio of the measured wave height to significant wave height as well as the relationship of crest to crest wave period to modal period (see Figure 21) so that the data can be applied to adjacent portions of the envelope of extremes using the approximation suggested in section 2.2.2(1). With respect to wave height measurements, it is important to note that in situ measurements must be accurate otherwise confusing, if not misleading, results will be obtained. As discussed in reference 2 (pp 43-61), indiscriminate use of data from wave rider buoys can lead to such an undesirable result.

4.2 Wave Height Spectra

Climatic wave data can and should be generated from NOAA's archived wave spectra data base (see Figure 5). Following this, envelopes of extreme combinations of significant wave height and modal period should be estimated for specific buoy locations based in part upon the results of the climatic spectra survey which will include extreme cases as indicated in Figure 5.

4.3 Extreme Time Series Waves

The amount of accurate and continuous time series wave height data measured during severe storm conditions which are available for analysis is extremely limited. Two possibilities exist for improving this situation both of which derive from on-going, public domain oceanographic research programs. The first is the enlargement of NOAA data buoy wave measurement capabilities to include time series data. Continuous, accurate data are needed from the data buoys during severe storm conditions, especially from buoy locations 46001, 46003, 46004, and 46005 (see section 2.2.3(2)). Continuous data are likely to be required for intervals of 24 to 48 hours on the order of 2 or 3 times a year as a minimum. The second possibility involves the state funded ocean data gathering program associated with Norwegian off-shore platforms. While a significant change in data gathering procedures is needed (i.e. continuous data gathering during extreme conditions vs the current 17 minutes data sample every 3 hours) this on-going, public domain program is a potential source of important time series wave height data. The need for analyzing time series data in half-cycle as well as frequency domain format is implicit in both cases.

In the meanwhile a complete analysis of hurricane Camille wave and wind data (see below) should be undertaken because of their considerable importance to deep water platforms in the Gulf of Mexico. Selected data from the oil company sponsored Off-Shore Data Gathering Program (ODGP) of 1969-71 should also be analyzed for periods of rapid wave development in seaways initially containing very little swell wave energy.

4.4 Wind Velocity Spectra

Wind velocity spectra are needed in general to determine platform dynamic response at surge, sway and yaw modal frequencies. The same data permit determination of the mean square wind velocity which is needed to determine time average restraint

forces associated with wind loads. Since it may be possible to generalize the spectral characteristics of wind velocity for various types of storms, it is suggested that time series velocity data be analyzed first for hurricane Camille and the limited number of winter storms for which such data are now available. (In the case of the former it will be necessary to apply a correction factor to the wind velocity data to compensate for anemometer installation effects.) The data analyses should also provide hourly 8.5 minute averaged wind velocities to permit correlations with the wind data available from the NOAA data buoys.

It is recommended that the use of joint probability statistics involving averaged wind velocity and significant wave height for a range of storm conditions be avoided since misleading results can be obtained. During the winter storm which is analyzed in Figure A13 an extreme value of significant wave height was measured. However, maximum winds occurred well before maximum significant wave height and they were not in any case of an extreme nature at that time (40.8 knots averaged wind speed). On the other hand, during hurricane Camille maximum winds and maximum values of significant wave height occurred together. It is recommended therefore that such statistical correlations as are made be limited to specific types of storm conditions which have been analyzed in the manner of Figure A13.

4.5 Assessment of Critical Wave Conditions for Tension Leg Platforms

It is apparent from the results obtained in reference 9, that tank testing of models is an important means of assessing the effects of specific types of waves on TLP's especially when non-linear effects are present. It follows that they can also be useful in determining those specific environmental conditions which may result in critical loadings (see section 3.2.2). Thus the ability to create the time domain wave conformations of Figure 21 at specific locations in a test tank is an important capability. Inasmuch as this represents an unusually deterministic wave making requirement, it is recommended that the wave making equipment and control systems required for generating such waves be investigated.

4.6 Coordination of Wave and Wind Data for Critical Storm Conditions

Coordination between the users of wave and wind data such as TLP designers and agencies such as NOAA who gather environmental data is essential if data of critical importance and appropriate format are to become available to designers. For example, the developments which are summarized in section 2.2 now place considerable importance on the acquisition of time series wave height data during severe storms. Implementation of this initiative would represent a major additional requirement for the data acquisition and processing systems employed in NOAA's data buoys. The fact that essential climatic wave spectra data have been acquired by NOAA but not processed into a useable format for lack of a statement of user needs, further suggests the importance of the recommended coordination. It is therefore suggested that means be established for assuring that essential coordination is undertaken between parties involved in ocean data gathering and in platform design.

ACKNOWLEDGEMENTS

Most of the environmental data and storm descriptions contained in the appendices of this report were obtained from among the following agencies of the National Oceanic and Atmospheric Administration: NOAA Data Buoy Center, National Oceanographic Data Center, and Environmental Data and the Information Service of the National Climatic Data Center. Wave and wind data gathered, summarized, and archived by NOAA have been of fundamental importance to the preparation of this report. In particular, the author wishes to acknowledge the assistance of Messrs. David Gilhousen and Kenneth Steele of the NOAA Data Buoy Center. He also wishes to acknowledge the help of Mr. Elwyn Wilson editor of NOAA's Publication Mariners Weather Log who furnished needed storm description and observational data. The project, which was monitored by Mr. Richard Dai, is the result of the support of the United States Coast Guard, Office of Merchant Marine Safety.

REFERENCES

1. Gilhousen, D., et. al., "Climatic Summaries for NOAA Data Buoys", U.S. Department of Commerce, January 1983.
2. Earle, M.D., "Uncertainties Affecting Comparisons of Satellite and In-Situ Wave Measurements", Marine Environments Corporation, January 1982.
3. Buckley, W.H., "The Application of Half-Cycle Counting Techniques to the Analysis of Ocean Wave Data", Proceedings of the Nineteenth General Meeting American Towing Tank Conference, Volume 1, 9-11 July 1980, pp 429-466.
4. Rice, S.O., "Mathematical Analysis of Random Noise", Selected Papers on Noise and Stochastic Processes, Dover Publications, 1954, pp 133-294.
5. Longuet-Higgins, M.S., "On the Statistical Distribution of the Heights of Sea Waves", Journal of Marine Research, Volume XI, No. 3, 1952, pp 245-266.
6. Buckley, W.H., et. al., "Use of Half-Cycle Analysis Method To Compare Measured Wave Height and Simulated Gaussian Data Having the Same Variance Spectrum", Ocean Engineering, Volume 11, No. 4, pp 423-445.
7. Bendat, J.S. and A.C. Piersol, "Random Data: Analysis and Measurement Procedures", Wiley-Interscience, 1971, pp 119-122.
8. Buckley, W.H., "A Study of Extreme Waves and Their Effects on Ship Structure", Ship Structure Committee Report No. SSC-320, 1983.
9. Mercier, J.A. et al., "Evaluation of Hutton TLP Response to Environmental Loads", Offshore Technology Conference paper OTC 4429, Volume 4, 1982.
10. de Boom, W.C. et. al., "Motion and Tether Force Prediction for a Deepwater Tension Leg Platform", Offshore Technology Conference Paper OTC 4487, Volume 1, 1983.
11. Teigen, P.S., "The Response of a TLP in Short Crested Waves", Offshore Technology Conference Paper OTC 4642, Volume 3, 1983.
12. Spidsøe, N. and H.P. Brathaug, "Measured Motions of a North Sea Articulated Loading Platform", Offshore Technology Conference Paper OTC 4639, Volume 3, 1983.
13. "Appendices to Requirements for Verifying the Structural Integrity of OCS Platforms", United States Geological Survey, Conservation Division, OCS Platform Verification Program, October 1979.
14. Spidsøe, N. and B. Hilmarssen, "Measured Dynamic Behavior of North Sea Gravity Platforms Under Extreme Environmental Conditions", Offshore Technology Conference Paper OTC 4613, Volume 3, 1983.
15. Mariners Weather Log, Volume 24, No. 5, October 1980, pp 365, 366.
16. Mariners Weather Log, Volume 24, No. 2, March 1980, pp 100-102.

17. Pierson, W.J. Jr., G. Neuman, R.W. James, "Practical Means for Observing and Forecasting Ocean Waves By Means of Wave Spectra and Statistics", H.O. Pub. No. 603, 1955, Table 2.1.

18. Mariners Weather Log, Volume 27, No. 3, Summer 1983, p 166.

19. Ocean Industry, Volume 18, No. 2, p 68.

APPENDIX A

WAVE AND WIND DATA FOR SELECTED STORMS

The Climatic Summaries for NOAA Data Buoys (reference 1) identifies by month, the date and hour of the highest significant wave height measurements made at the seventeen buoy locations covered by the summary. As a result, it has been a relatively simple matter to retrieve wave height spectra and related wave and wind data for the particular storms which resulted in the highest significant wave height measured at a buoy location. These storms are considered to be severe since it has been found that they have generally appeared in NOAA's publication Mariners Weather Log under the heading "Monster of the Month." It is clear from the seven storm analyses which follow that the occurrence of a maximum value of significant wave height at a buoy location can depend upon both the intensity of the storm as well as how close its region of maximum wave heights happened to pass with respect to the buoy in question. It is implicit that storms with locally higher significant wave heights could have occurred in the general ocean area of the buoy during the survey period.

No attempt has been made to classify data sample intervals for the individual buoy locations as to duration because, as indicated by the data of Table A1, the average observation rate per year varied from buoy to buoy. Variations in rate are due in part to incremental increases in observation rate from an early value of once every six hours to the current standard of once an hour as well as equipment malfunctions, non-operating periods associated with buoy maintenance and finally storm damage (e.g. buoy capsizings).

The climatic data summary of reference 1 was prepared by NOAA for those buoy locations for which a minimum of three years of data were available. These are shown in Figures 3 and 4 together with maximum significant wave height measured at each of the buoy locations. (In the case of buoy location 46006, a recent storm which produced a higher significant wave height than that of the survey has been included because of the relatively extreme modal period of the wave height spectra involved. Data from buoy location 46022 have also been considered as part of this particular storm review.) The location of the outer edge of the continental shelf is shown in these figures for reference purposes. It can be seen that along the East Coast the maximum measured significant wave height decreases significantly for continental shelf locations as compared to deep water locations to the east (at least for the types of storms involved in the NOAA climatic summary). This trend is less evident along the West Coast of the United States and Canada. The particular storms which have been reviewed here are those which produced maximum measured significant wave heights among the eighteen NOAA data buoy locations of the climatic summary and therefore are from deep water rather than continental shelf locations. This selection was made because of a primary interest in extreme wave conditions rather than an assertion that wave criteria for TLF design should correspond to wave environments in deep ocean waters.

The storm analyses which follow consist of: (a) a time sequence plot covering 24 hours or more of significant wave height (H_{m0}), modal period (T_p , peak of the wave energy spectrum), wind velocity (V_w) and direction (D_w), (b) wave energy spectra of particular interest during the analysis interval, (c) the storm track relative to the data buoy, and (d) the surface weather map at or near the time of measurement of maximum significant wave height. Particulars of the measurement of wave and

wind parameters are summarized in Table A2. In the case of modal period, tabulated values correspond to discrete spectrum frequencies so that modal period changes in discrete jumps, which in the case of the longer wave periods are relatively large. Interpolated modal periods at or near maximum significant wave height are available in some cases from plots of individual spectra.

A1. Buoy Location 41001: Winter Storm of 3 March 1980

The surface weather map at 0Z on the 3rd reveals an elongated low pressure area resulting in relatively strong winds from the northeast in the vicinity of the buoy which was 200 nautical miles east of Cape Hatteras. At that time, Figure A1 shows that the buoy measured an 8.5 minute averaged wind velocity of 31 knots from the northeast and a significant wave height of 13.4 feet with a modal period of 9.1 seconds. During the next 12 hours a local region of low pressure in the vicinity of the buoy intensified explosively with a 20 mb drop in central pressure to 976 mb see Figure A2. At 09Z the buoy reported local winds of 61 knots (virtually of hurricane strength) from the south, a significant wave height of 30.5 feet and modal period of 12.5 seconds. During the next 3 hours the wind veered to the northwest and decreased slightly to 57 knots. The wind shift caused a decrease in significant wave height to 23.8 feet and a drop in modal period to 11 seconds. In the next 3 hours the northwest wind dropped to 48 knots while the seaway built to a significant wave height of 32.3 feet with a modal period of 14.3 seconds. Following this, the wind continued to hold from the northwest while both wind velocity and significant wave height dropped with modal period remaining constant at 14.3 seconds. The wave energy spectra for 9Z, 12Z, and 15Z hours are presented in Figure A3.

With the exception of the early elongated northeasterly wind field and associated seaway this storm is a good example of a severe winter storm rapidly intensifying over the Gulf Stream. The reasons for the exceptional value of significant wave height at buoy location 41001 are that the center of the storm passed very near the buoy, see Figure A4, and that the peak winds were unusually strong. (For a description of ship damages caused by the storm, see reference 15.)

A2. Buoy Location 42003: Hurricane Frederic, 12 September 1979

Figure A5 shows that the track of hurricane Frederic carried it almost directly over buoy location 42003 which is approximately 240 nautical miles south of Panama City, Florida. At the time it passed the buoy the central pressure was 960 mb (28.4 inches of Hg). Twenty four hours later it made landfall near Mobile, Alabama with a central pressure of 946 mb (28 inches of Hg) and caused 2.3 billion dollars in damage, reference 16.

The wave and wind data of Figure A6 were influenced by the fact that the hurricane was intensifying during the 24 hour period prior to its arrival at the buoy (990 mb at 0Z the 11th to 960 mb at 0Z on the 12th) and by its relatively slow speed of advance (approximately 8 knots) during the 12 hour period prior to its arrival at the buoy. At 12Z on the 11th, modal period was 10 seconds with an averaged wind velocity of 30 knots from the northeast and a significant wave height of 15 feet. By 20Z the modal period had increased to 11 seconds, wind speed to 39 knots and a significant wave height to 20 feet. Over the next two hours significant wave height increased to 28.8 feet and modal period to 12.5 second with the averaged wind speed increasing only to 42 knots. The wave energy spectrum for 22Z, Figure A9,

shows an increase in energy at wave periods less than modal period. It is clear from the delayed increase in wind velocity beginning at 22Z that the seaway associated with the strong central winds of the hurricane have outrun the central wind field by approximately 2 hours. This is apparently due to the group velocity of waves corresponding to a modal period of 11 seconds (approximately 17 knots) being greater than the speed of advance of the hurricane (approximately 8 knots).

The eye of the hurricane began to pass over the buoy at 0Z and completed its passage at 03Z on the 12th with a change in wind direction of 180° and a return to stronger winds. The wave energy spectrum now has a modal period of 10 seconds and a decrease in total energy corresponding to a reduction in significant wave height from 29.2 ft at 0Z to 18.7 ft at 03Z.

A3. Buoy Location 44004: Winter Storm of 8 February 1980

This storm which developed off Savannah, Georgia on the 6th produced 23 knot winds from the northeast and a significant wave height of 3.9 feet at 0Z on the 7th at the buoy location (about 115 nautical miles east of Cape May, New Jersey), Figure A8. The storm intensified and moved rapidly in a northeasterly direction to a point due south of the buoy at 12Z on the 7th, Figure A9. During this 12 hour period the averaged wind speed increased to 45 knots still from the northeast while significant wave height increased to 25 feet with a modal period of 11 seconds. Wind speed reached 52 knots at 10Z and then dropped to 37 knots at 13Z at which time it began to increase again. Between 14Z and 15Z the wind shifted abruptly to the north (presumably backing) and increased in velocity to 52.5 knots at 16Z as the center of the storm passed south of the buoy, see Figures A9 and A10. After this, the wind velocity decreased slowly with its direction remaining relatively constant from the north, northwest.

From 13Z on, the hourly values of significant wave height shown in Figure A8 exhibit considerable variability beginning at about 13Z on the 7th. With the exception of the interval from 13Z to 16Z when the wind strength and direction were changing, there is no obvious reason these variations. (See discussion of similar variations under Item A4.)

The wave energy spectra of Figure A11 show limited variations in spectrum shape before and after the wind shift, i.e. between 13Z and 17Z. The spectrum for 6Z on the 8th when maximum significant wave height occurred also shows limited change in shape other than that necessarily associated with the increase in significant wave height. Modal period for all three spectra remained at about 12.5 seconds.

A4. Buoy Location 46001: Winter Storm of 28 November 1979

This particular storm resulted in the highest significant wave height measured to date at any of the NOAA data buoy locations. During the time of interest, the storm followed a northwesterly track due to the presence of a blocking high pressure area over the western Canadian provinces. This track while not typical of winter storms, is not unusual for the month of November judging from storm track information contained in past issues of the Mariner's Weather Log. Based upon the following central pressure data it can be said that the storm was both intense and sustained during the time interval of interest:

Date	Time	Central Pressure	
		(mb)	(inches Hg)
27 Nov 1979	18Z	960	28.3
28 Nov 1979	0Z	956	28.2
28 Nov 1979	06Z	952	28.1
28 Nov 1979	12Z	968	28.6

Surprisingly, the closest the storm center came to the buoy location was 275 nautical miles to the southwest at 06Z on the 28th at which time maximum significant wave height was measured, see Figures A12 and A13. The unusually high value of significant wave height is attributable in part to the straightening and tightening of the isobars as the low pressure center and the blocking high came close to one another which resulted in a large wind field of relatively constant direction, see Figure A14. The fact that hurricane strength barometric pressures persisted during the entire period of interest obviously contributed to the unusual values of significant wave height which were measured.

The chronological development of wave and wind measurements presented in Figure A13 shows a steady build up of wind velocity and significant wave height from 12Z to 20Z on the 27th. At this point the local averaged wind velocity peaked out at just under 50 knots. Significant wave height and modal period, however, continued to build until 06Z on the 28th when a significant wave height of 48.6 feet and a modal period of just under 20 seconds were measured. Wind velocity at 06Z had decreased to 41 knots while the wind direction changed from east northeast to east southeast. Beginning at 02Z marked variations in significant wave height began to occur at 1 to 2 hour intervals. Wind velocity during this time decreased slowly as did the general trend of significant wave height while wind direction was nearly constant from the southeast. Wave energy spectra corresponding to selected maxima and minima of significant wave height are presented in Figures A15 and A16. It is apparent from these figures that the changes in wave energy occurred primarily near modal period, i.e., the large variations in wave energy were associated with the longest waves in the seaway.

One explanation of this behavior derives from the possible existence of large grouped waves in storm winds which are no longer increasing, or which have begun to decrease (item II.a of Table 3). The occurrence rate cited for such waves given in reference 8 section 5.21(3) is such that the NOAA data buoy measurements might well include several occurrences of large grouped waves or alternatively none at all. Such an hypothesis cannot be verified in the absence of time series wave height data for the 20 minute intervals in question so that this explanation is necessarily speculative.

Of greater certainty is the observation that wave data gathered at intervals substantially greater than one hour would fail to detect these variations in wave energy. (Sampling at intervals of 3 hour, for example, is common practice.) Substantial hourly variations in significant wave height are not confined to the storm reviewed here. Examination of the hourly variations in significant wave height presented here in Figures A8, A19, A23, and A25 show that somewhat less dramatic variations in significant wave height are not uncommon under the relatively severe storm conditions being examined.

A5. Buoy Location 46003: Winter Storm of 16 December 1979

This storm featured a complex pattern of lows lying east and west of a dominant low as shown in Figure A17. The track of the low nearest to the buoy, which is located approximately 395 nautical miles south by east of Kodiak Island, Alaska, is shown in Figure A18. Its central pressure at the time of maximum significant wave height was 980 mb (28.9 inches of Hg). The dominant low which lay even further south had a central pressure of 956 mb (28.2 inches of Hg). The surface weather map of Figure A17 shows that the circulation around the complex pattern of lows in the vicinity of the buoy was largely from the east with a considerable fetch. Straightening of the isobars in this region was due to the presence of an elongated high pressure area to the northeast which lay over parts of Alaska and the Yukon Territory.

Figure A19 provides a chronological plot of significant wave height and modal period. In this instance no wind data are available due to an anemometer malfunction. Significant wave height was 18.8 feet at 0Z on the 15th with a modal period of 10 seconds. Both increased gradually during the next 17 hours until a significant wave height of 36.7 feet was reached with a modal period of 19.3 seconds. During this development, variations in significant wave height are evident which are of 2 to 4 hours duration. Following attainment of maximum significant wave height, these variation cycle over intervals of about 2 to 3 hours.

Hourly variations in the wave height spectra near the time of maximum significant wave height are shown in Figure A20 from which it can be seen that the build up in wave energy from 16Z to 17Z occurred principally near modal period. The decrease in energy in the following hour, however, involves a significant energy loss below modal period as well as an increase in modal period itself.

A6. Buoy Location 46005: Winter Storm of 26 November 1981

This storm passed approximately 165 nautical miles east of the buoy location during its progress in a southeasterly direction, the buoy itself being located approximately 300 nautical miles east of Portland, Oregon, see Figure A21. The storm was somewhat unusual in that its minimum central pressure reached a low of only 996 mb (29.4 inches of Hg) although it had a maximum averaged wind velocity at the buoy of 48.1 knots, Figures A22 and A23. The fetch for the northwesterly winds was greater than inferred by the isobars of the surface weather map since wind vectors associated with point measurements show northwesterly winds persisted for at least 400 nautical miles north of the buoy. The chronology of wave and wind data shows an averaged wind velocity of 29.3 knots and a significant wave height of 15.6 feet with a modal period of 10 seconds at 0Z on the 28th. Wind velocity peaked at 07Z and then began to slowly decrease. Significant wave height continued to increase, however, until 12Z at which time a value of 36.2 feet was reached with a modal period of 12.5 seconds. Figure A24 shows a growth in wave energy from 09Z to 12Z followed by an abrupt decrease at 14Z. The gains and losses of wave energy from 07Z to 14Z were centered near modal period but were spread over a range of wave periods from about 9 seconds to 16 seconds.

A7. Buoy Locations 46006 and 46022: Winter Storm of 9 February 1983

This particular storm occurred after the wave and other data of reference 1

were compiled. It has been included here primarily because of the unusually long period waves and high significant wave heights involved. The buoy position is far to the west of any location of likely interest for TLP installation, i.e., approximately 635 nautical miles west of Cape Mendocino. The synoptic development of the storm and its long period waves, however, are of considerable interest with respect to the occurrence of long period waves of high energy.

The chronological wave and wind data of Figure A25 show that the averaged wind velocity at the buoy location varied from about 30 to 40 knots up to the time of maximum significant wave height (13Z on the 9th) after which it slowly decreased. Significant wave height increased slowly from 0Z (22.6 feet) to 09Z (26.5 feet) with a noticeable increase in modal period occurring at 07Z. From 09Z to 11Z both significant wave and modal period show dramatic increases, i.e., from 26.5 to 40 feet and from 14.3 to 25 seconds respectively. The wave energy spectra of Figure A26 clearly indicate the arrival at the buoy of wave energy generated at more distant location, there being no logical reason for the wind field then arriving at the buoy to have generated waves of such long period. A fully developed sea of 25 seconds modal period, for example, would require sustained winds averaging approximately 60 knots, reference 17. The wave energy spectra of Figure A27 are exceptionally narrow-band with the majority of wave energy contained between 15-25 second wave periods, especially at 13Z when maximum significant wave height was measured. Large variations in significant wave height can be seen to occur after 11Z which are similar to those measured at buoy location 46001 in the Gulf of Alaska (Figure A13). Again the major variations in wave energy occur near modal period.

The storm track of Figure A28 confirms that no storm center is in the vicinity of buoy location 46006 during the period of interest. The surface weather map of Figure A29, which corresponds closely to the time at which maximum significant wave height was measured, suggests that winds from the west southwest had a considerable fetch before arriving at the buoy.

It is of interest at this point to examine wave and wind data measured at buoy location 46022 which is less than 10 miles off Cape Mendocino. The chronological wave and wind data of Figure A30 show waves of 25 second modal period arriving at the buoy between 3Z and 4Z on the 10th. The local averaged wind velocity is about 20 knots at 0Z, decreasing slowly to 11 knots at 15Z. Wind direction varied from southwest to west and then back during this interval. Since the long period wave energy arrived at buoy location 46006 at about 10Z on the 9th, an average speed of advance for the wave energy can be estimated as follows: (a) elapsed time from 10Z on the 9th to 04Z on the 10th is 18 hours, (b) the distance between buoys is approximately $(138-124.5) 60 \cos 41^\circ = 611$ nautical miles so that wave energy advanced at an average speed of about $611/18 = 34$ knots. The theoretical group velocity for wave energy of 22 to 25 second period is close to 33 to 37.5 knots which is in good agreement with the observed group velocity. The extremely narrow band spectrum of Figure A31 derives from the fact that the longest and hence fastest waves arrive first at the buoy (over a distance of 600 miles), which effectively filters out swell wave energy at wave periods less than maximum.

The observed speed of advance estimated above permits a rough check of the origin of the long period waves considering the storm center time and position information of Figure A28. Reference 18 reports a severe winter storm centered at 42°N , 161°W at 0Z on the 8th together with observed wind and barometric pressure

information. The observed central pressure at that time was 952 mb (28.1 inches of Hg) which is virtually a hurricane barometric pressure. The SEA-LAND-DEFENDER reported measured winds of 75 knots from 260° at 41°N, 160°W at 0Z on the 8th confirming the severity of the westerly winds associated with the storm. Long period waves traveling from the vicinity of the storm center at 0Z on the 8th and arriving at buoy location 46006 at 10Z on the 9th would imply a group velocity of approximately (161-138) $6G \cos 41^\circ/34 = 30.6$ knots. This is reasonably close to the theoretical velocity of 33 knots for waves of 22 second modal period which arrived at the buoy at 10Z on the 9th (Figure A26) which tend to confirm that these wave were indeed generated by the storm located near 42°N, 161°W at 0Z on the 8th. The fact that such large amounts of wave energy traveled the considerable distance to buoy location 46006 and ultimately to buoy location 46022 is apparently attributable to the strong (but by no mean severe westerly winds blowing over a distance of 1000 nautical miles or more to the east of the storm). This wind field resulted in part from the low pressure center which existed to the east of the storm and which produced an overall circulation at latitude 41°N of great extent and uniformity in direction, see Figure A29. The arrival of long period wave energy in relatively abrupt fashion at buoy location 46006 at 10Z on the 9th is due in part to the slow speed of advance of the storm from 0Z on the 8th to 0Z on the 9th, Figure A28. The westward travel of the storm during this 24 hour period was approximately 360 nautical miles which corresponds to an average speed of advance to the east of about 15 knots. It is clear that long period waves having a group velocity of over 30 knots would tend to outrun the storm which they evidently did.

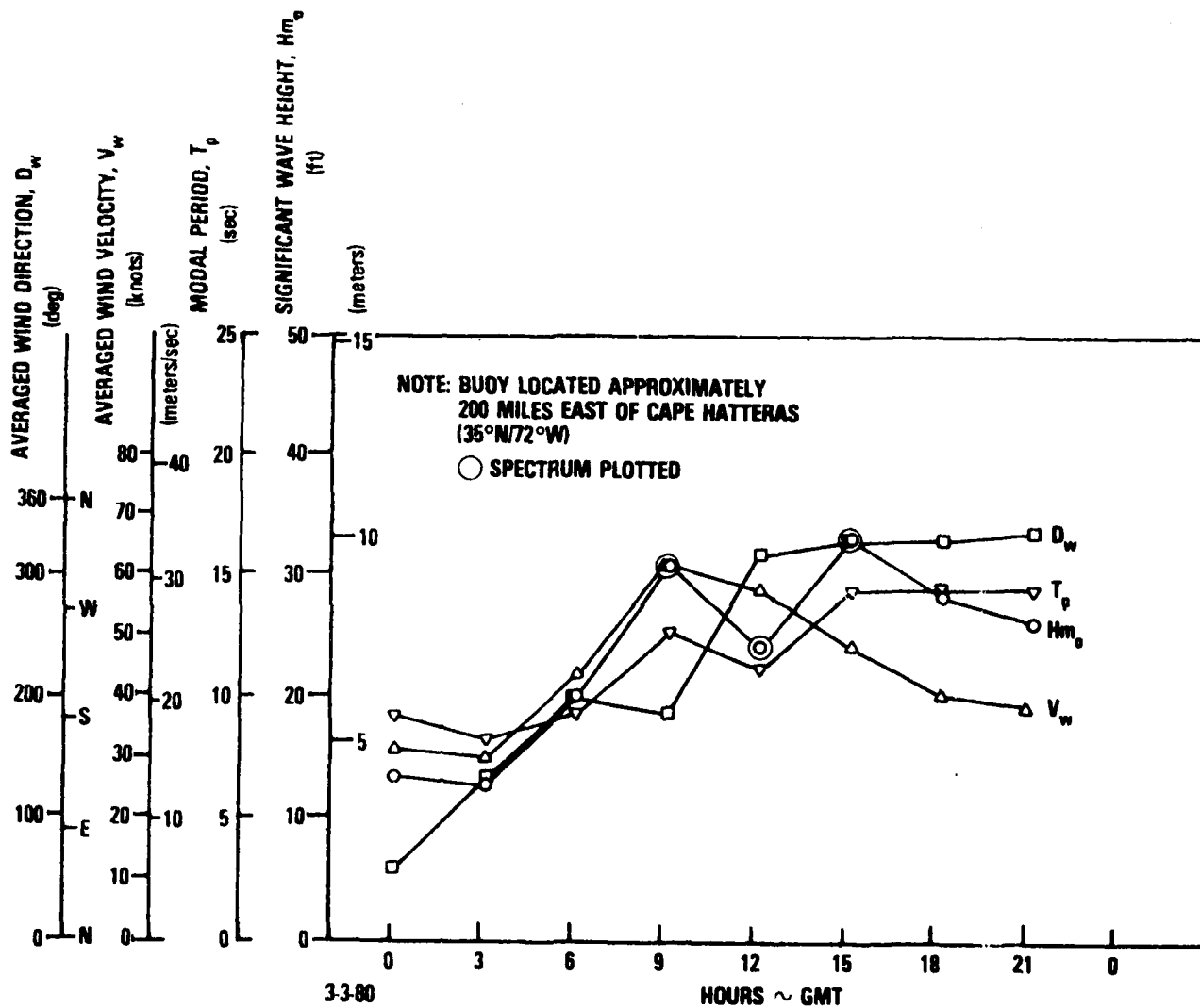


Figure A1 - Wave and Wind Data from Buoy Location 41001:
Winter Storm of 3 March 1980

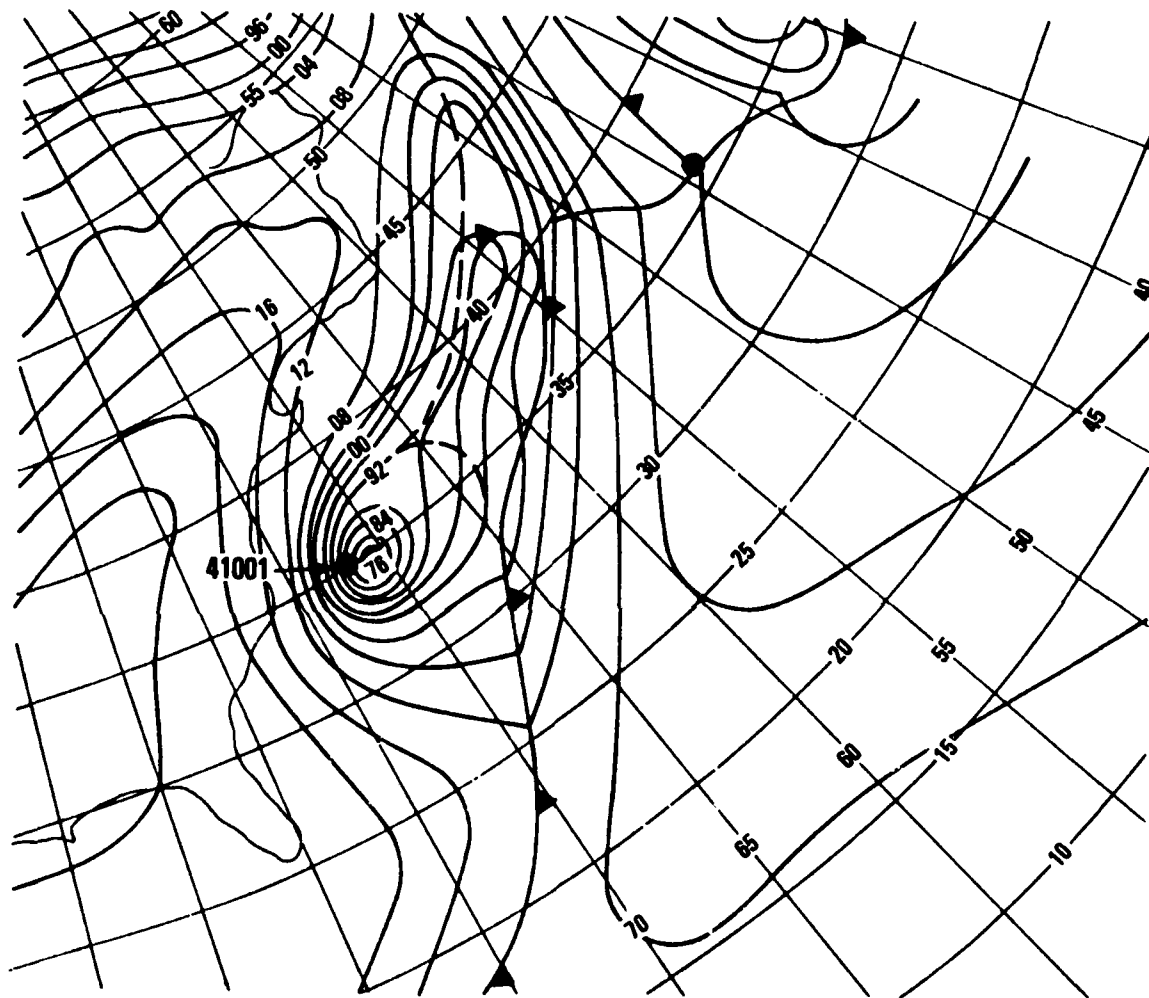


Figure A2 - Surface Weather Map for Buoy Location 41001
at 1200Z on 3 March 1980

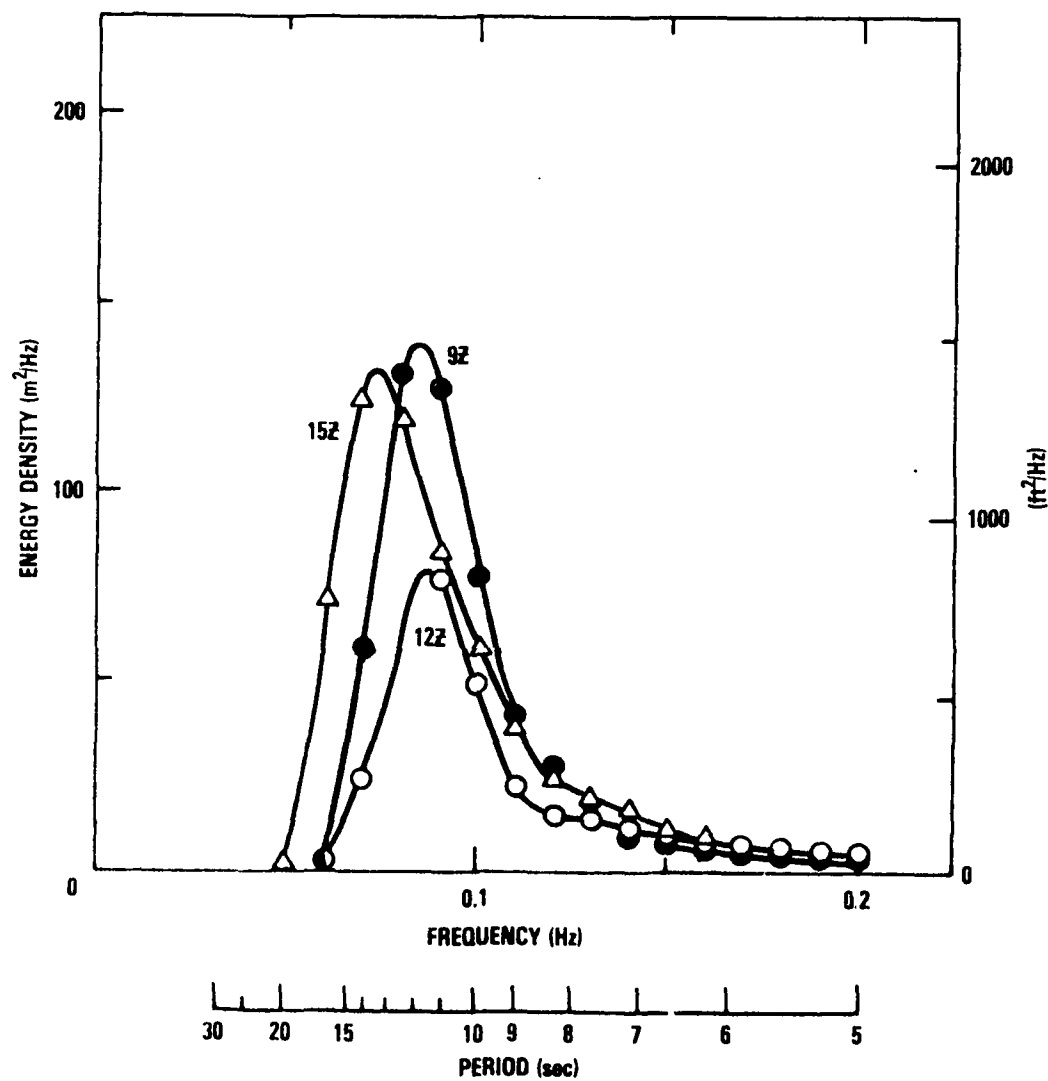
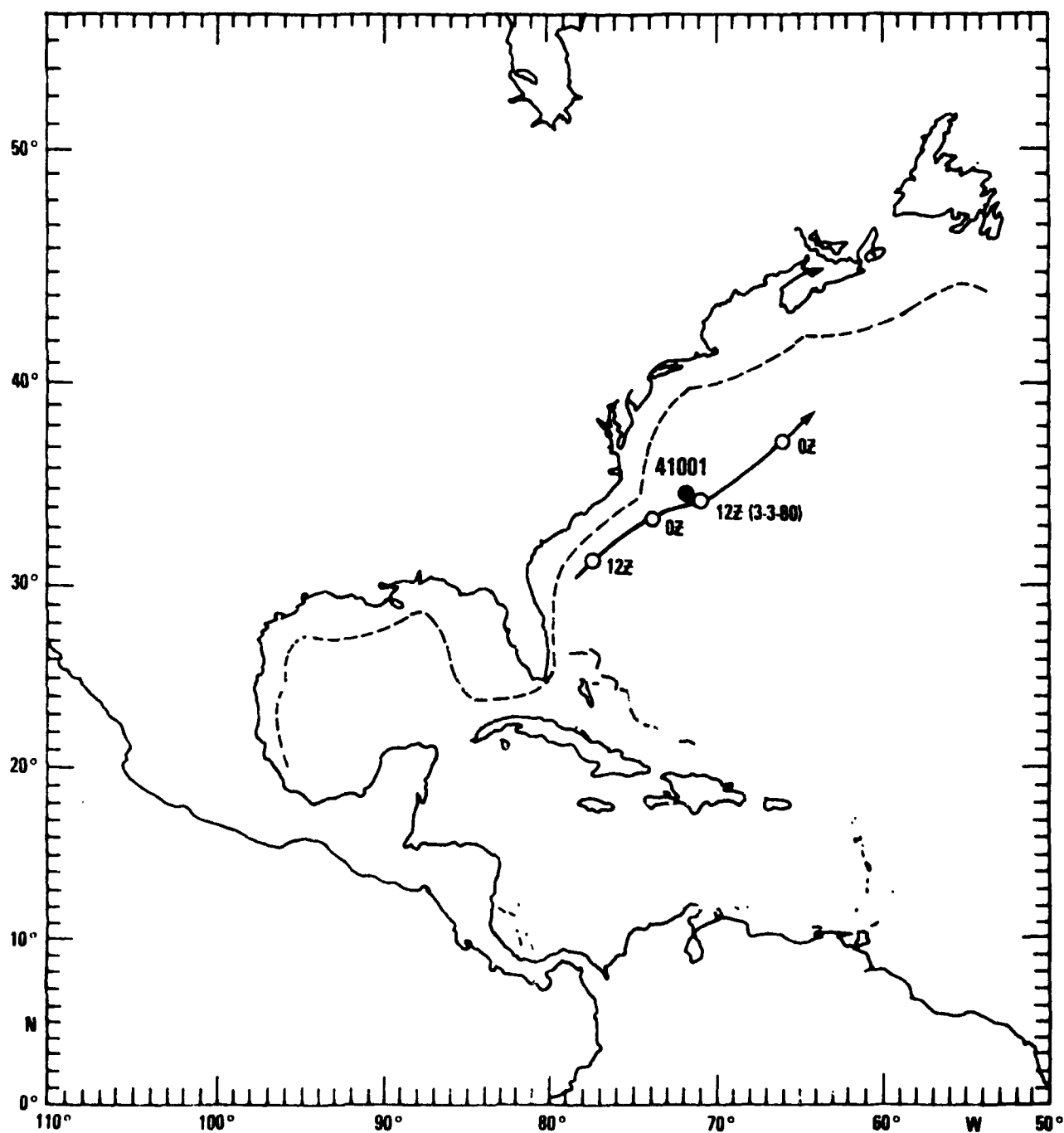


Figure A3 - Wave Height Spectra from Buoy Location 41001:
Winter Storm of 3 March 1980



NOTE: STORM TRACK DATA FROM REFERENCE 15

Figure A4 - Track of Winter Storm Relative to Buoy
Location 41001: 3 March 1980

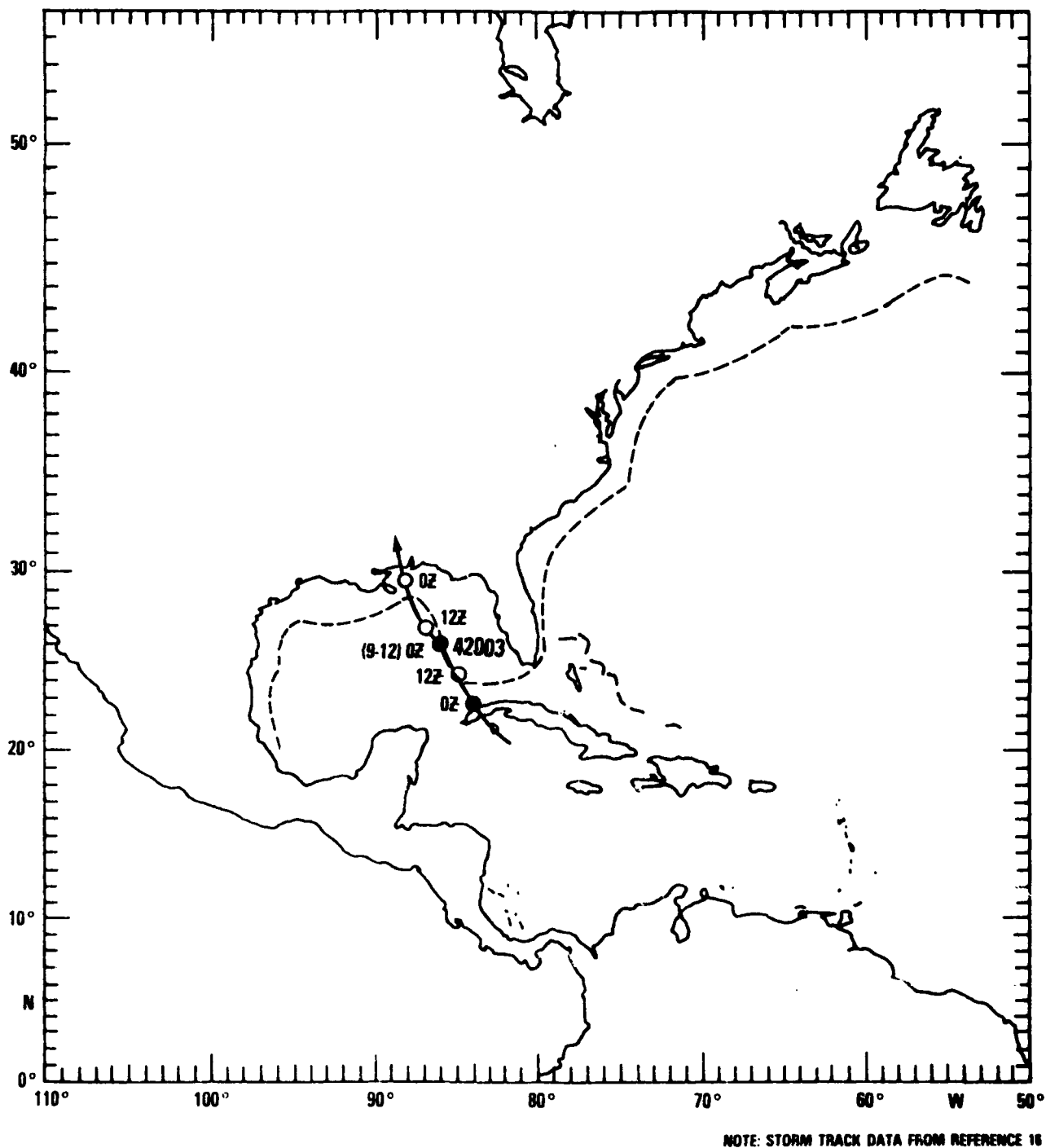


Figure A1 - Track of Hurricane Frederic Relative to Buoy
Location 42003: 12 September 1979

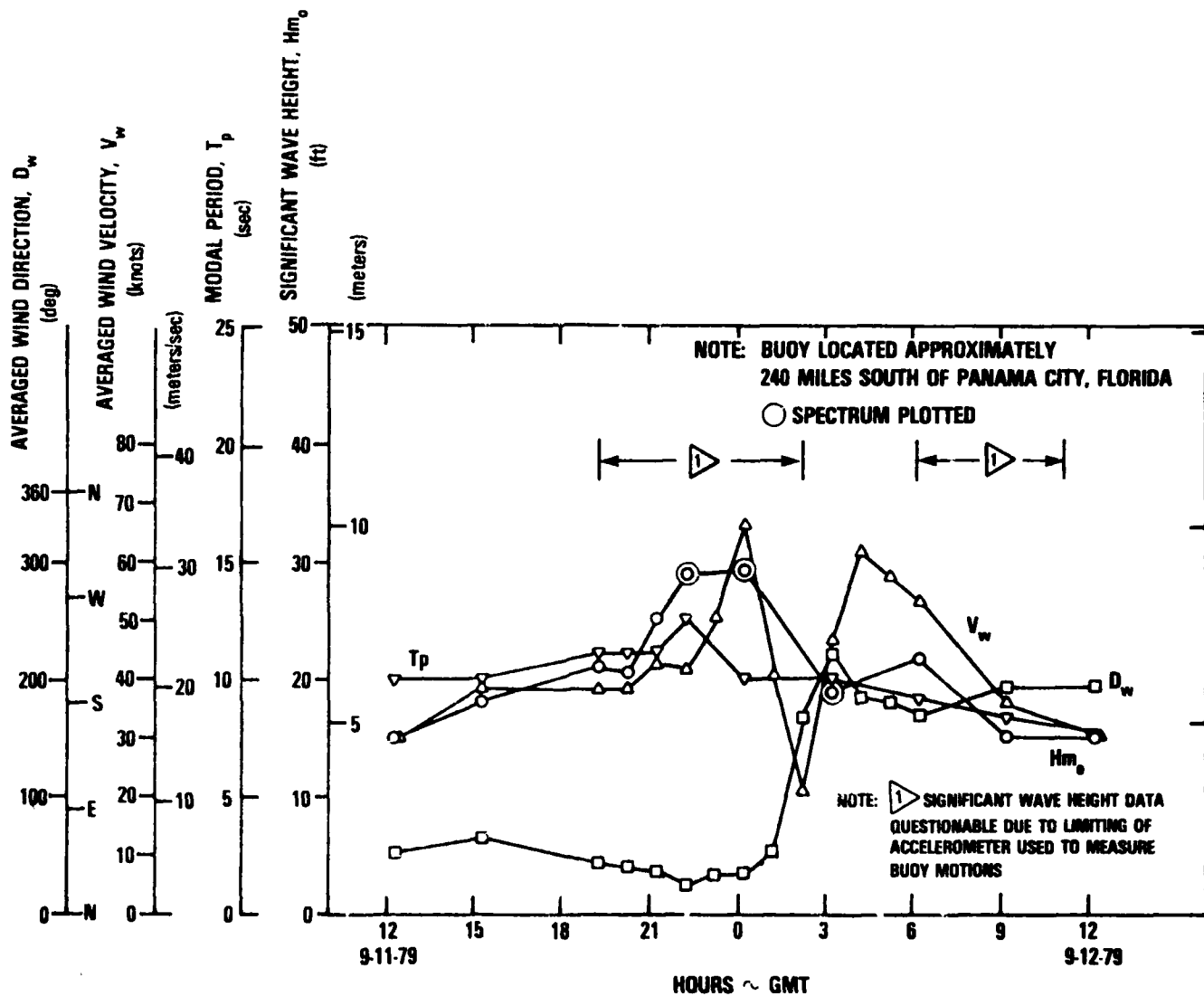


Figure A6 - Wave and Wind Data from Buoy Location 42003:
Hurricane Frederic 12 September 1979

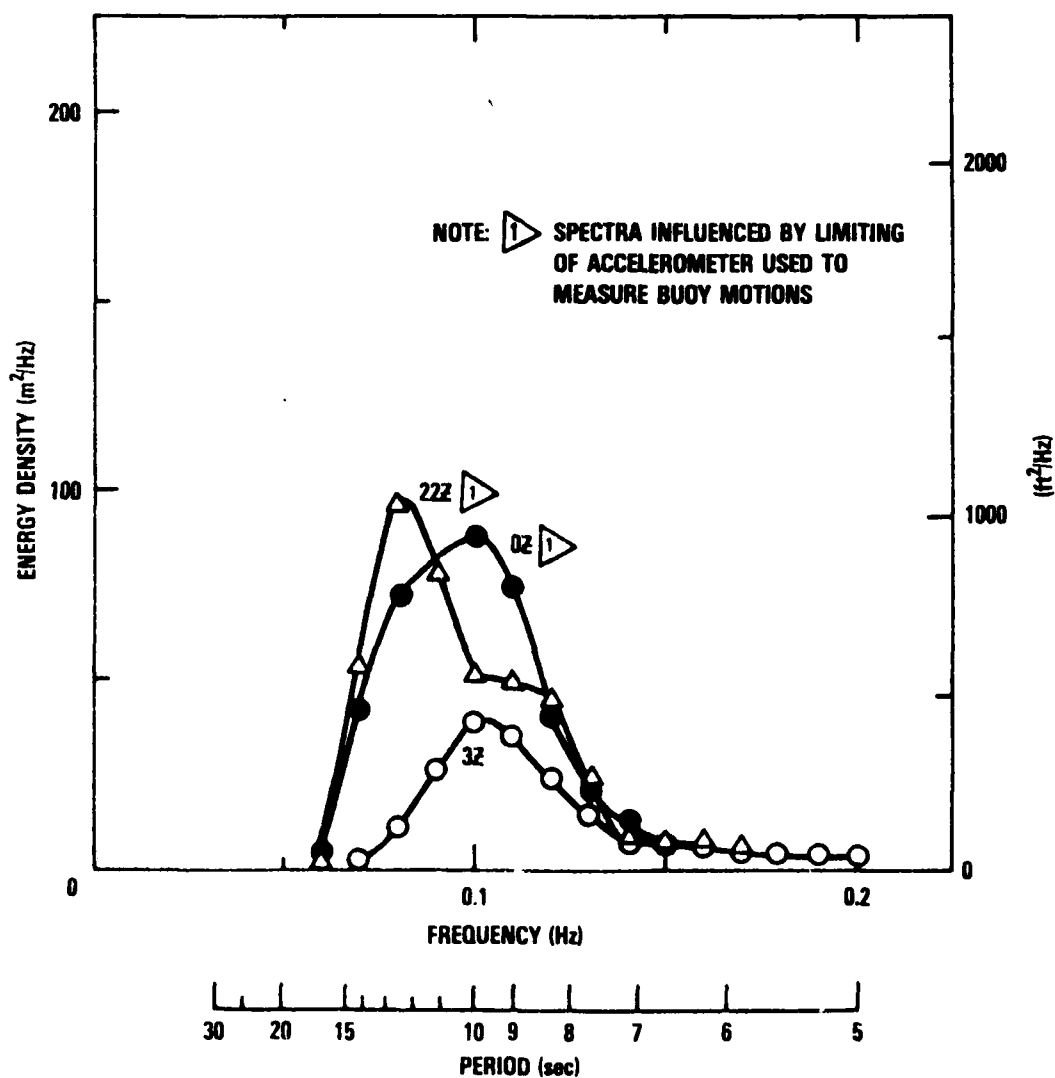


Figure A7 - Wave Height Spectra from Buoy Location 42003:
Hurricane Frederic 12 September 1979

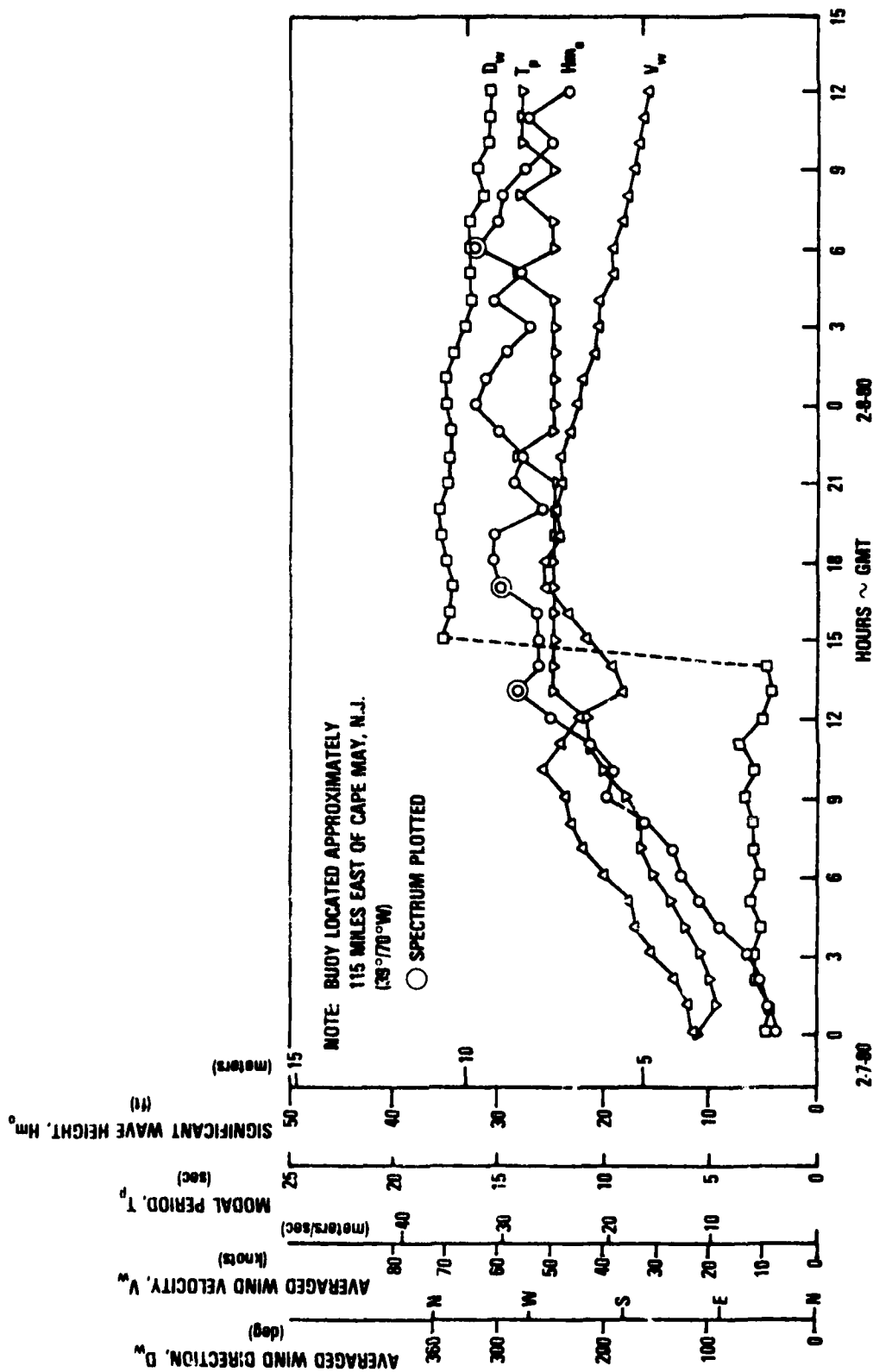


Figure A8 - Wave and Wind Data from Buoy Location 44004:
Winter Storm of 7 February 1980

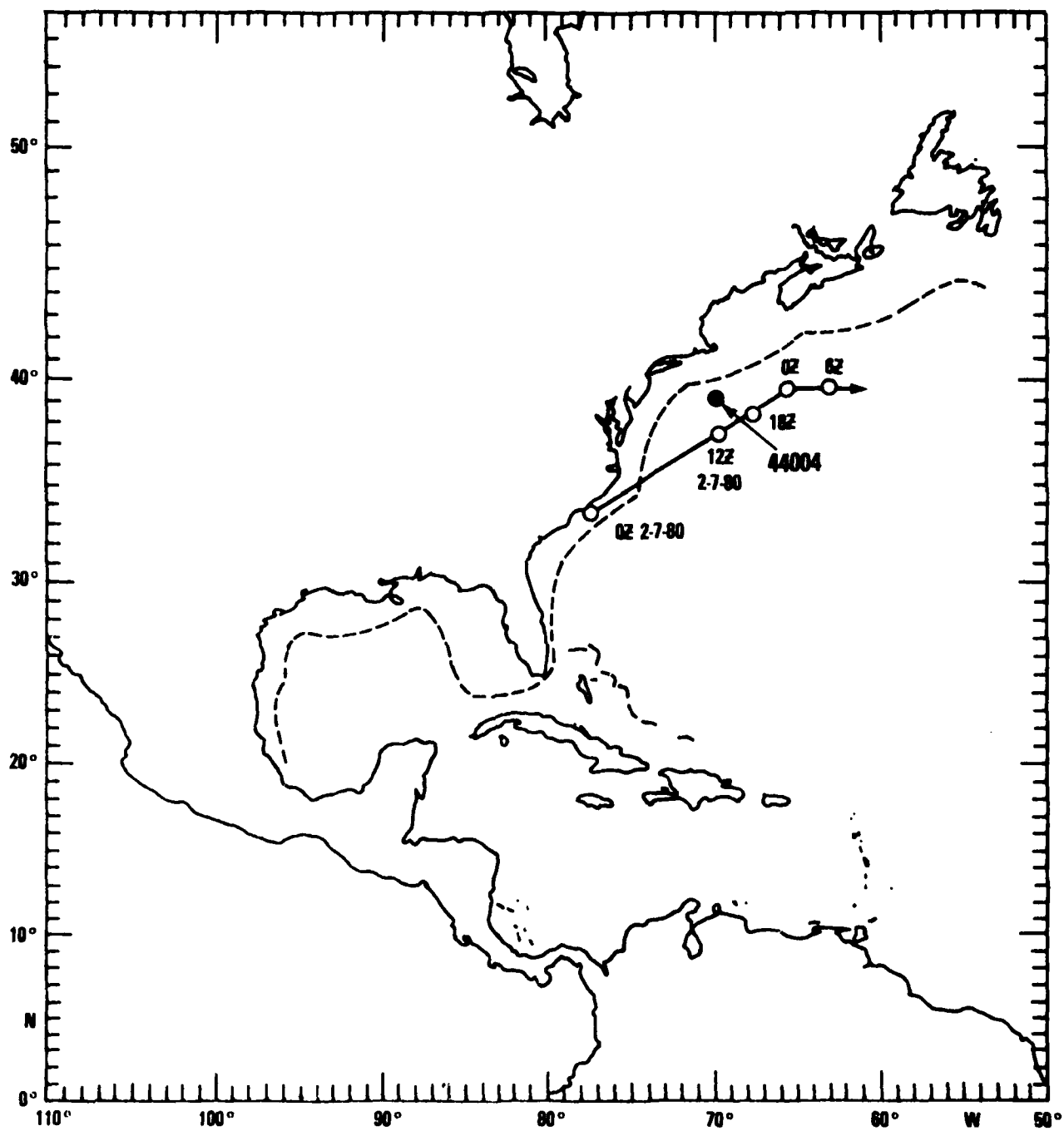


Figure A9 - Track of Winter Storm Relative to Buoy Location 44004:
7 February 1980

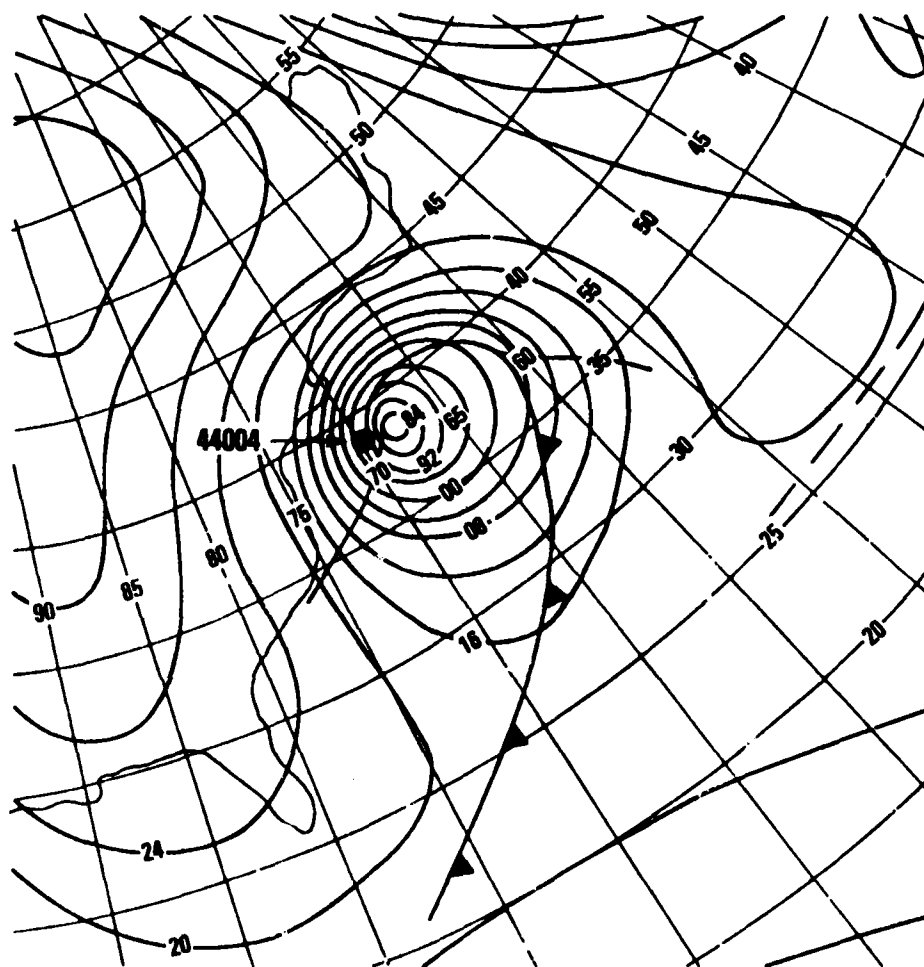


Figure A10 - Surface Weather Map for Buoy Location 44004 at 1800Z
on 7 February 1980

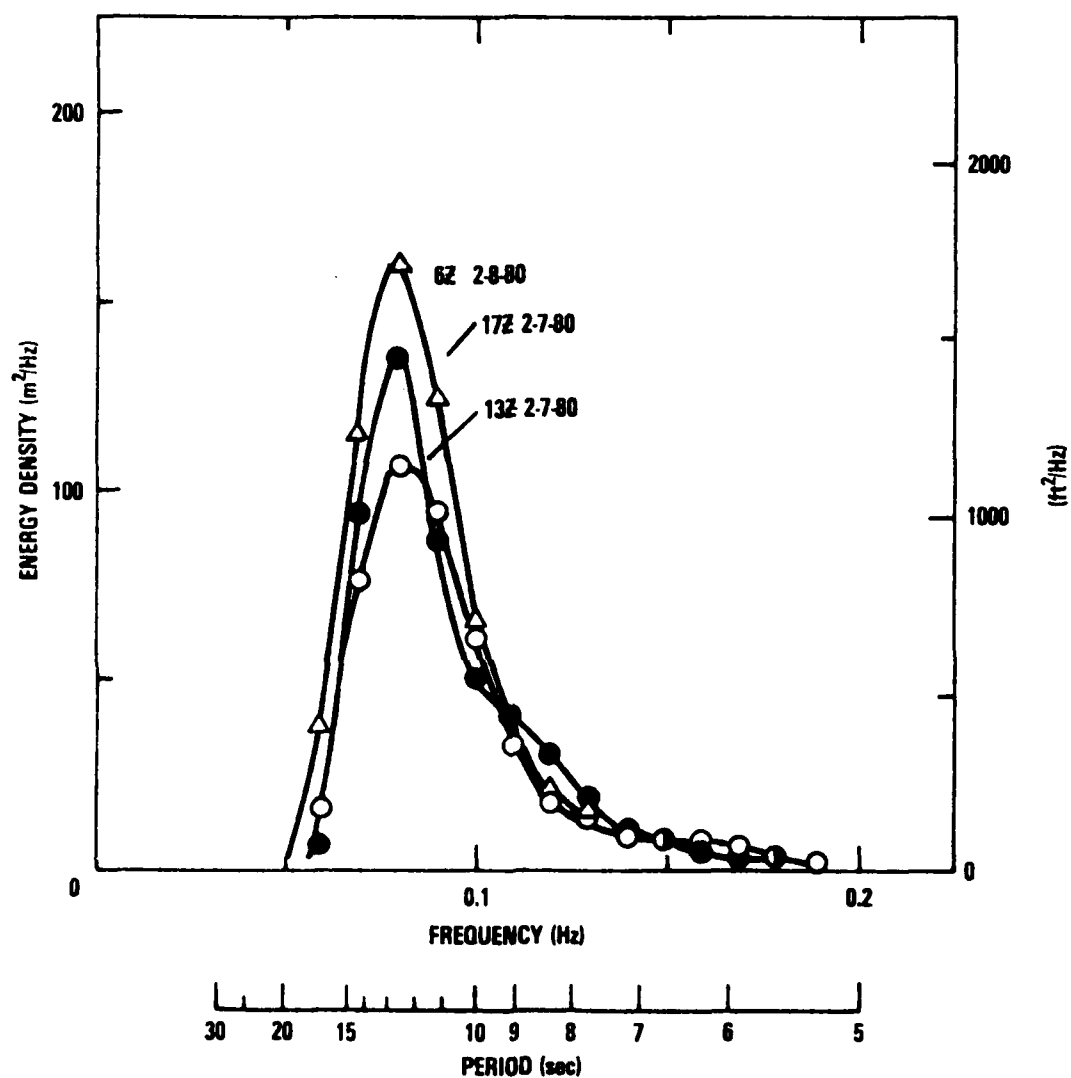


Figure A11 - Wave Height Spectra from Buoy Location 44004:
Winter Storm of 7 February 1980

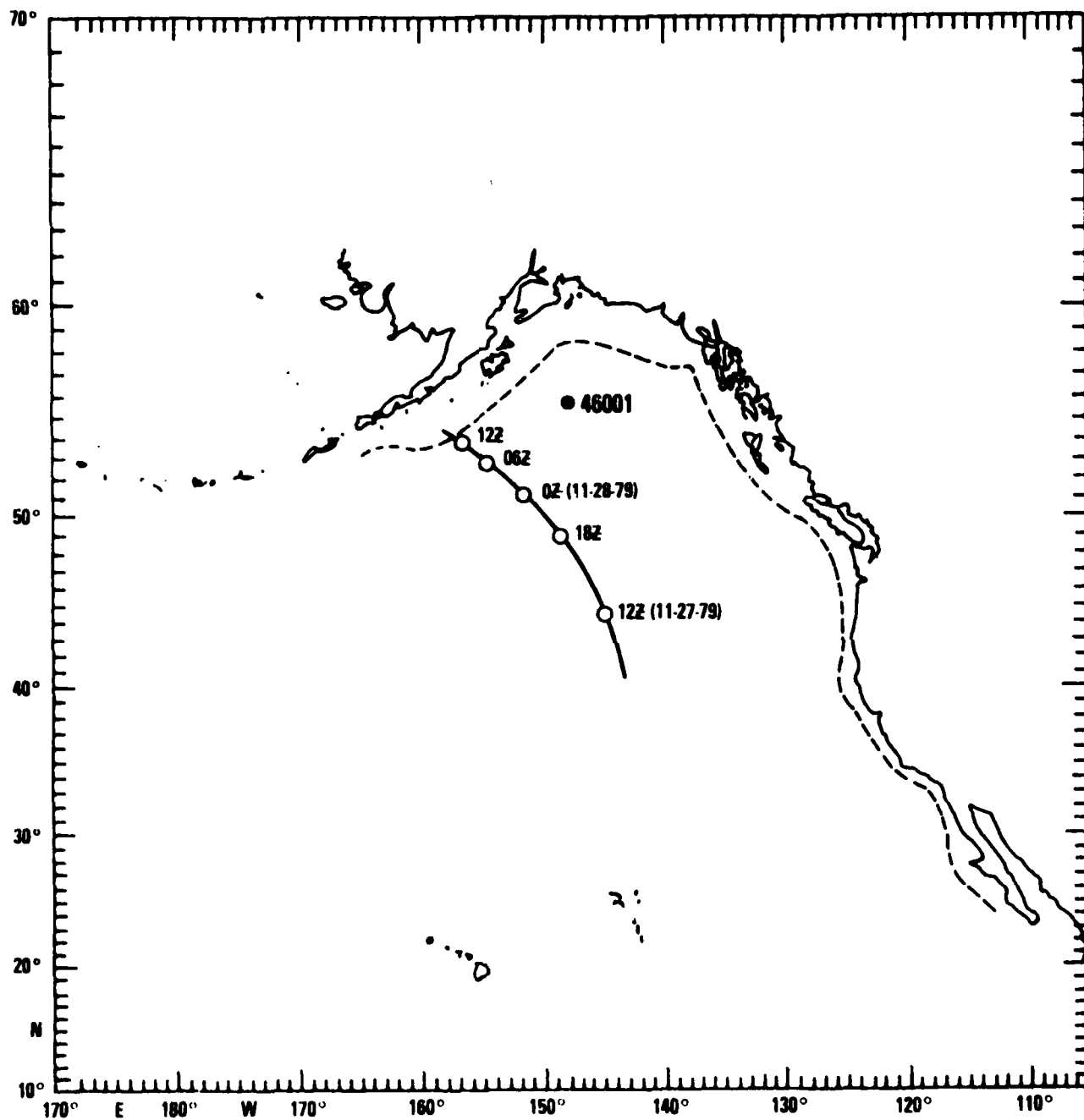


Figure A12 - Track of Winter Storm Relative to Buoy Location 46001:
28 November 1979

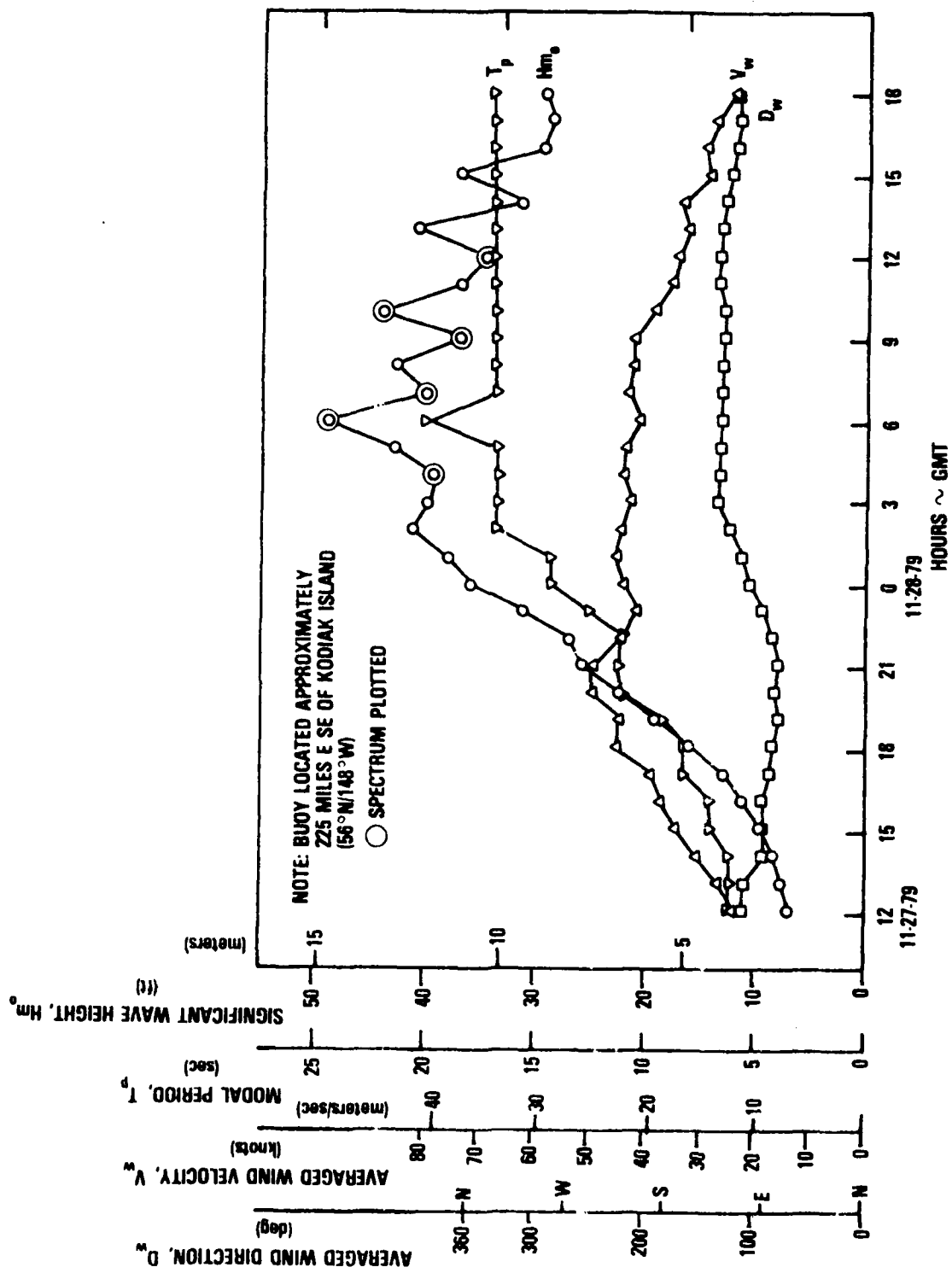


Figure A13 - Wave and Wind Data from Buoy Location 46001:
Winter Storm of 28 November 1979

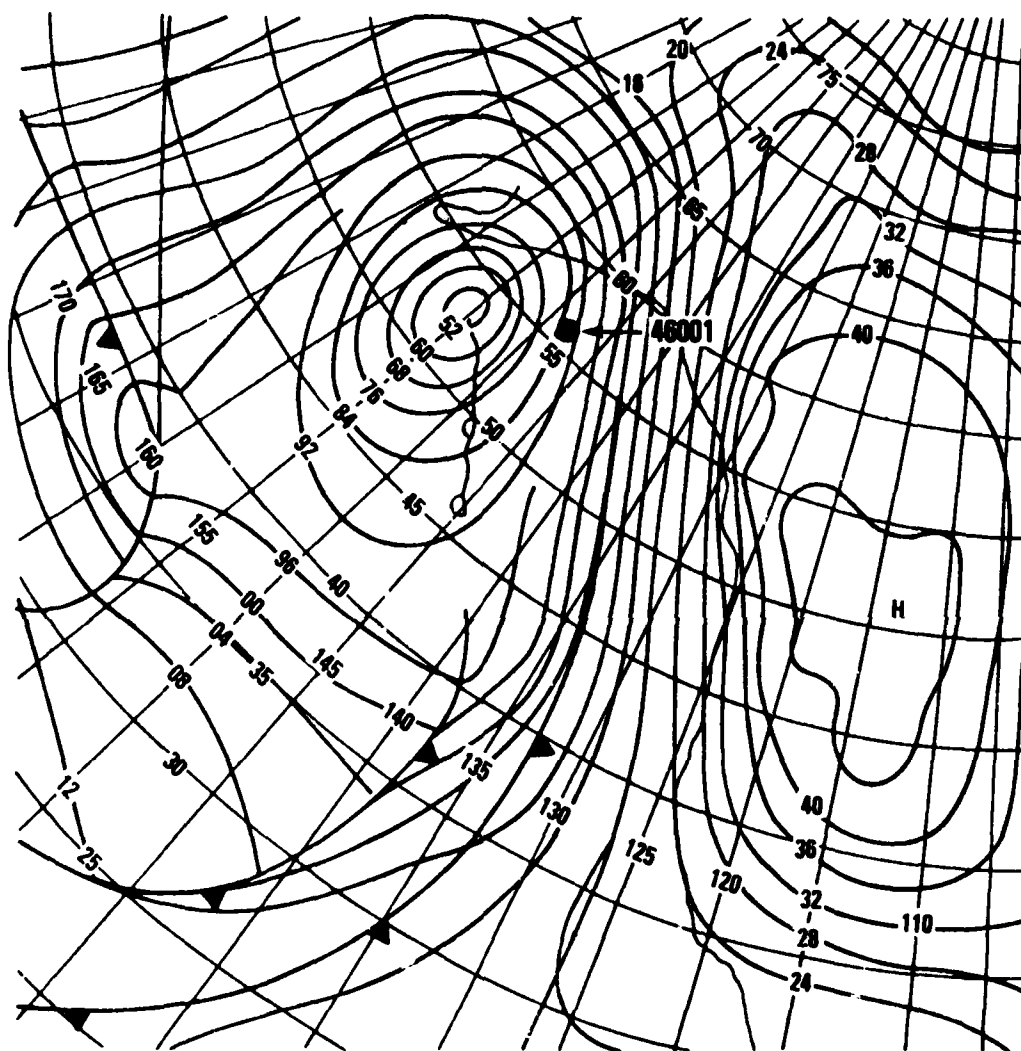


Figure A14 - Surface Weather Map for Buoy Location 46001 at 0600Z on 28 November 1979

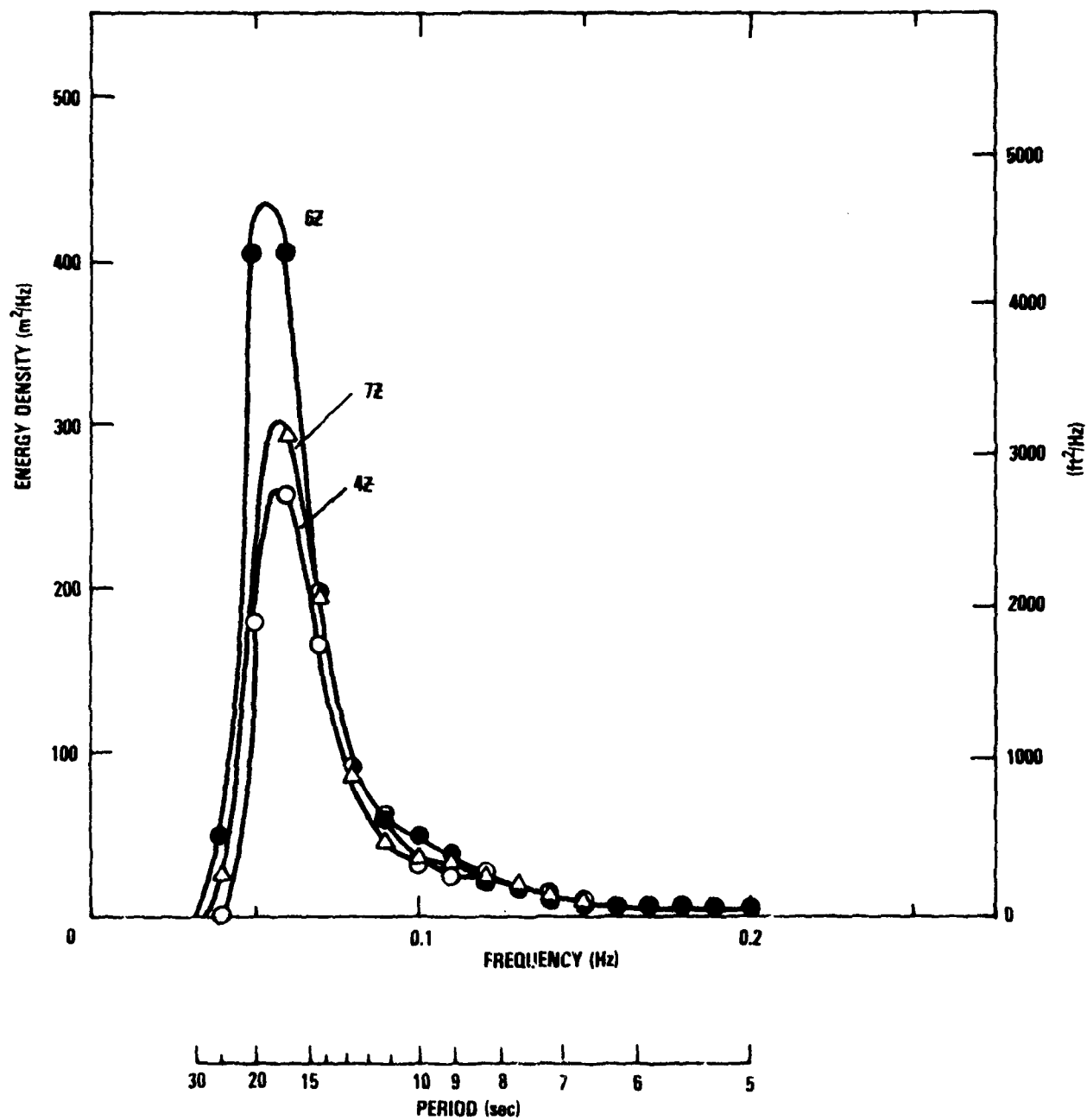


Figure A15 - Wave Height Spectra from Buoy Location 46001:
Winter Storm of 28 November 1979

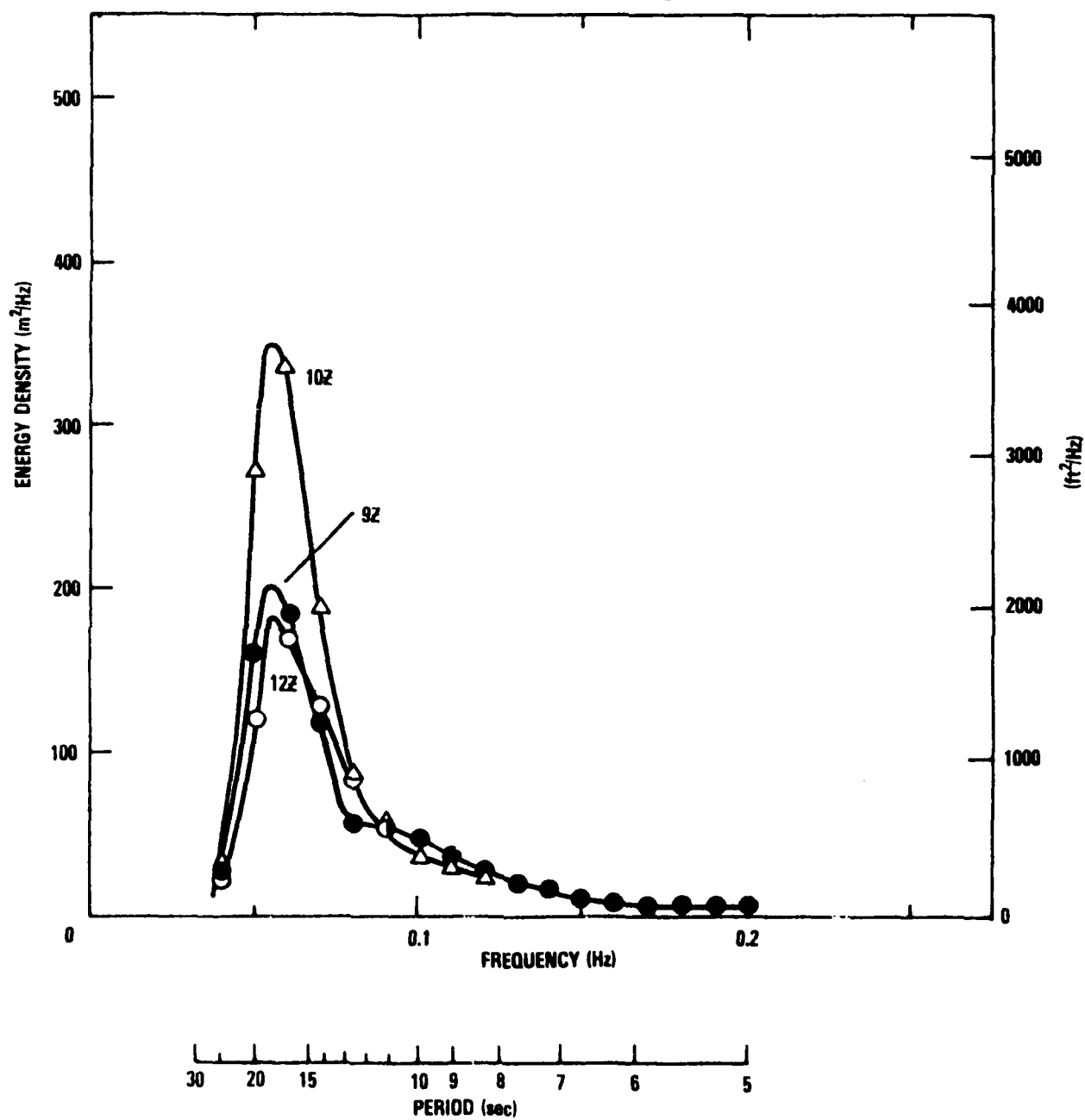


Figure A16 - Wave Height Spectra from Buoy Location 46001:
Winter Storm of 28 November 1979 - 09Z to 12Z Hours

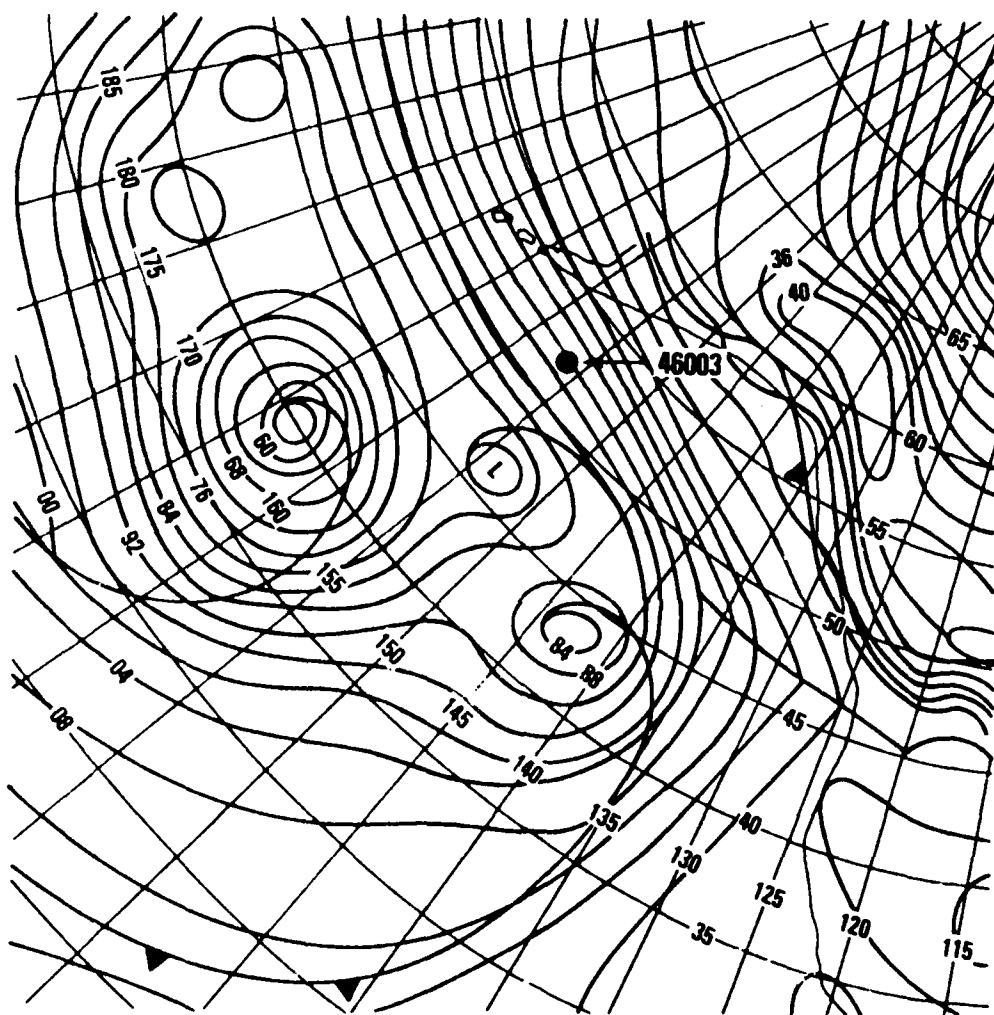


Figure A17 - Surface Weather Map for Buoy Location 46003 at 1800Z
on 15 December 1979

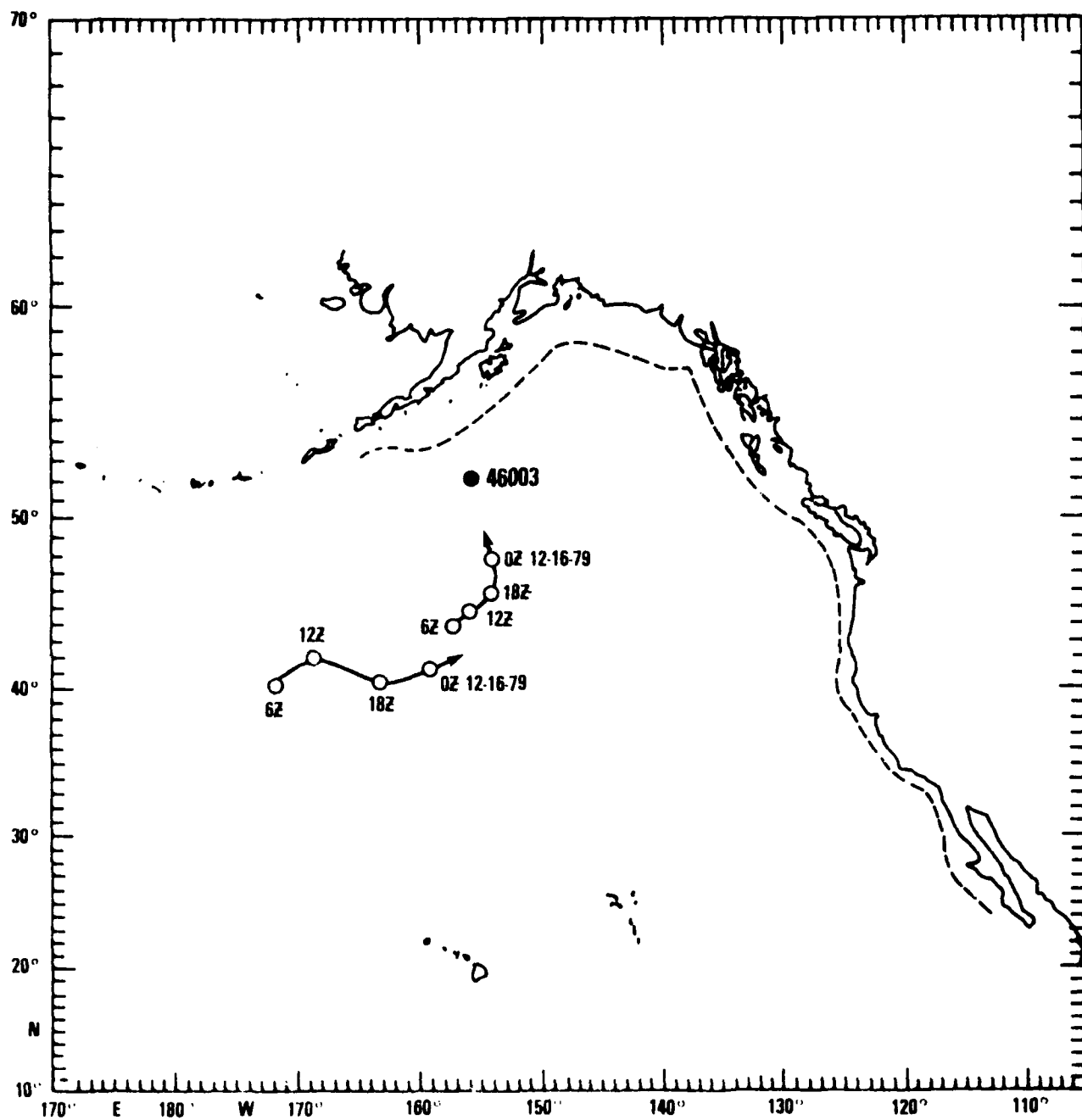


Figure A18 - Track of Winter Storm Relative to Buoy Location 46003:
15 December 1979

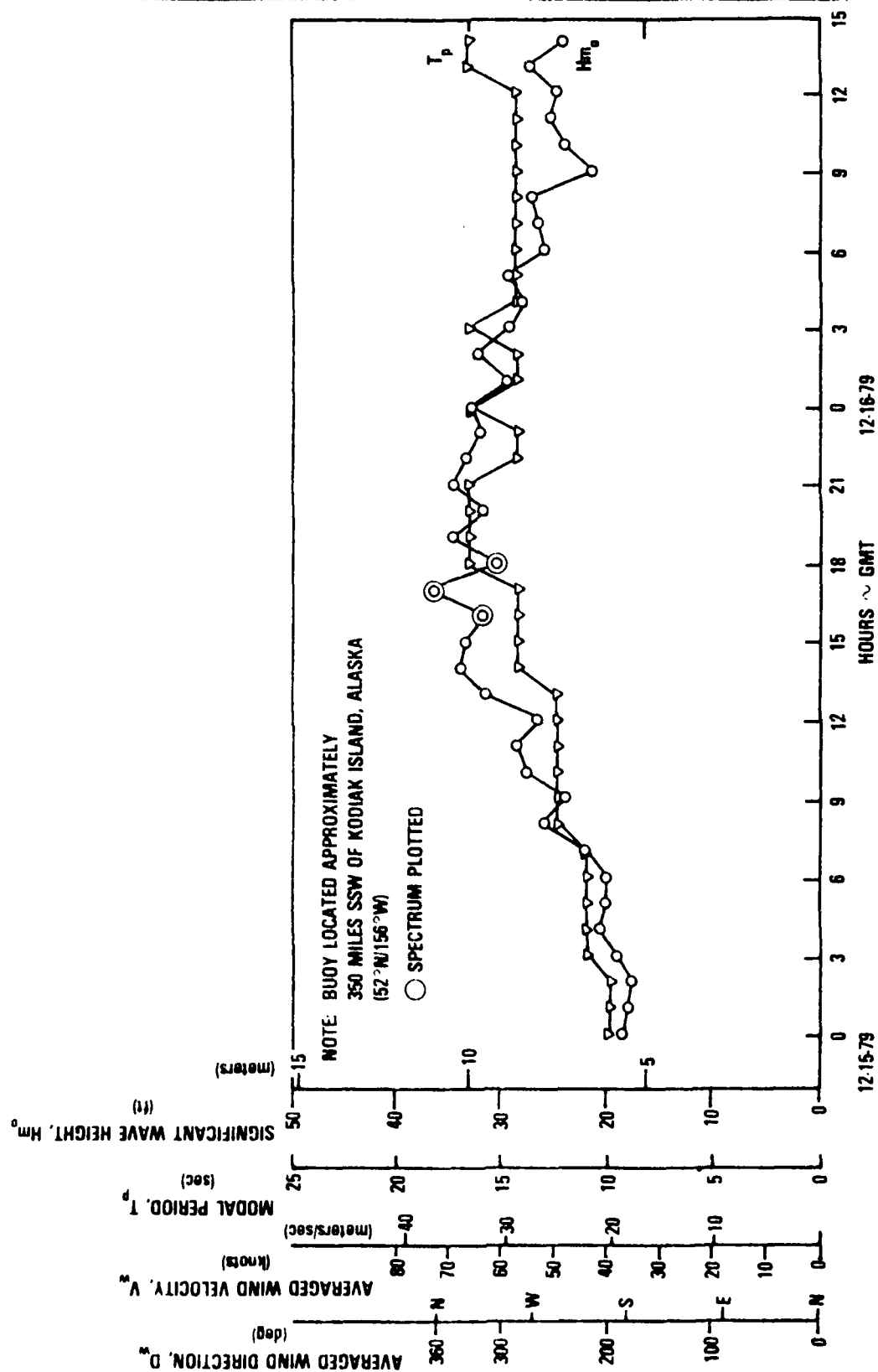


Figure A19 - Wave Data from Buoy Location 46003:
Winter Storm of 15 December 1979

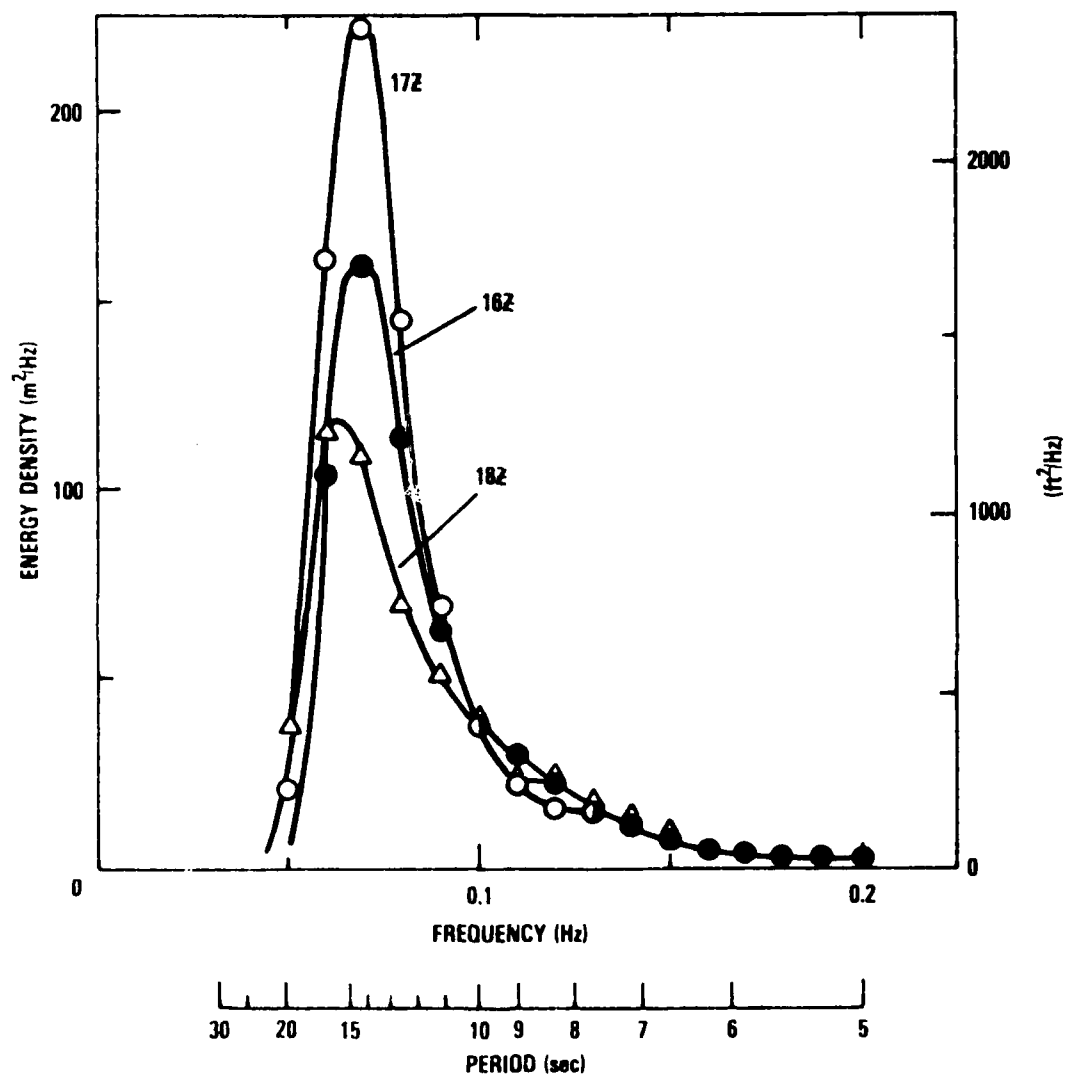


Figure A20 - Wave Height Spectra from Buoy Location 46003:
Winter Storm of 15 December 1979

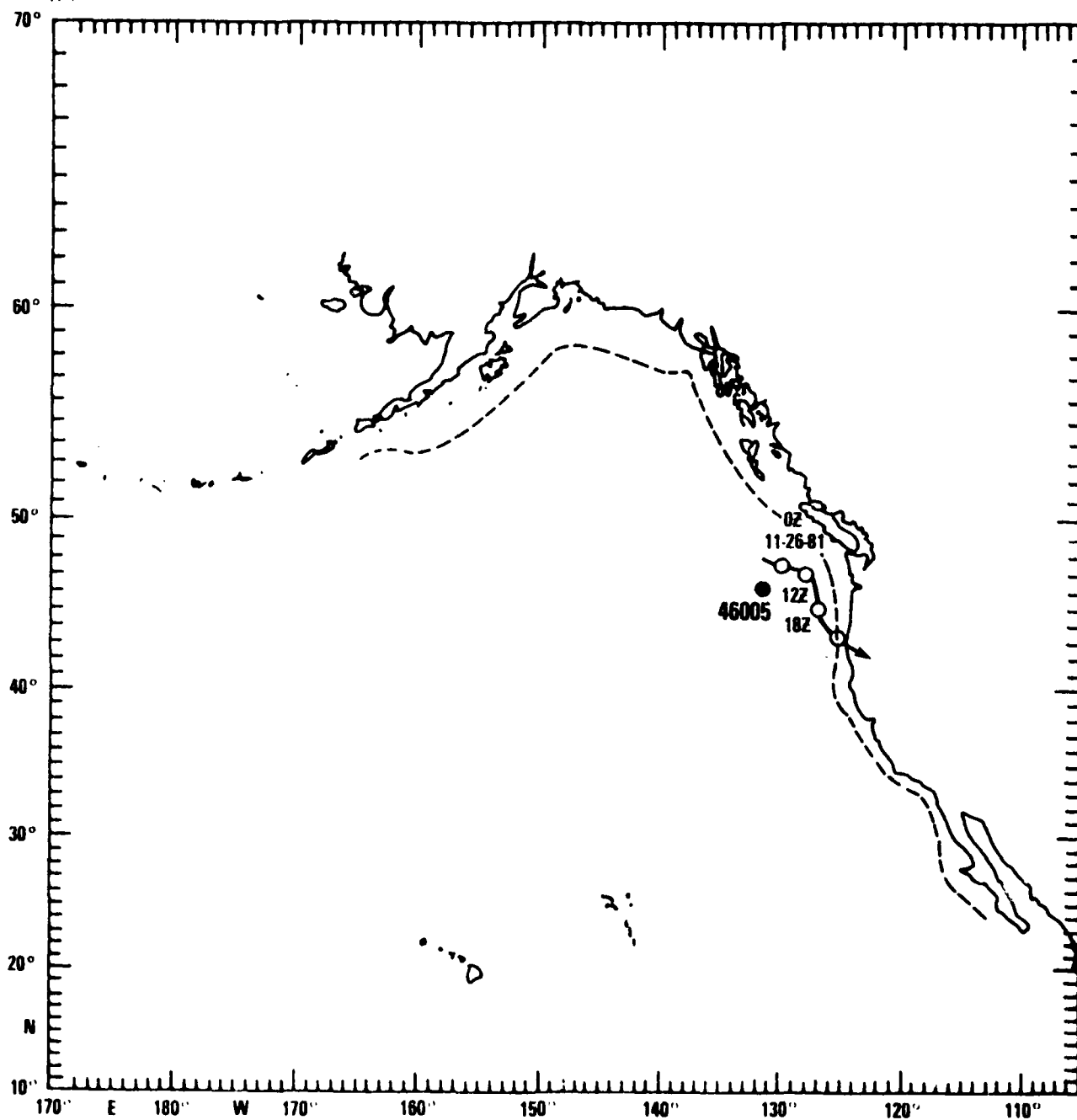


Figure A21 - Track of Winter Storm Relative to Buoy Location 46005.
26 November 1981

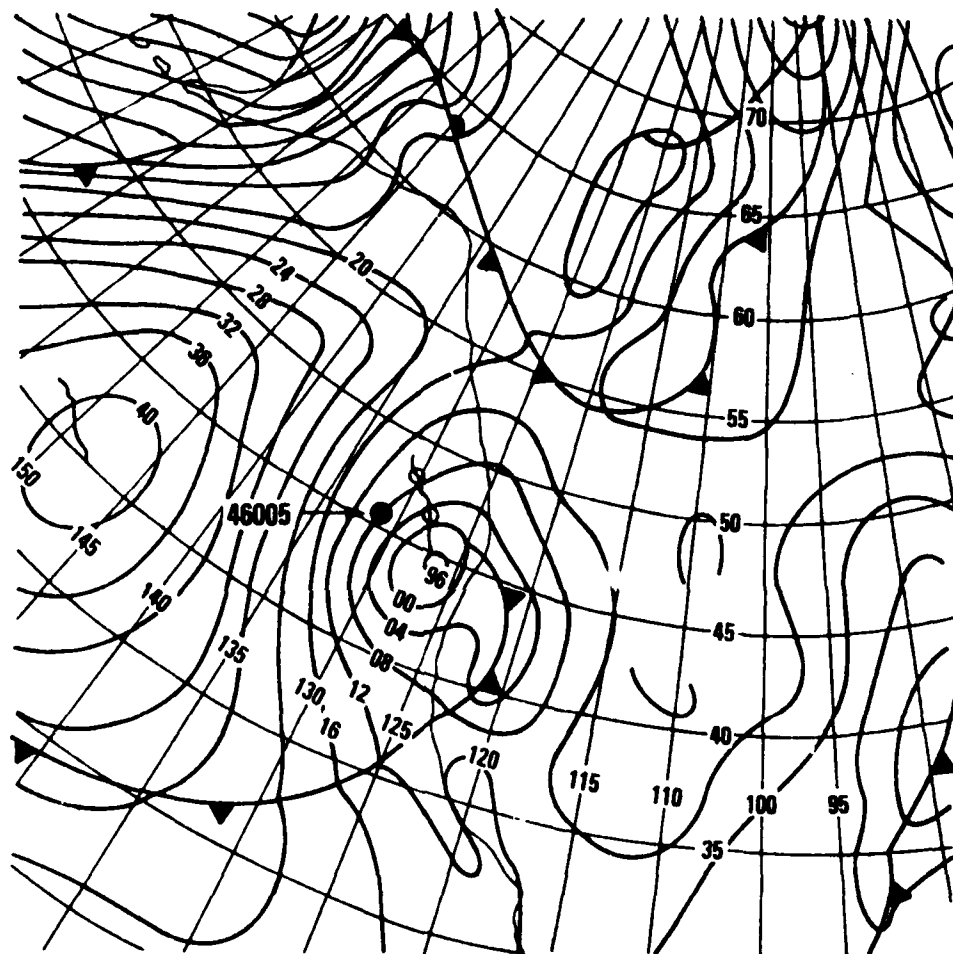


Figure A22 - Surface Weather Map for Buoy Location 46005 at 1200Z
on 26 November 1981

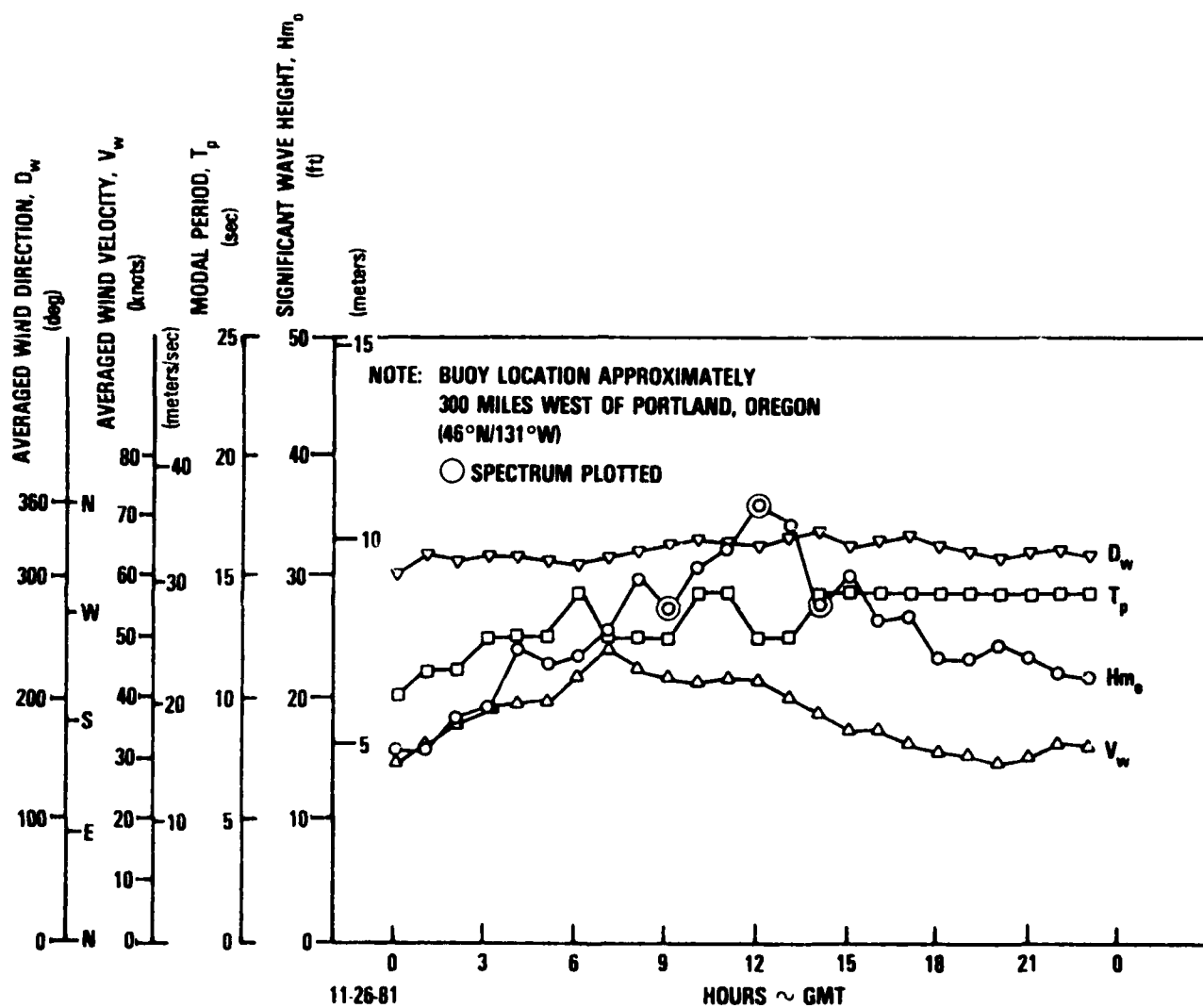


Figure A23 - Wave and Wind Data from Buoy Location 46005:
Winter Storm of 26 November 1981

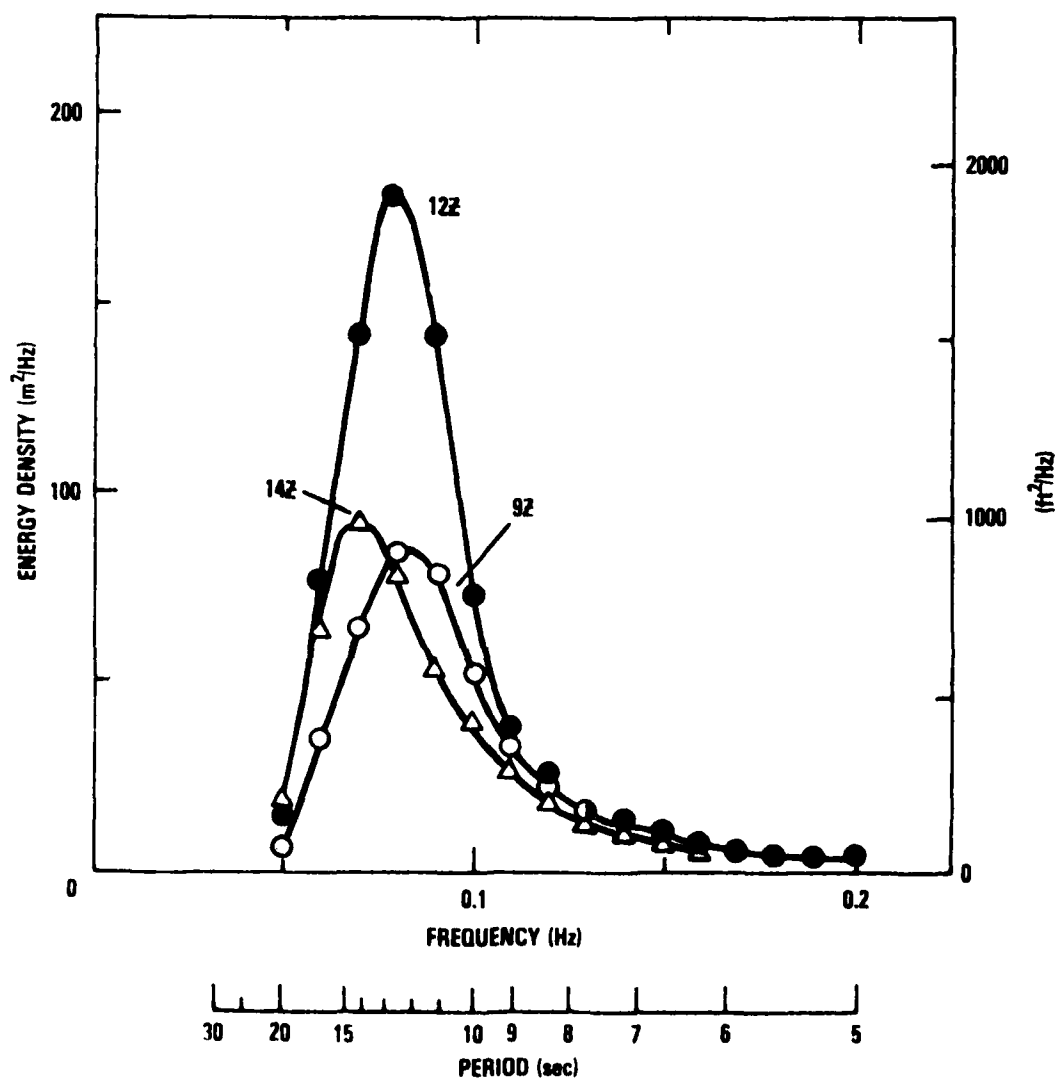


Figure A24 - Wave Height Spectra from Buoy Location 46005:
Winter Storm of 26 November 1981

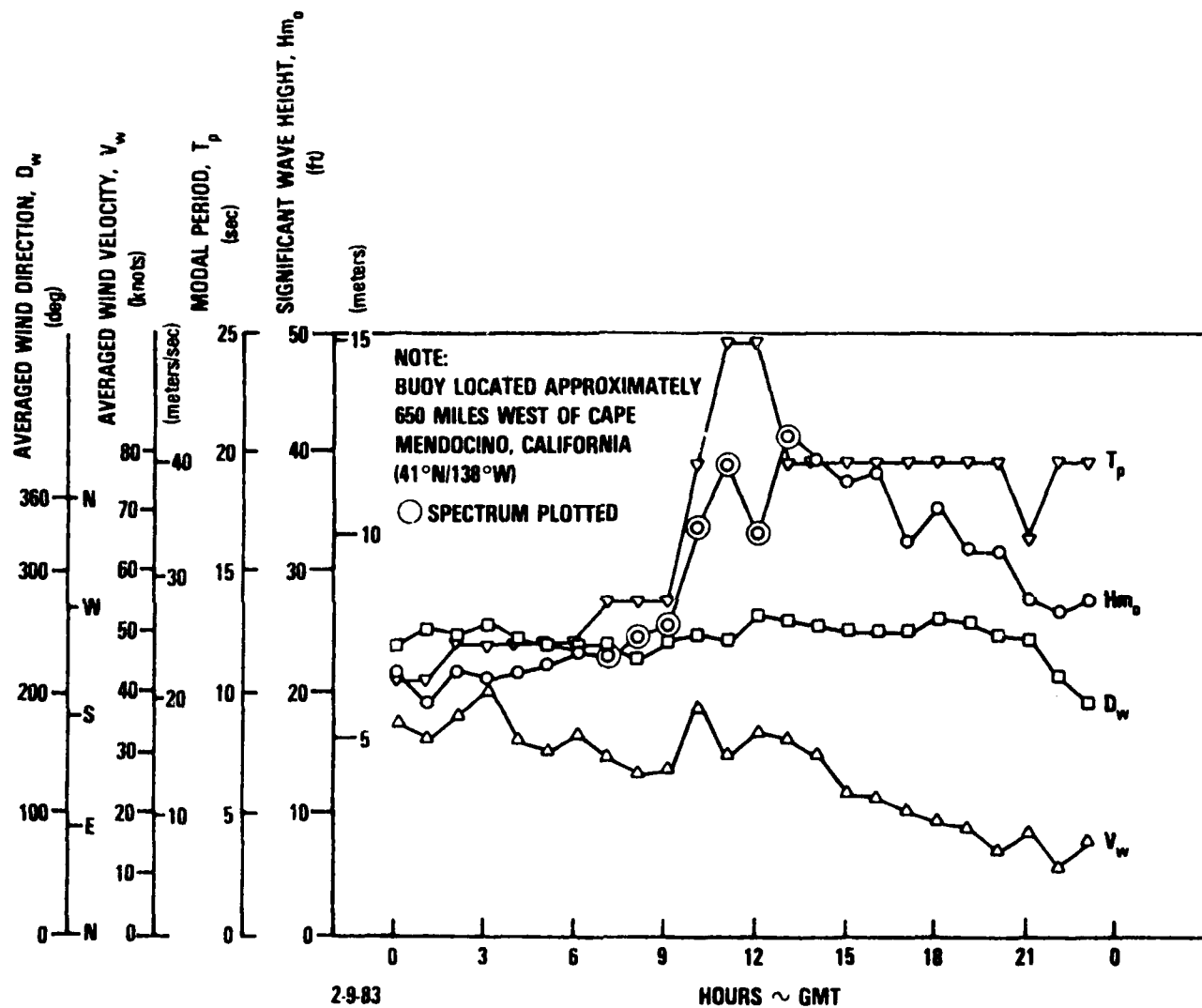


Figure A25 - Wave and Wind Data from Buoy Location 46006:
 Winter Storm of 9 February 1983

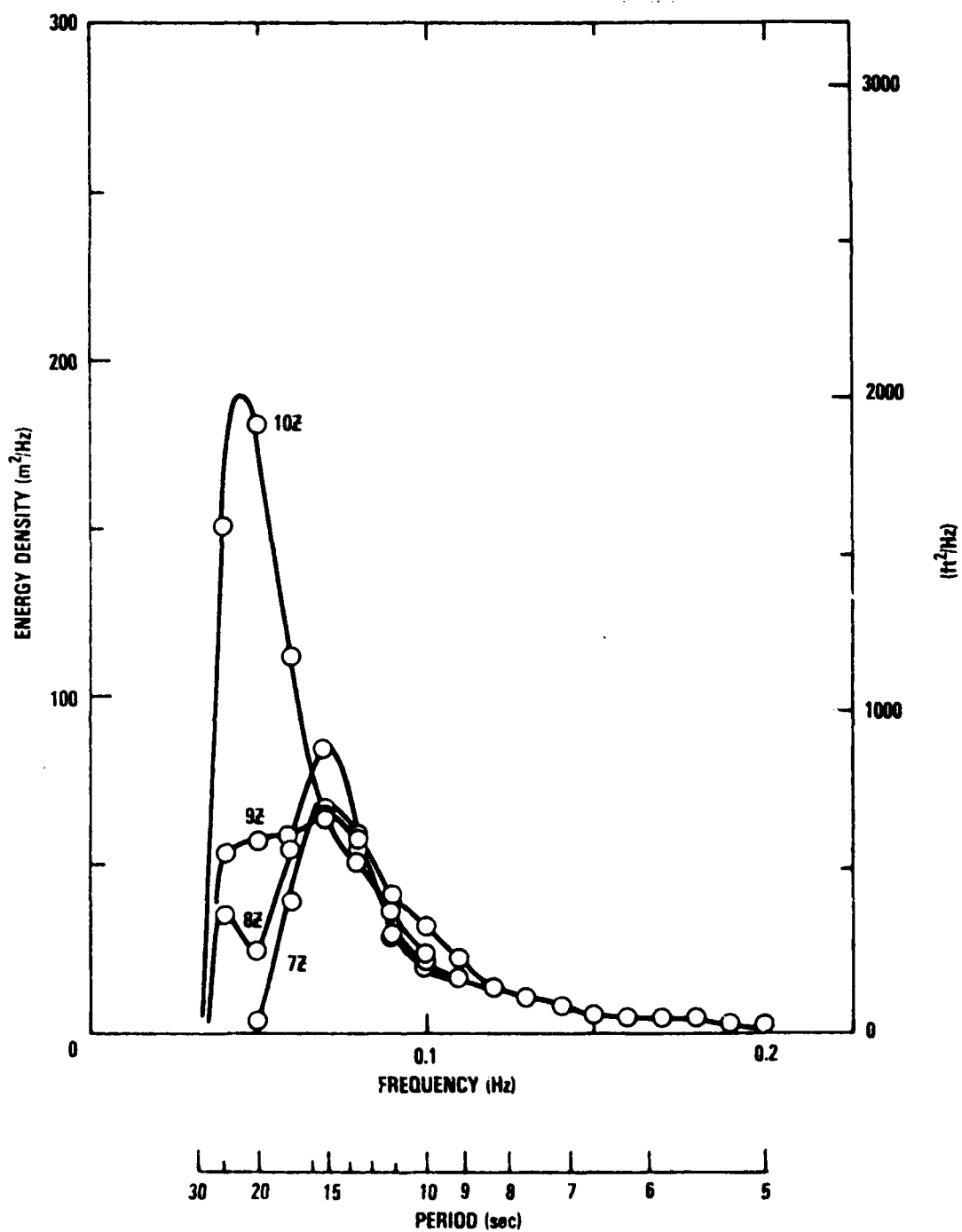


Figure A26 - Wave Height Spectra from Buoy Location 46006:
Winter Storm of 9 February 1983 - 0700Z to 1000Z

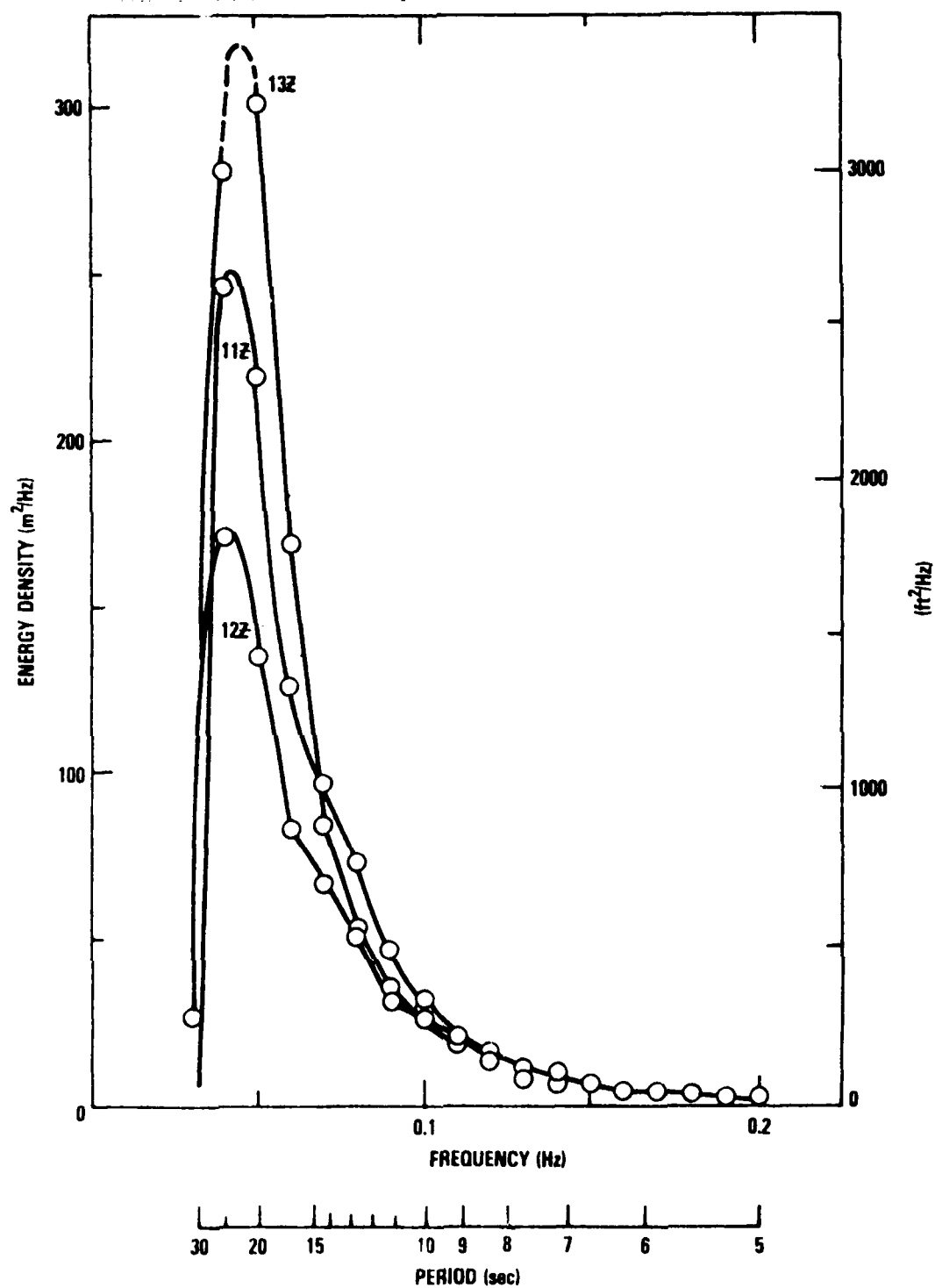


Figure A27 - Wave Height Spectra from Buoy Location 46006:
Winter Storm of 9 February 1983 - 1100Z to 1300Z

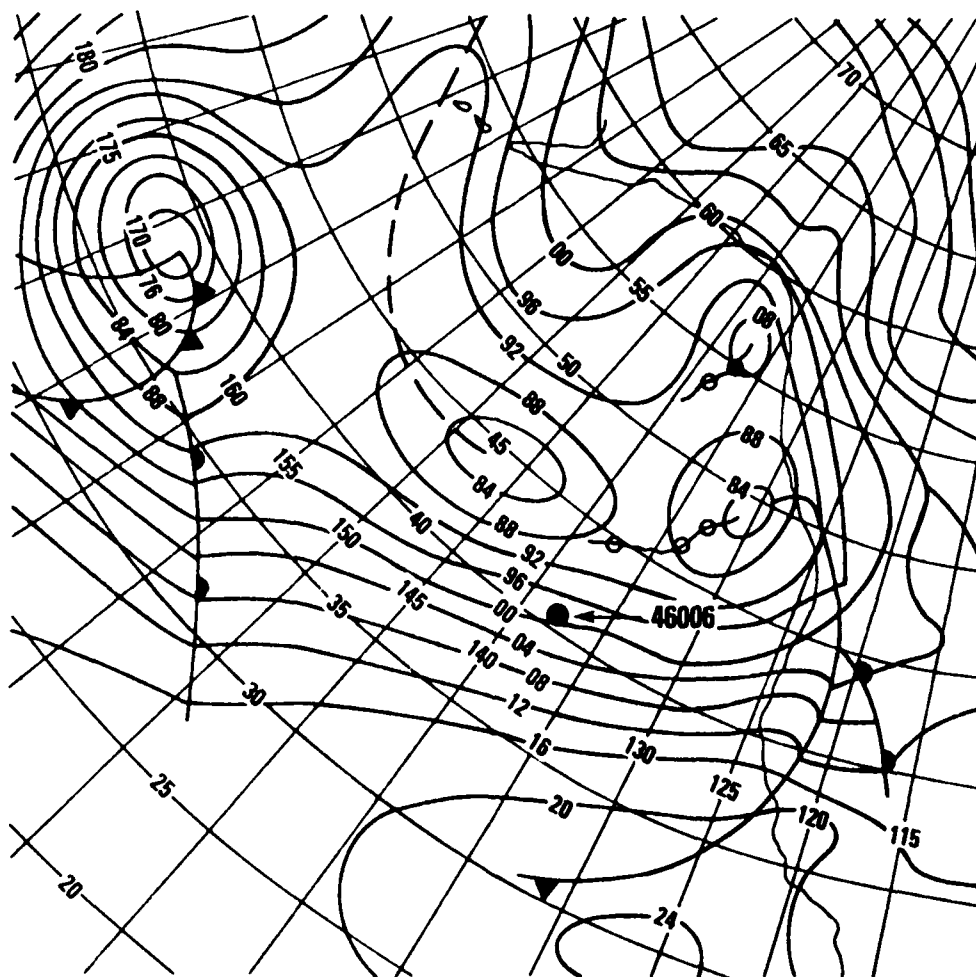


Figure A29 - Surface Weather Map for Buoy Location 46006 at 1200Z
on 9 February 1983

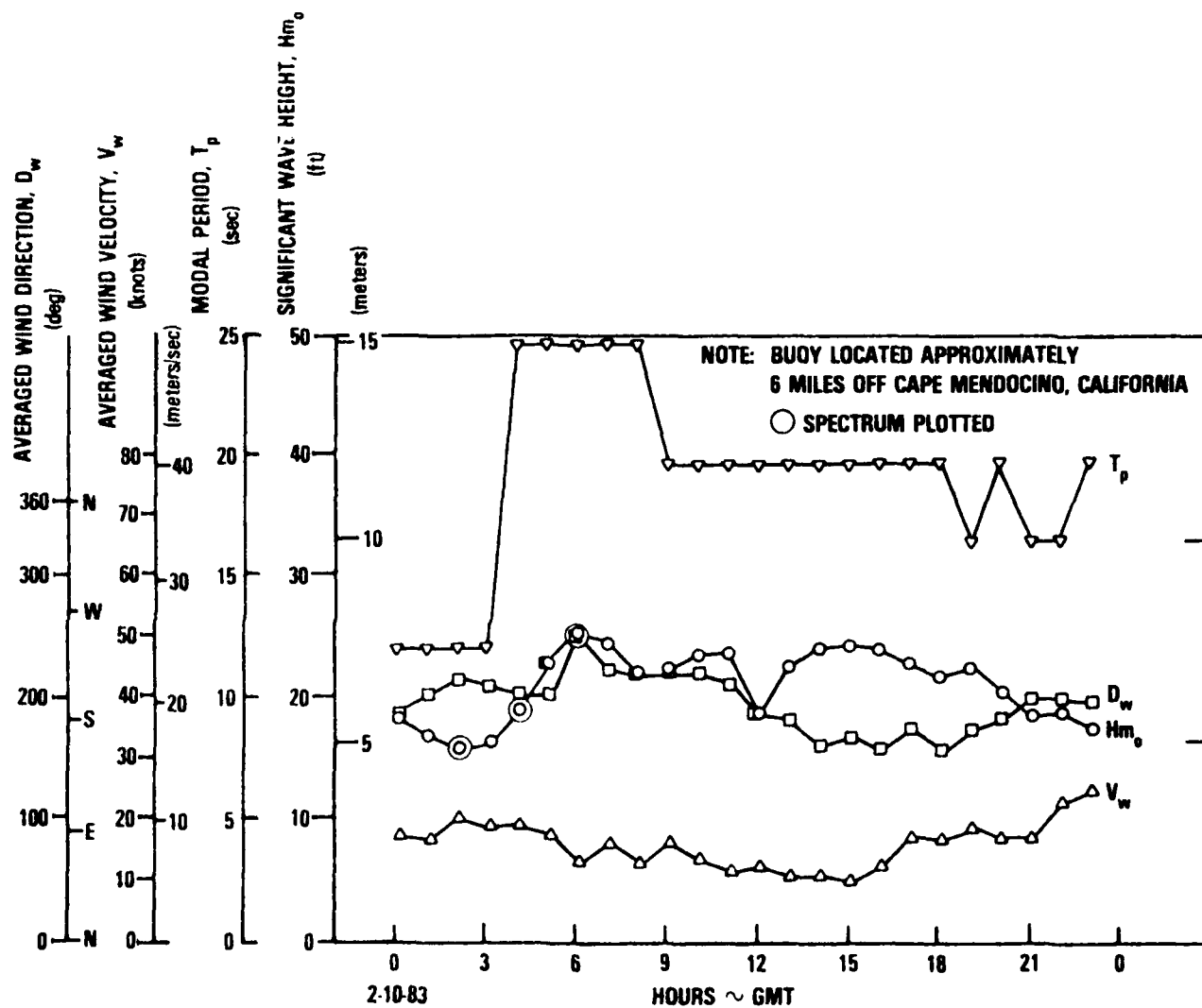


Figure A30 - Wave and Wind Data from Buoy Location 46022:
Winter Storm of 9 February 1983

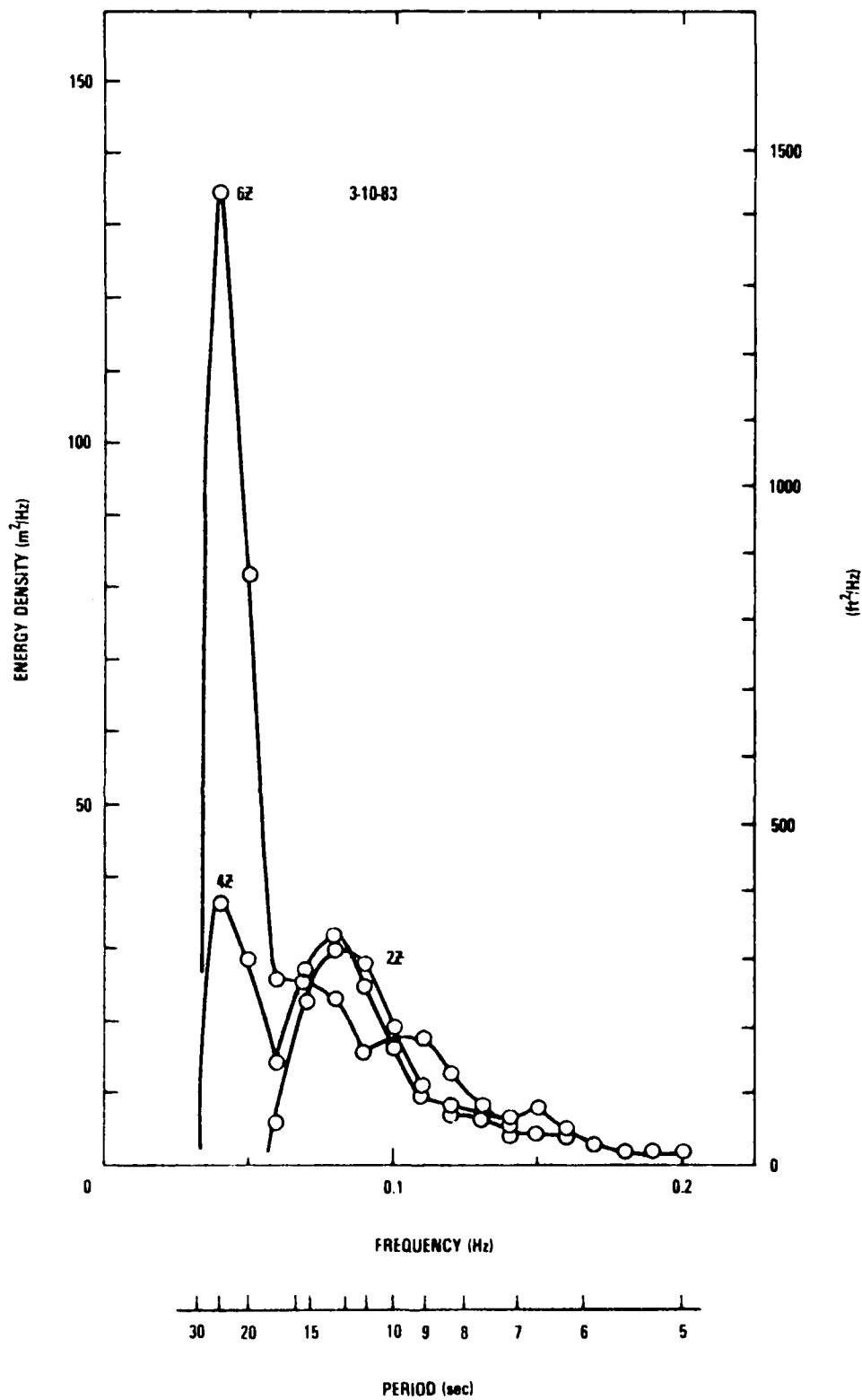


Figure A31 - Wave Height Spectra from Buoy Location 46022:
Wave Energy from Winter Storm of 9 February 1983

AD-R159 723

AN ASSESSMENT OF WAVE AND WIND DATA FOR USE IN DESIGN
OF TENSION LEG PLAT (U) DAVID W TAYLOR NAVAL SHIP
RESEARCH AND DEVELOPMENT CENTER BET W H BUCKLEY

2/2

UNCLASSIFIED

JUL 84 USCG-M-84-5 DTICG23-83-F-04433

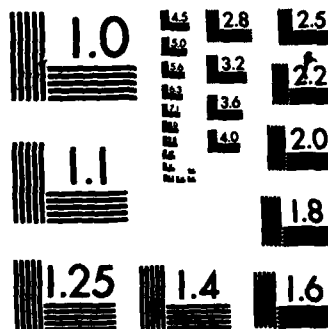
F/G 8/3

NL

END

FILED

DTIC



MICROCOPY RESOLUTION TEST CHART
NATIONAL BUREAU OF STANDARDS-1963-A

TABLE A1 - SUMMARY OF OBSERVATION PERIODS AND AVERAGE OBSERVATION RATE FOR SELECTED BUOYS

Buoy	Observation Period*		Number of Individual Observations*	Average Observation Rate (per year)	Date of Observation of Maximum Significant Wave Height
	(Elapsed)	(years)			
41001	1976-81	(5)	11,300	2260	Mar. 1980
42003	1976-82	(6)	24,500	4080	Sept. 1979
44004	1977-81	(4)	18,500	4630	Feb. 1980
46001	1972-81	(9)	37,300	4140	Nov. 1979
46003	1976-81	(5)	27,700	5540	Dec. 1979
46005	1976-82	(6)	32,700	5450	Nov. 1981
46006	1977-82	(5)	15,200	3040	Oct. 1979 ($H_{m_0} = 12 \text{ m}$)
*Data from Reference 1.					

TABLE A2 - TYPICAL REPORTING RANGES, SAMPLING INTERVALS, AND AVERAGING PERIODS FOR NOAA BUOY MEASURED WAVE AND WIND PARAMETERS (From Reference 1)

Measurement	Reporting Range	Sampling Interval	Averaging Period	Total System Accuracy (1 σ)
Wind Speed, V_w	0 to 155 knots	1 sec	8.5 min	± 1.9 knots or 10%
Wind Direction, D_w	0 to 360°	1 sec	8.5 min	$\pm 10^\circ$
Significant Wave Height, H_{m0}^*	0 to 20 m	0.67 sec	20.0 min	± 0.5 m
Wave Period, T_p	2 to 30 sec	0.67 sec	20.0 min	± 1 sec
*Calculated from the area under the wave energy spectrum.				

APPENDIX B

AN OBSERVATION OF EPISODIC WAVE PACKETS

The following excerpt is taken from Mariners Weather Log, Vol. 13, No. 4, July 1969, pp. 158-159.

LETTER TO THE EDITOR

"We have received word that the "monster of the month" for March (Rough Log, p. 182) was well chosen. The Commander, Military Sea Transportation Service, Atlantic, received the following memorandum from Captain G. Gundersen, Master, USNS BALD EAGLE (fig. 19), after the captain transited close to the center and then into the severe southwest quadrant of this gigantic, late-winter extratropical cyclone:

"During the period Mar. 7-9, 1969, this vessel, on voyage 141 (Bremerhaven to Norfolk), traveling in a light condition while in the vicinity of the Grand Banks (42°57'N, 49°32'W) transited a storm of such severity and eccentric features that is considered noteworthy.

"Reports of this storm were received over regular weather broadcasts. These reports indicated that the storm covered a very large area. Due to its relative position to the BALD EAGLE, and its huge area, a diversion to remove the ship from the storm's track was not feasible and not recommended by NAVOCEANO.

"March 7 entered with a barometric pressure of 998 mb. Winds during the day were westerly from 10-25 kt with an average of 15 kt; the day cleared with west-southwesterly winds of 10 kt. Seas from 2 to 8 ft were westerly to west-southwesterly; the final seas were west-southwesterly at 3 ft. Swells were westerly at an average height of 16 ft. March 8 opened with a pressure of 1001 mb, southwesterly winds of 10 kt, southeasterly seas of 2 ft, and westerly swells of 15 ft. At 1700, the wind was east by south at 10 kt accompanied by east by south seas of 3 ft and south by west swells of 14 ft; the barometer had plummeted to the very low value of 956 mb. Between 1600 to 1730, the BALD EAGLE passed through the "eye" of this storm from its easternmost to its southernmost point while on a westerly course. At 1745, the wind had increased to a steady 65 kt while sea and swell increased to 25 ft, all from west by south. The approach of these high seas, wind, and swell could be seen for approximately 15 min prior to the ship's entry. The ship's speed was reduced to 70 rpm, the minimum required to maintain steerageway; the ship's head was maintained slightly off the seas to prevent her from "pounding." From 1800 on March 8 to 1800 on March 9, visibility was 1 mi or less, and steady winds blew at 70 kt with gusts to 87 kt. Seas and swell to 45 ft, with numerous "freak" seas up to 70 ft, were encountered while the barometer was rising slowly. These freak seas were often 20° to the left or right of the average seas. Due to the severity of this storm and the numerous

freak seas, it was impossible to prevent some pounding of the vessel. However, every possible effort was made to keep it to a minimum. To further indicate the severity of this storm, it is noteworthy that the vessel succeeded in attaining a course of 220° true, while steering generally 270° into westerly winds, seas, and swells.

"On March 10, an inspection of the ship, in so far as possible, revealed no apparent storm damage.

"All the above data is contained in the ship's log book. This by far is one of the worst storms the undersigned has experienced."

"Editor's note: A synoptic weather map for 1200 on March 8 shows the storm at its probable peak intensity. Several ships in the dangerous southwest quadrant reported winds in excess of hurricane force (fig. 20). Table B1* is the Weather Log of the BALD EAGLE."

*Designation in this report.

TABLE B1 - SELECTED DATA FROM THE WEATHER LOG OF THE
BALD EAGLE MARCH 7-10, 1969

Lat. (°N)	Long (°W)	Day	Time	Wind		Barometric Pressure (mb)	Waves	
				Direction (10's deg)	Speed (kn)		Wind Waves (ft)	Swell (ft)
46.1	39.7	7	00	28	20	997.3	5	10
45.6	41.0	7	06	28	14	998.6	3	8
45.2	42.3	7	12	24	25	999.0	8	16
44.2	43.7	7	18	21	12	998.3	3	15
43.8	45.7	8	00	26	10	1001.7	3	15
43.5	46.4	8	06	13	12	993.2	3	15
43.3	48.3	8	12	14	15	973.2	3	15
43.3	50.6	8	18	26	65	958.3	X	33
42.8	51.2	9	00	26	60	970.2	30	33
42.4	51.2	9	06	27	50	974.6	25	30
42.1	51.7	9	12	27	65	978.3	39	43
42.0	52.1	9	18	27	60	982.4	34	34
41.8	52.4	10	00	27	30	988.5	X	34
41.5	52.8	10	06	32	30	988.2	10	18
41.3	54.4	10	12	31	08	986.1	5	10
X = Indeterminate								

APPENDIX C

UNIQUENESS OF SYNOPTIC WIND FIELDS ASSOCIATED WITH THE OCCURRENCE OF EXTREME SIGNIFICANT WAVE HEIGHTS AND MODAL PERIODS

Synoptic wind fields associated with the development of extreme values of significant wave height and modal period have relatively consistent development patterns. In general one or more relatively intense lows (generally in close proximity) find their normal eastward or northeastward track blocked by a large high pressure center. As a consequence of this blockage a large, elongated wind field is developed between them with strong winds blowing over a relatively long period of time and distance so that a seaway of extreme significant wave height and modal period is generated. It is implicit that this large, undirectional wind field be directed on-shore or along-shore.

Points (8) and (9) in Figure 8 correspond to synoptic wind field developments of this type. Figure A14 shows, for example, that the highest value of significant wave height yet recorded by the NOAA buoys resulted from blockage of the eastward passage of an intense low (952 mb or 28.1 inches of Hg) by a massive high pressure region lying over the Rocky Mountains. Figure A12 shows that the path of the storm was then directed toward the northwest and that its speed of advance had slowed considerably by 0600Z on the 28th when the buoy at location 46001 recorded a significant wave height of 48.6 feet.

Point (9) of Figure 8 derives from a storm in which a significant wave height of 42.2 feet was measured at Buoy location 46006 at 1200Z on 9 February 1983. Figure A29 shows a synoptic pressure field in which a major low near 38° N and 168° W had two less intense lows to the east and a relatively stationary high pressure region to the southeast. The elongation of the associated wind field was due to the orientation of the easterly lows with respect to the high pressure region to the south. Since the westerly surface winds were stronger to the west of Buoy location 46006, the significant wave height was quite likely greater than 42.2 feet in that area. Slowing of the eastward travel of the primary low during the twelve hours preceding 1200Z on the 9th is evident in Figure A28.

The characteristic synoptic weather pattern described above is uncommon for East Coast offshore areas and in fact the two highest significant wave heights measured by the NOAA Buoys (32.2 feet at Buoy location 41001 and 32.7 feet at Buoy location 44004) resulted from rapidly developing winter storms as discussed in Appendix A. One might be tempted to conclude that an intense, rapidly developing winter storm (or possibly hurricane) with a 50 or 100 year return period would result in a seaway of maximum significant wave height. The surface weather maps of Figures C1 and C2, which are taken from reference 19 suggest another possibility. The storm in question is the Ash Wednesday Storm of March 6 and 7, 1962 which resulted in wide spread and severe damage to the East Coast from Long Island to Cape Hatteras. It is apparent from Figures C1 and C2 that this record storm was the result of the same type of synoptic pressure development as that which resulted in extreme values of significant wave height and modal period off the U.S. and Canadian West Coasts. In this instance the blocking high pressure area lay over the Canadian Eastern provinces. The tightening and elongation of the isobars between the two lows and the high pressure center is very similar to that shown in Figure A14 as is

the relatively slow speed of advance from noon GMT on the 6th to noon on the 7th (on the order of 15 knots). The primary difference between the two synoptic developments appears to be that the Pacific storm had a lower central pressure of 952 vs 980 mb (28.1 vs 28.9 inches Hg) and a somewhat higher speed of advance. In any event, the characteristic synoptic pressure field development associated with the occurrence of extreme values of significant wave height and modal period is evident.

~~26~~

95

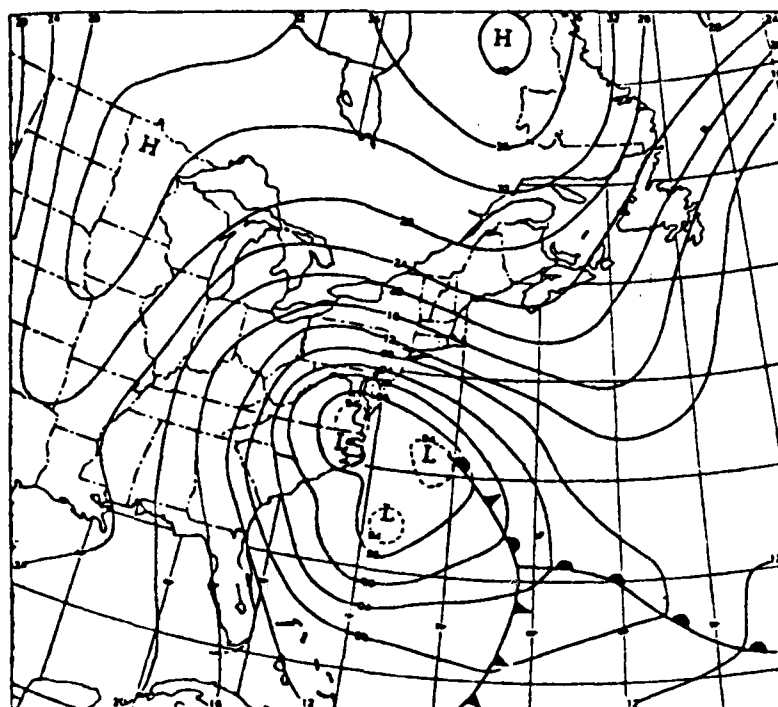
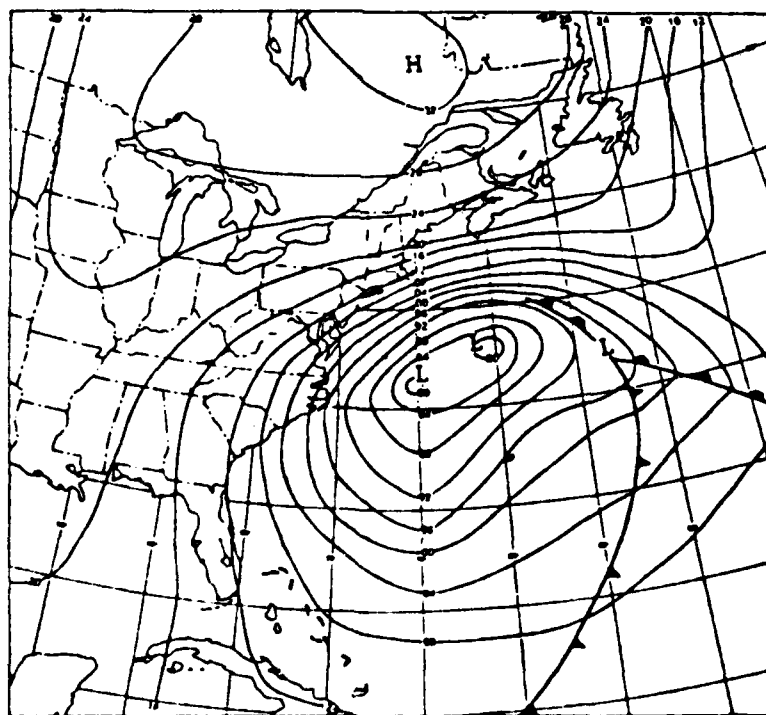


Figure C1 - Sea Level Pressure Chart (mb.) at 1200 GMT
March 6, 1962



NOTE: FROM REFERENCE 19.

Figure C2 - Sea Level Pressure Chart (mb.) at 1200 GMT
March 7, 1962

27
96

APPENDIX D

COMPARISON OF HURRICANE AND SEVERE WINTER STORM WAVES

Reference 14 presents spectral wave data measured during a severe winter storm at a gravity platform located in the northern North Sea in 343 feet of water (60° N and 2° E). At the height of the storm the authors report that significant wave height attained 13.3 meters (43.6 feet) with a modal period of $1/0.07 = 14.3$ seconds. These data have been plotted in Figure D1 to determine their relationship to those of Figure 8 of this report. It can be seen that the wave energy characteristics approached those encountered during Hurricane Camille in the Gulf of Mexico.

With respect to time series wave characteristics measured during the storm reference 14 states that:

"The non-Gaussianity of the waves at the Frigg field appears as a clear positive skewness of the parent distribution for the surface elevation. This means that the wave crests are higher and the troughs lower than linear theory allows for, and it indicates thus a pattern which seems to be consistent with the Stokien wave models. This is, in disagreement with the commonly accepted wave models used in stochastic dynamic analyses of gravity platforms, as described previously."

While the findings employ less conclusive methods of data analysis and are based upon sampled data (18 minutes every 60 minutes) as opposed to continuous data, they are remarkably similar to the findings of reference 6 in regard to the elevation of the larger waves and the fact that they are non-Gaussian* in character (see Section 2.2.2 of this report). Unfortunately, reference 14 does not present time-series wave height data so that the extreme steepness of the waves implied by the Camille data could be confirmed.

Some evidence of the wave characteristics is available, however, from a photograph appearing in reference 19, the profile of which has been traced in Figure D2. The information** contained in the photo caption is as follows:

"Actually, measuring wave heights at sea is difficult. Floating vessels move with the action, and only seldom does a wave line up with a fixed structure to permit measurement. In this case, the trough lined up almost perfectly with the small structure at left as the wave crest brushes against the underside of the platform deck at right (the only unknown factor is whether the white portion of the wave shown at right is foam of the actual

*That is to say, if the wave height time series were truly Gaussian such waves would not appear in it.

**The following additional information together with an original print of the wave photo was kindly furnished by Mr. Dillard Hammett of SEDCO, Inc.:

"The photo was taken in November, 1982. The location was the Ekofisk Field which is at a latitude of 54° N and a longitude of 4° E. The water depth was 240 ft and the waves were from the North North-East. The storm reached its peak 32 hours after initiation. The maximum wave height observed in the area was 86-92 ft. The maximum wave period observed was 12.8 seconds."

99

97

crest of the wave). In either case, the known dimensions of the two structures assures that the wave exceeds 70 ft in height, and might reach a total height of up to 90 ft. This photo was made in wet, wintry 1981-82 season at one of Phillips Petroleum's approximately 30 fixed structures in the Ekofisk area of the Norwegian North Sea - near the site where the Pentagone-class floatel ALEXANDER KIELLAND sank in March 1980 after losing one of its pontoons. To date, Phillips has suffered no major failure with any of its fixed structures in the area despite continuous attacks by rough wintry seas."

The wave traced from the photo has a height of at least 70 feet and a trough to crest length of approximately 255 feet for an implied height to length ratio of $70/(2 \times 255) = 1/7.3$. The Camille wave height time series shown corresponds to wave (C) of Figure 21 above. Assuming that wave length is given approximately by $L = 5.12 T^2$ (L in feet and T in seconds), the length of the Camille wave is roughly $5.12 (9.6)^2 = 472$ feet. The measured height was 65 feet which leads to an estimated height to length ratio of $65/472 = 1/7.3$ which corresponds closely to that of the wave photographed in the North Sea. If the Camille wave were to be modified to reflect the difference between the significant wave height existing when it was measured and the value reported in reference 14, its height would become $(43.6/40.5) \times 65 = 70$ feet for design purposes (i.e., for time domain response analyses or tank testing of a North Sea platform model). It is apparent that such a "design wave" would be similar to the wave which was photographed in the North Sea.

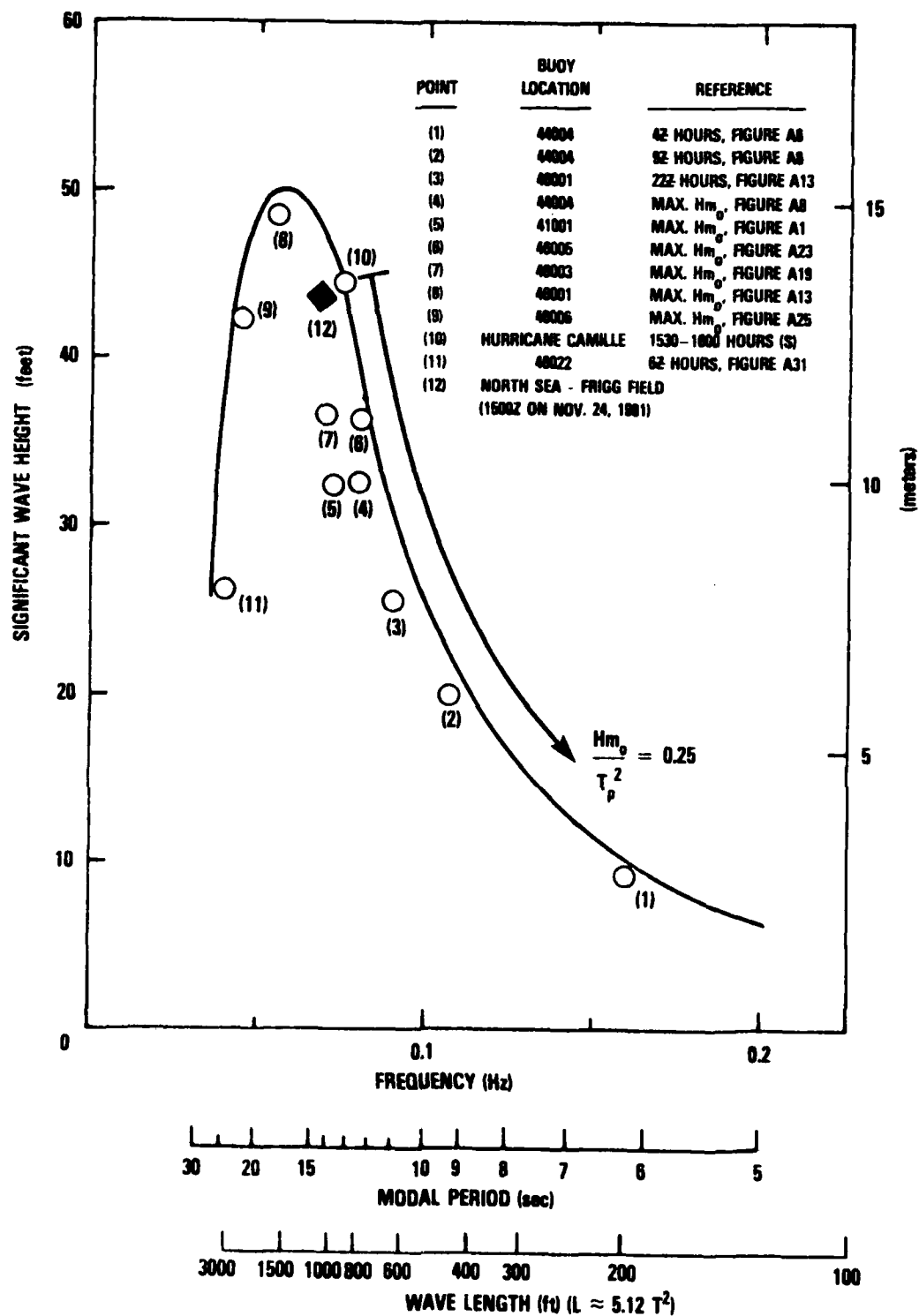


Figure D1 - Maximum Measured Significant Wave Heights vs Frequency
Corresponding to Modal Period - Including
North Sea Storm

101
99
~~100~~

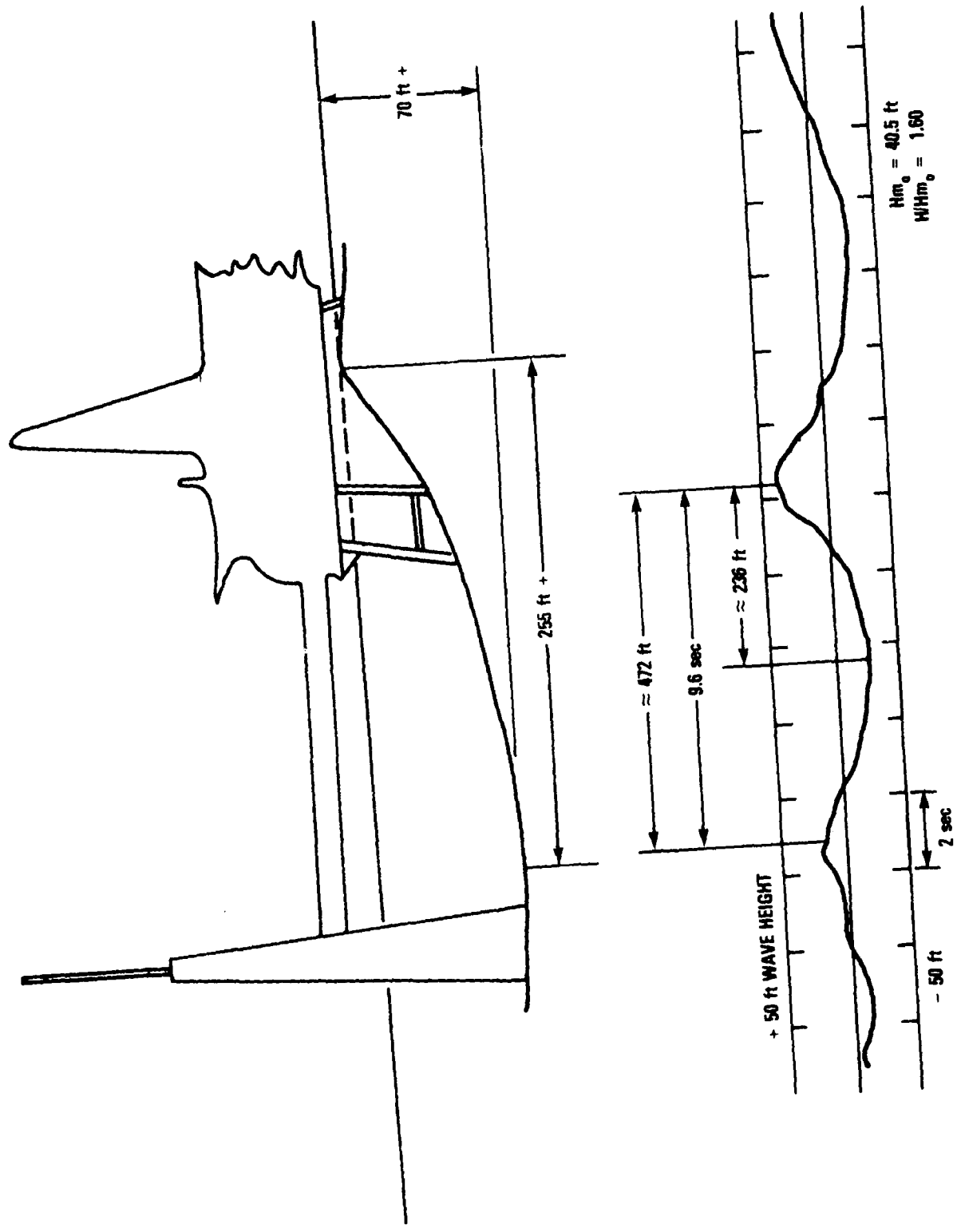


Figure D2 - Similarity of Waves in a Severe North Sea Winter Storm and Hurricane Camille

102
100
101

END

FILMED

11-85

DTIC